BLIND ESTIMATION OF MULTI-PATH AND MULTI-USER SPREAD SPECTRUM CHANNELS AND JAMMER EXCISION VIA THE EVOLUTIONARY SPECTRAL THEORY

by

Abdullah Ali Alshehri

B.S. E.E., University of Detroit, Detroit, USA, 1993

M.S. E.E., University of Pittsburgh, Pittsburgh, USA, 1999

Submitted to the Graduate Faculty of

the School of Engineering in partial fulfillment

of the requirements for the degree of

Doctor of Philosophy

University of Pittsburgh

2004

UNIVERSITY OF PITTSBURGH

SCHOOL OF ENGINEERING

This dissertation was presented

by

Abdullah Ali Alshehri

It was defended on

November 19, 2004

and approved by

Dr. Luis F. Chaparro, Associate Professor of Electrical Engineering

Dr. J. Robert Boston, Professor of Electrical Engineering

Dr. Patrick Loughlin, Professor of Electrical Engineering

Dr. Ching-Chung Li, Professor of Electrical Engineering

Dr. David Tipper, Associate Professor of Information Science

Dissertation Director: Dr. Luis F. Chaparro, Associate Professor of Electrical Engineering

ABSTRACT

BLIND ESTIMATION OF MULTI-PATH AND MULTI-USER SPREAD SPECTRUM CHANNELS AND JAMMER EXCISION VIA THE EVOLUTIONARY SPECTRAL THEORY

Abdullah Ali Alshehri, PhD

University of Pittsburgh, 2004

Despite the significant advantages of direct sequence spread spectrum communications, whenever the number of users increases or the received signal is corrupted by an intentional jammer signal, it is necessary to model and estimate the channel effects in order to equalize the received signal, as well as to excise the jamming signals from it. Due to multi-path and Doppler effects in the transmission channels, they are modeled as random, time-varying systems. Considering a wide sense stationary channel during the transmission of a number of bits, a linear time-varying model characterized by a random number of paths, each being characterized by a delay, an attenuation factor and a Doppler frequency shift, is shown to be an appropriate channel model. It is shown that the estimation of the parameters of such models is possible by means of the spreading function, related to the time-varying frequency response of the system and the associated evolutionary kernels. Applying the time-frequency or frequency-frequency discrete evolutionary transforms, we show that a blind estimation procedure is possible by computing the spreading function from the discrete evolutionary transform of the received signal. The estimation also requires the synchronized pseudo-noise sequence for either of the users we are interested in. The estimation procedure requires adaptively implementing the discrete evolutionary transform to estimate the spreading function and determine the channel parameters. Once the number of paths, delays, Doppler frequencies and attenuations characterizing the channel are found, a deci-

sion parameter can be obtained to determine the transmitted bit. We have also shown that our estimation approach supports multiuser communication applications such as uplink and downlink in wireless communication transmissions. In the case of an intentional jamming, common in military applications, we consider a receiver based on non-stationary Wiener masking that excises such jammer as well as interference from other users. Both the mask and the optimal estimator are obtained from the discrete evolutionary transformation. The estimated parameters from the computed spreading function, corresponding to the closest to the line of sight signal path, provide an efficient detection scheme. Our procedures are illustrated with simulations, that display the bit-error rate for different levels of channel noise and jammer signals.

keywords: Multipath channel fading, Direct sequence spread spectrum, Discrete evolutionary transform, Frequency-frequency kernel, Spreading suction, Time-varying frequency response, Channel characterization, Wiener filtering and masking, Doppler shifts, Attenuation factors, and Bifrequency function..

TABLE OF CONTENTS

LIST OF TABLES

LIST OF FIGURES

PREFACE

I would like to thank my advisor Dr. Luis F. Chaparro for the guidance and support he has provided me throughout my Ph.D. studies. I would like also to express my appreciation to all of the members serving on my dissertation committee for their time and invaluable feedback.

Also I am grateful to my friends and colleagues Hakki Ilgin, Nazeeh Alothmani, Fawzi Alorafi, Hussam Zaman, Rashida Afroz, Jongchin Chien and Dr. Aydin Akan.

I would like to express my gratitude to the Saudi Arabian Government for sponsoring my graduate studies.

Finally, my deepest regards go to my mother Norah for her unconditional love and awaiting my return, my wife Norah for her patience and support, and to my lovely kids, Ghadah, Khaled, and Afnan. I dedicate this dissertation to them.

1.0 INTRODUCTION

1.1 MOTIVATION AND SCOPE

The transmission channel of a radio communication system is in most cases a multipath one [2, 3]. When changes take place in the propagation environment (e.g. the radio stations are mobile), reflectors and scatterers are moving, or the medium itself is changing, then the channel response also changes as a function of time. The signals that arrive from various paths are added to form a distorted signal. Due to multipath effects, each signal has a different time delay, gain amplitude, and carrier frequency shift [4, 7, 55]. Channel time-variation and inter-symbol interference affect the strength of the received signal. This effect is called channel fading, and it poses a challenge in mobile wireless communications. One fundamental characteristic of wireless communications is that the channel is time-varying due to the mobility of the user, or of objects in the propagation environment[5, 6, 64, 65].

Fading due to multi-path is a major limitation in mobile wireless communication systems. Fluctuations in the received signal degrade the performance of the receiver. For instance, the RAKE receiver typically used in the code division multiple access (CDMA) works optimally in slow-fading situations, but a significant loss of performance occurs whenever rapid channel changes take place, causing fast fading. Moreover, the increased mobility of users in cellular communications make the effect of Doppler spread in the transmitted signal more significant, as the state of the channel is much more difficult to estimate.

In this thesis we propose an estimation approach for direct-sequence spread-spectrum wireless communications (DSSS) channels using the discrete time-frequency evolutionary transform [16, 20]. The model is characterized by parameters such as time-delays, frequency shifts, and attenuation factors associated with signals coming from various paths. This

model contains all-pass filters that characterize the delays, constant attenuation factors, and exponential modulators that characterize the frequency shifts, or Doppler shifts. During the transmission of a single data symbol or frame the channel is almost constant, and the channel response to the the symbol can be calculated using the formulas of linear time invariant systems [7, 57, 59, 60, 80, 81, 83]. When the channel changes significantly during the transmission of a data frame, new channel representations must be used. The discrete evolutionary transform DET was used to estimate the time-frequency kernel from the received signal. We will show that this kernel can be used to obtain the channel time-varying frequency response, and we present a special adaptive windowing method to compute the time-frequency evolutionary kernel of the received signal, which can then be related to the channel frequency response function [7, 8]. Once the channel frequency response is obtained, it is possible to compute the spreading function (SF) that depicts the parameters of the channel. A DSSS receiver is constructed based on the channel parameters obtained from the received signal by means of the spreading function. Practical communication systems are often multiuser in nature since mobile users share a common air interface and the receiver must detect one of the user's signal only. Multiuser communication is substantially more complicated compared to single-user communication, mainly due to limited physical resources such as power and bandwidth. We will show that it is possible for our estimation method to work for multiuser communication channels both in the down and up links.

Recently there has been a great deal of interest in the application of time-frequency signal analysis to problems in communications, particularly to spread spectrum communications [41, 42, 48, 49]. The direct sequence spread spectrum technique to some degree reduces interference power. Therefore, the interference immunity of a DSSS system can be reduced if the power of the interferences during transmission is very strong. Additional preprocessing techniques before despreading such as transform domain excision can enhance the interference immunity of the system. In many of these situations the type of jammer is known and the methods are adapted accordingly. Different methods have been proposed to mitigate broad-band jammers; many of the available excision techniques assume characteristics of the interference (e.g., sinusoidal or chirp interference), and then project the received signal either onto the signal-plus-noise space, or use time-varying filtering to excise the interference

[41, 42, 43, 44, 46, 49]. The Wigner-Hough transform method characterizes the jammer by a parametric model of its instantaneous frequency. Time-varying filtering and masking methods based on bilinear time-frequency distributions can excise jammers characterized by their instantaneous frequency, bandwidth, and support in the time-frequency plane [50, 52]. The method of the projection excision technique improves the time-varying notch filtering [44, 45]. In most situations the characterization of the jammer is not known, only its support may be available or obtained. However, the users' spreading sequences are always known at both the transmitter and at the receiver, and the direct sequence has the same spectrum independent of the sign of the sent bit. The problem can be treated as a deterministic masking problem, or as a mean-square estimation problem. We will show that the jammer excision can be determined using the frequency-frequency evolutionary transformation which shows a better performance when the interference is narrowly concentrated; conversely the Wiener masking method is more capable of dealing with interference spread over the whole or most of the frequency space. It will be shown that in the case of broadband jamming signals a simplified version of the Wiener masking approach [54] can be used to excise such jammers. In fact, it can be combined with the channel estimation approach to generate a special DSSS receiver.

1.2 DISSERTATION OVERVIEW

The research presented in this dissertation is primarily concerned with aspects of reliable channel estimation and interference excision of DSSS wireless communication in the presence of multipath phenomenon. The time-frequency representation of the signal is connected to a spreading function using the relation of LTV channel functions. The discrete time-frequency evolutionary transform DET is used to obtain the time-frequency representation of the multipath signal. Furthermore, detection schemes that follow channel estimation are presented to develop robust receivers.

This thesis is organized as follows: in Chapter 2 the necessary theoretical backgrounds are introduced, such as direct sequence spread spectrum communications, linear time-varying

(LTV) channels, and multipath channel fading. In the same chapter, we define the frequency-frequency evolutionary spectrum obtained from the discrete evolutionary transform (DET) via Gabor expansion. It is also shown how this kernel can be obtained from the time-frequency evolutionary kernel, or directly from the signal. An example is provided comparing the frequency-frequency evolutionary spectrum to the time-frequency evolutionary spectrum of a multi-component signal.

Modeling and estimation of multipath wireless CDMA channels is discussed in Chapter 3, where an all-pass multipath channel model is used to characterize channel parameters. We consider a single user case, showing how the evolutionary kernel is related to the channel frequency response, and the spreading function of the channel that depicts the channel parameters. Examples are given to illustrate the estimation approach for different fading environments. A bit detection scheme based on the proposed channel modeling and estimation technique is presented also in Chapter 3. This approach involves obtaining the transmitted signal closest to the line of sight, with the smallest delay, the least attenuation, and some Doppler shift for use in determining the transmitted bits. Such a signal is clearly the strongest signal being sent, and thus its parameters are probably more easily estimated than those of weaker signals. Two computational aspects showing a significant reduction in the computational cost are presented as well.

In Chapter 4 channel modeling and estimation are extended to support the multiuser levels encountered in DSSS wireless communications during both uplink and downlink transmissions. The estimated spreading function of a particular user depicts peaks that correspond to that user, while other users' spreading functions appear as noise. The detection scheme is similar to the single user scheme, which uses information corresponding to the strongest path signal.

In Chapter 5 we present two interference mitigation schemes based on spectrum masking of the time-frequency, and the frequency-frequency evolutionary spectrums of the desired signals. In the instance of jammers with narrow support, frequency-frequency masking performs best, while Wiener masking performs well in situations involving non-stationary jammers. Also, a Wiener masking receiver capable of excising broad band jammers in multiuser and multipath transmission channels is presented.

Many examples are provided with illustrations explaining the ideas of this thesis. Several simulations were performed and their plotted results are included in Chapters 3, 4, and 5. Finally, a general conclusion with the contributions of this thesis and some ideas for future work are provided in Chapter 6.

2.0 BACKGROUND

In this chapter we briefly present some issues that will be used in the rest of the thesis. In particular, we generally review spread spectrum, then consider the physical propagation of transmitted signals, and ways the transmission channels can be characterized. In addition to that, the time-frequency evolutionary spectral theory is reviewed and a new frequency-frequency evolutionary spectral representation is presented.

2.1 SPREAD SPECTRUM

Spread-spectrum techniques for digital communications were originally developed and used for military communications either to provide resistance to jamming, or to hide the signal by transmitting it at low power, thus making it difficult for an unintended listener to detect its presence in noise [9]. Therefore, spread-spectrum communications have advantages in the areas of security, resistance to jamming, resistance to multipath fading, and supporting multiple-access techniques such as the code division multiple access (CDMA) [1, 3, 57].

2.1.1 Spread Spectrum Schemes

There are a number of different ways to generate spread spectrum signals. One spreading scheme is the direct-sequence spread-spectrum (DSSS), which is achieved by phase modulation. Another spreading scheme is known as frequency-hop spread-spectrum (FHSS) achieved by rapid changes in the carrier frequency. When both direct-sequence and frequency-hop techniques are employed, the resultant scheme is called a hybrid DS-FHSS. Another way

to generate a spread-spectrum signal is the time-hop spread-spectrum (THSS) signal. In this case, the transmission time is divided into intervals called frames. Each frame is further divided into time slots. During each frame, only one time slot is modulated with a message; all the message bits accumulated in previous frames are transmitted.

2.1.2 Direct-Sequence Spread Spectrum (DSSS)

In direct-sequence spread spectrum (DSSS) the baseband data pulse is spread by multiplying it with a pseudo-noise (PN) sequence produced by a code generator (see Appendix B). The PN sequence is a deterministic, periodic signal that is known to both the transmitter and the receiver. A single pulse or symbol of the PN sequence is called a *chip* [4]. The name pseudo-noise, or pseudo-random comes from having similar statistical properties as white noise. For an unauthorized listener, it appears to be a truly random signal. A more general DSSS transmitter with binary phase shift keying (BPSK) is shown in Fig. 1, where a single bit $m(t)$ of duration T_b seconds is considered for transmission.

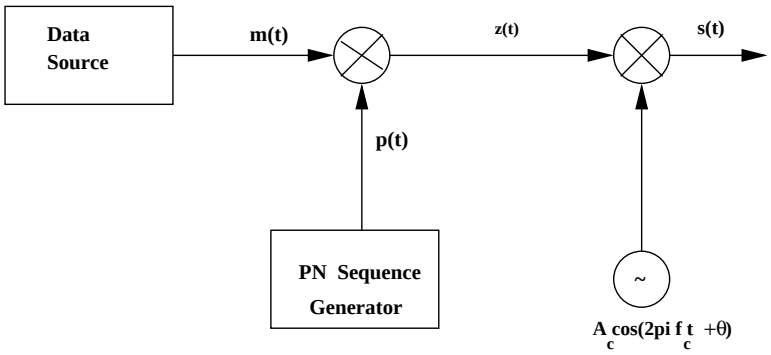

Figure 1: Transmitter for DSSS system

Let us consider the transmission of a binary information sequence of rate R bits per second with duration interval $T_b = \frac{1}{R}$ seconds. The available transmission bandwidth is B_w Hz, where $B_w \gg R$. The information-bearing baseband signal $m(t)$, which is transmitted at

a rate of R, and has the duration period of $T_b = \frac{1}{R}$ seconds can be expressed as

$$m(t) = \sum_{k=\infty}^{\infty} d_k g(t - kT_b)$$

where $d_k = \pm 1$, and $g(t)$ is a rectangular pulse of duration T_b. The baseband signal can then be spread by multiplying it by the spreading code. The pseudo-noise signal is generated using shift registers (see Appendix B for generating PN) and can be expressed as

$$p(t) = \sum_{k=-\infty}^{\infty} c_k q(t - kT_c) \tag{2.1}$$

where $c_k = \pm 1$ represents the binary code sequence, and $q(t)$ is a rectangular pulse of duration equal to the chip interval T_c.

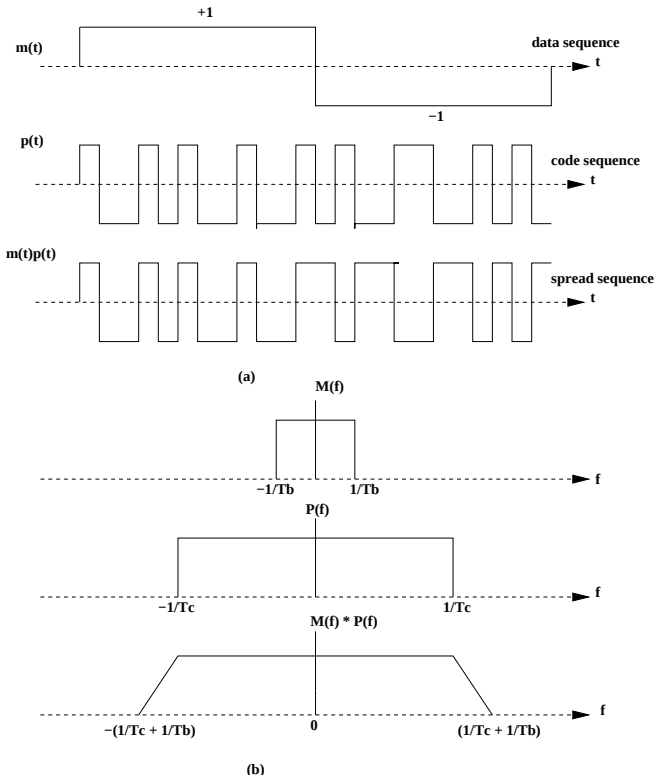

Figure 2: Spreading operation: (a) in time domain, (b) in frequency domain.

By the multiplication operation, we try to spread the bandwidth of the information-bearing signal of narrow bandwidth R into a broad bandwidth.Figure 2 illustrates the spreading processes in both the time and the frequency domains respectively.

The product signal $z(t) = p(t)m(t)$ is then used to modulate the carrier $A_c cos(2\pi f_c t + \theta)$. The transmitted signal can be expressed as

$$s(t) = A_c m(t)p(t)cos(2\pi f_c t + \theta) \tag{2.2}$$

We notice here that for any t, the product signal $m(t)p(t) = \pm 1$, thus, the modulated transmitted signal $s(t)$ may also be expressed as

$$s(t) = A_c cos(2\pi f_c t + \theta(t)) \tag{2.3}$$

where $\theta(t)$ has two distinct values, $\theta(t) = 0$ when $m(t)p(t) = 1$, and $\theta(t) = \pi$ when $m(t)p(t) = -1$. Therefore, the carrier-modulated transmitted signal is a binary PSK signal. At the receiver side, a demodulation process takes place by multiplying the received signal by the replica of the spreading signal p(t) generated synchronously at the receiver. This operation is called despreading and is shown in Figure 3. The despread signal is

$$\begin{aligned} r_o(t) &= A_c m(t)p^2(t)cos(2\pi f_c t + \theta) \\ &= A_c m(t)cos(2\pi f_c t + \theta) \end{aligned} \tag{2.4}$$

where $p^2(t) = 1$ for all t. The resultant signal $r_o(t)$ will have approximately the same original bandwidth R, which means that the spreading does not have any effect on the demodulation. After despreading, the output signal will be demodulated by the PSK to recover the desired signal.

However, the despreading has other effects on interference. Suppose that the received signal is

$$r(t) = A_c m(t)p(t)cos(2\pi f_c t + \theta(t)) + j(t) \tag{2.5}$$

where j(t) is the interference. The despread signal will then have the form

$$\begin{aligned} r_o(t) &= (s(t) + j(t))p(t) \\ &= A_c m(t)p^2(t)cos(2\pi f_c t + \theta(t)) + j(t)p(t) \\ &= A_c m(t)cos(2\pi f_c t + \theta(t)) + j(t)p(t) \end{aligned} \tag{2.6}$$

We notice from $r_o(t)$ that it has the modulated signal in the first term with the original bandwidth R, and in the second term it spreads the interference across the bandwidth of the spreading code. If the interference has a narrow-band spectrum after despreading, demodulating, and filtering with bandwidth R, the power of the interference will be reduced by an amount equal to the bandwidth expansion factor, or what the so-called the processing gain

$$G = \frac{T_b}{T_c} = \frac{B_w}{R}.$$

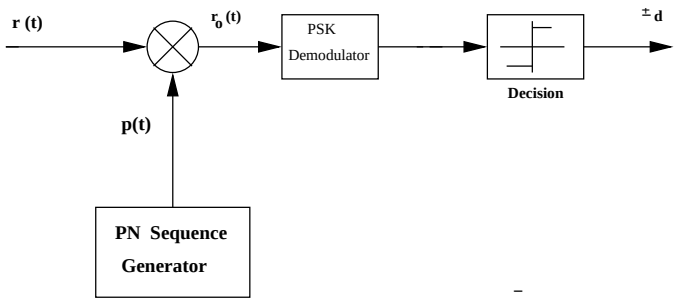

Figure 3: Receiver for DSSS system

2.1.3 RAKE Receiver

In CDMA spread spectrum systems, the chip rate is typically much greater than the flat fading bandwidth of the channel $R_m = \frac{1}{T_m}$, where T_m is the maximum access time delay. The spreading code, or pseudo-noise PN sequence, is designed to provide very low correlation between successive chips. Thus, the multipath channel provides multiple versions of the transmitted signal at the receiver. If the multipath components are delayed in time by more than a chip duration T_c, they appear as uncorrelated noise at the receiver [55, 57, 59]. In 1958, Price and Green [68] proposed a method for resolving multipath wide-band pseudo-random PN sequence using the property that time-shifted versions of itself with $T_m > T_c$ are almost uncorrelated. Thus, a signal that propagates from transmitter to receiver over multiple paths, and hence multiple time delays can be resolved into separately

fading signals by cross correlating the received signal with multiple time-shifted versions of the PN sequence. The receiver is called a RAKE receiver because the block diagram looks like a garden rake. Thus, the RAKE receiver is essentially a diversity receiver designed specifically for CDMA, where diversity is provided by the fact that the multipath components are practically uncorrelated from one another when their relative propagation delays exceed a chip period. The performance of the RAKE receiver is governed by the combining scheme used. The RAKE receiver utilizes multiple correlators to separately detect the M strongest multipah components (see Appendix C for details).

2.2 PHYSICAL PROPAGATION ENVIRONMENT

The communication link between a transmitting and a receiving antenna is called free space path if it is a free of all objects that might absorb or reflect radio frequency energy [1, 2]. Within this path, the atmosphere behaves as a perfectly uniform medium, and the reflection effect of the earth is neglected as being far away from the path. At the receiver, the received signal is attenuated by a free space path loss factor $L_s(d)$ and is giving by [4]:

$$L_s(d) = \left[\frac{4\pi d}{\lambda}\right]^2$$

i.e, it depends quadratically on the distance d between the transmitter and the receiver, and the wavelength λ of the transmitting signal. Thus, the received signal power is predictable and the attenuation factor is the only channel parameter that can determine the power level of the received signal.

2.2.1 Multipath Fading

In practical channels, a signal typically propagates from transmitter to receiver over multiple reflective paths. The effect of this phenomenon is that it causes fluctuations in the amplitude and the phase of the received signal, and is referred to as multipath fading. Therefore, in practice a channel model has to be introduced since the free space propagation model is

inadequate to describe the channel and predict the system performance [4, 5, 7, 55]. Figure 4 illustrates this manifestation with three reflective paths and one direct path.

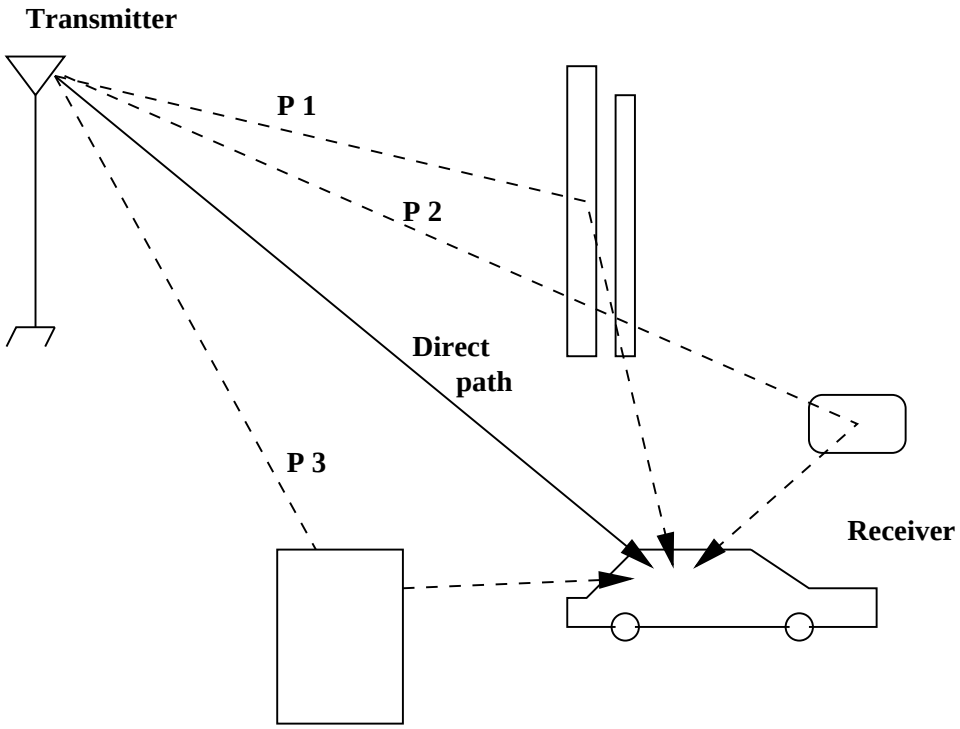

Figure 4: Multipath fading environment

Thus, the characterization of mobile communication depends on the types of channel-fading. The variations are characterized by two main manifestations: large-scale and small-scale fading [5]. Furthermore, these manifestations give rise to specific types of degradations of the signal. Figure 5 shows the fading manifestations and their associated degradations [4].

2.2.1.1 Large-Scale Fading The first fading manifestation, large-scale fading, refers to path loss caused by the effects of the signal traveling over large areas [5]. Large-scale fading characterizes the losses due to sizable physical objects in the signal's path such as hills or forests. The statistics of large-scale fading provide a way of computing an estimate of path

loss as a function of distance. This is often described in terms of a mean-path loss, and a log-normally distributed variation about the mean [3, 7].

2.2.1.2 Small-Scale Fading The second fading manifestation, small-scale fading, characterizes the effects of small changes in between a transmitter and a receiver. These changes can be caused by mobility of the transmitter, receiver, or intermediate objects in the path of the signal. Small scale changes result in considerable variations of signal amplitude and phase. Small-scale fading is also known as Rayleigh fading since the fluctuation of the signal envelope is Rayleigh distributed when there is no predominant line-of-sight between the transmitter and receiver. The Rayleigh probability density function is expressed as:

$$f_{Ray}(r) = \frac{r}{\sigma^2} exp\left(-\frac{r^2}{2\sigma^2}\right), \qquad r \geq 0 \tag{2.7}$$

where r is the envelope amplitude of the received signal, and $2\sigma^2$ is the pre-detection mean power of the multipath signal. When there is a predominant line of sight between the transmitter and receiver, the fluctuations are statistically described by a Ricean probability density function expressed as:

$$f_{Ric}(r) = \frac{r}{\sigma^2} exp\left(\frac{-(r^2+k^2)}{2\sigma^2}\right) I_o\left(\frac{Kr}{\sigma^2}\right), \qquad r, K \geq 0 \tag{2.8}$$

where $I_0(x)$ is the Bessel function of the first kind of order zero. As the amplitude of the specular component (nonfaded component from the direct path when there is line-of-sight between the transmitter and receiver) approaches zero, the Ricean pdf approaches a Rayleigh pdf.

Small scale fading has two manifestations. The first one, signal dispersion, refers to the time-spreading of the signal. Dispersion causes the underlying digital pulses transmitted in the signal to spread in time. The second manifestation reflects the time varying of the channel that is due to relative mobility between a transmitter and a receiver, or the objects in the path of the signal. Both of these manifestations can be characterized in the time and frequency domain by fading degradation types.

As shown in Fig 5, the degradation types of the dispersion manifestation are frequency selective fading and flat fading. From the time domain point of view, frequency selective

fading occurs when the maximum spread T_m in time of a symbol is greater than the duration of the symbol. Consequently, another name for this fading degradation is channel induced inter symbol interference ISI. From the frequency domain point of view, frequency selective occurs when the spectral components of a signal are affected in different ways by the channel. In particular, frequency selective fading occurs when the channel coherence bandwidth is smaller than the signal's bandwidth [5, 57].

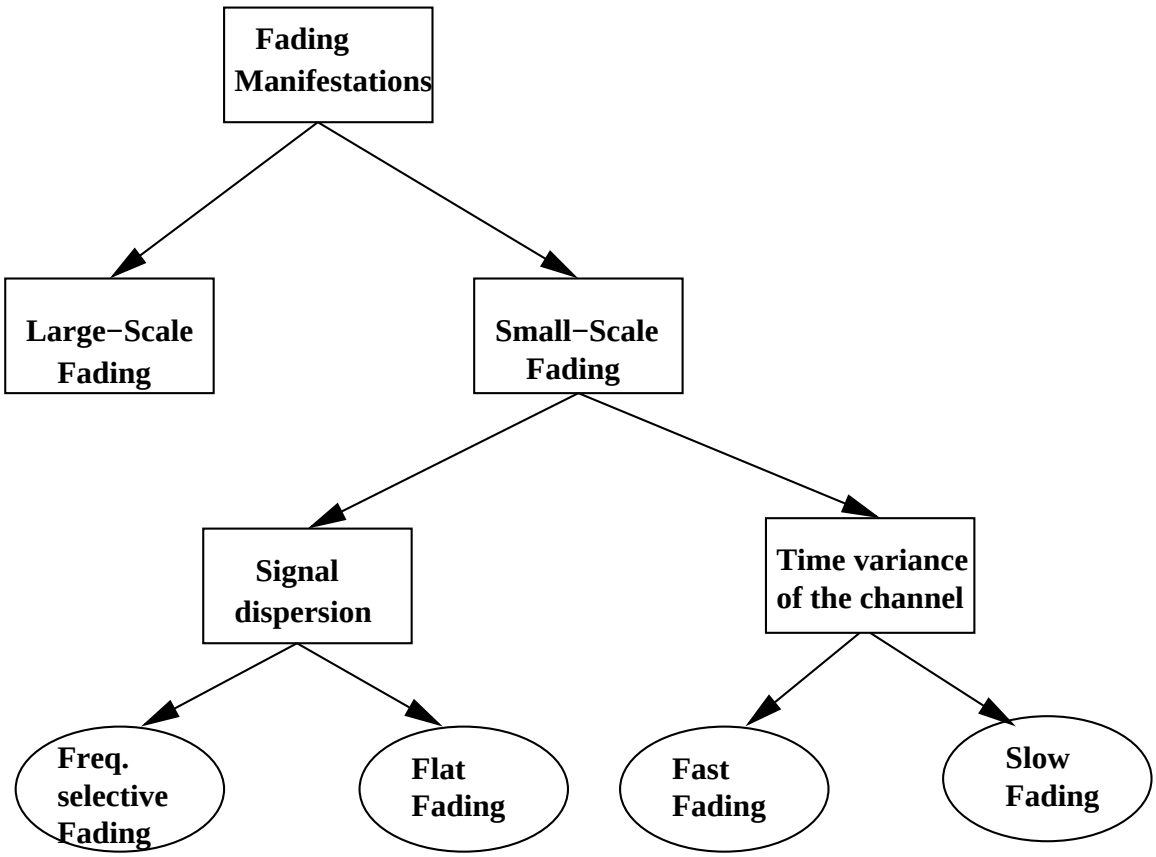

Figure 5: Channel fading manifestations and degradations

Figure 5 also shows the degradation due to the time variation of the channel. These are fast and slow fading. For fast fading, the channel state changes during the time in which the symbol is transmitted, leading to distortion of the received signal. But for slow fading, the

channel state remains unchanged for the time in which the symbol is transmitted.

An important parameter in a time-varying channel is the Doppler shift f_d caused by the movement of the receiver, and is expressed as:

$$f_d = \frac{\nu}{c} f_c \cos\beta$$

where ν is the speed of the mobile receiver, c is the speed of the radio wave, f_c is the carrier frequency, and β is the angle between propagation path and transmitter.

2.3 CHANNEL CHARACTERIZATION AND MODELING

In the case of the channel being invariant with respect to time, an impulse response h(t), or its corresponding transfer function H(f) fully describes it. In the characterization of a linear time-varying (LTV) channel, several system functions are introduced [3, 7].

The time-variation nature of the channel can be seen from the varying number, attenuations, and delays of the paths at different time instants. It can be said that the multipath channel response depends on both the time of arrival of the input pulse (time), and on the time passed since that (delay). The impulse response is a function of both time and delay, while in the time-invariant channel it is only a function of delay. Furthermore, if the transmitter in moving, a Doppler effect will also be seen at the receiver.

2.3.1 Multipath Channel Models

Several multipath channel models have been developed [4, 5, 6]. Proakis [1, 3] presented the most general time-varying multipath channel model. In this model, the transmitted signal was represented as

$$s(t) = R_e[z(t)e^{j2\pi f_c t}] = \frac{1}{2}[z(t)e^{j2\pi f_c t} + z(t)^* e^{-j2\pi f_c t}] \tag{2.9}$$

where $z(t)$ the transmitted data pulse.

It was shown that there were multiple propagation paths, and that each was associated with a time-varying propagation delay and a time-varying attenuation factor. Thus, the received band-pass signal is

$$y(t) = \sum_{k=0}^{M(t)-1} \alpha_k(t) s(t - \tau_k(t)) \tag{2.10}$$

where $\alpha_k(t)$ is the gain of the n^{th} propagation path as function of time, $\tau_k(t)$ is the propagation delay of the n^{th} propagation path as function of time, and $M(t)$ is the number of propagation paths as function of time. By substituting Equations (2.9) into (2.10) the received signal becomes

$$\begin{aligned} y(t) &= \sum_{k=0}^{M(t)-1} \alpha_k(t) R_e[z(t - \tau_k(t)) e^{j2\pi f_c(t-\tau_k(t))}] \\ &= R_e[\sum_{k=0}^{M(t)-1} \alpha_k(t) e^{-j2\pi f_c \tau_k(t)} z(t - \tau_k(t)) e^{j2\pi f_c t}] \end{aligned} \tag{2.11}$$

centered around the carrier frequency f_c and has the following low-pass form at the output of the demodulator

$$r(t) = \sum_{k=0}^{M(t)-1} \alpha_k(t) e^{-j2\pi f_c \tau_k(t)} z(t - \tau_k(t)) \tag{2.12}$$

From Equation (2.11), the impulse response of the channel can be written as

$$g(t, \tau) = \sum_{k=0}^{M(t)-1} \alpha_k(t) e^{-j2\pi f_c \tau_k(t)} \delta(\tau - \tau_k(t)) e^{j2\pi f_c t} \tag{2.13}$$

Thus, the characteristics of parameters $\alpha_k(t)$ and $\tau_k(t)$ determine the classification of the multipath channel. If they are slowly varying during the symbol time period, the channel can be called slow-varying.

The time-varying channels can be classified as either deterministic or statistic depending on whether its parameters are viewed as deterministic functions or as random processes. An example of statistical models are those that employ the Rayleigh and Ricean pdfs to describe the random fluctuations of the received signal's envelope [5, 66].

2.3.2 System Functions of a LTV-Channel

The basic system function of a deterministic LTV-channel is the time variant impulse response $g(t,\tau)$ obtained in (2.13). Other frequently used system functions are [7, 55]:

(1) The time-variant frequency response function:

$$G(t,f) = \int_{-\infty}^{\infty} g(t,\tau) e^{-j2\pi f\tau} d\tau \tag{2.14}$$

obtained by taking the Fourier transform of the impulse response with respect to the delay variable τ.

(2) The channel bifrequency function:

$$B(\Omega,f) = \int_{-\infty}^{\infty} G(t,f) e^{-j2\pi\Omega t} dt \tag{2.15}$$

obtained by taking the Fourier transform of the transfer function with respect to the time variable t.

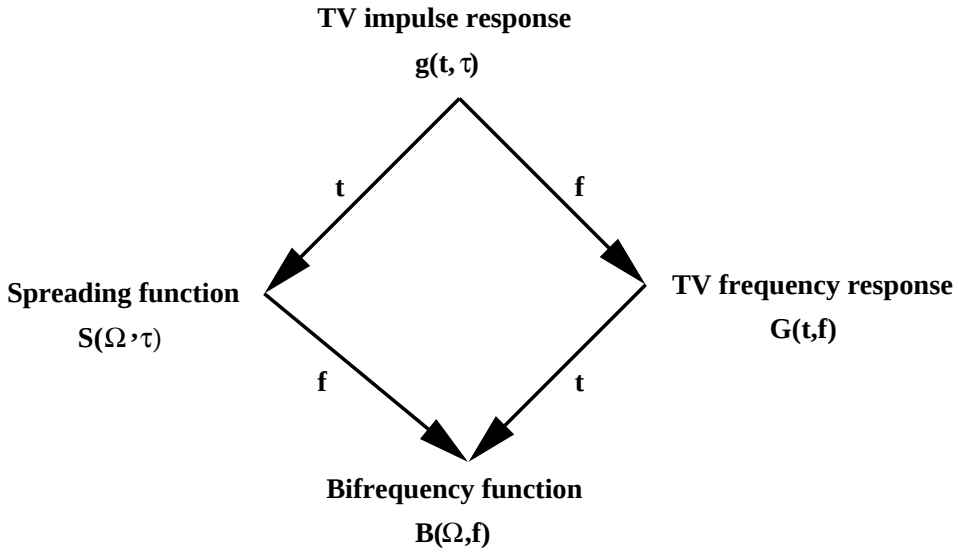

Figure 6: System functions representation.

(3) The Doppler spreading function:

$$S(\Omega, \tau) = \int_{-\infty}^{\infty} g(t, \tau) e^{-j2\pi\Omega t} dt \tag{2.16}$$

obtained by taking the Fourier transform of the impulse response function $g(t, \tau)$ with respect to the time variable t, or taking the inverse Fourier transform of the bi-frequency function with respect to frequency f. It gives the complex gain of the channel on the delay interval $[t + dt]$, and the Doppler-shift interval $[\Omega + d\Omega]$. The Fourier-transform relations of these four system functions are shown in Figure 6.

The output of the LTV channel $\zeta(t)$ can be expressed in terms of the system functions as

$$\begin{aligned} \zeta(t) &= \int_{-\infty}^{\infty} g(t, \tau) z(t - \tau) d\tau \\ &= \int_{-\infty}^{\infty} G(t, f) Z(f) e^{j2\pi f t} df \\ &= \int_{-\infty}^{\infty} \int_{-\infty}^{\infty} S(\Omega, \tau) z(t - \tau) e^{-j2\pi\Omega\tau} d\Omega d\tau \\ &= \int_{-\infty}^{\infty} \int_{-\infty}^{\infty} B(f - \Omega, \Omega) Z(f - \Omega) e^{j2\pi f t} d\Omega df. \end{aligned} \tag{2.17}$$

2.4 FREQUENCY-FREQUENCY EVOLUTIONARY SPECTRAL THEORY

The frequency content of the majority of signals encountered in our everyday lives such as speech, acoustic, stock indexes, and biomedical signals change over time, and their estimation has been a research topic of great interest [10, 11, 14, 15, 18, 26, 31]. Standard Fourier analysis allows the decomposition of a signal into individual frequency components, and establishes the relative intensity of each component with respect to frequency. The power spectrum indicates which frequencies exist in the signal and their intensities, but does not reveal when these frequencies occur. Therefore, time-frequency representations provide a characterization of a signal in terms of its joint time and frequency content. In this chapter, we introduce a new representation of the signal in terms of the frequency-frequency kernel which can be obtained from the time-frequency evolutionary kernel, or directly from the signal. Before

we get to the bi-frequency kernel, we will review in briefly about the evolutionary spectral theory and the discrete evolutionary transform DET.

2.4.1 Evolutionary Spectral Theory

According to the Wold-Cramer representation [29], a discrete-time non-stationary process $\{x(n)\}$ can be represented as the output of a casual, linear, time-varying system with impulse response $h(n,m)$, or

$$x(n) = \sum_{m=-\infty}^{n} h(n,m)e(m) \tag{2.18}$$

where $\{e(m)\}$ is a stationary, zero-mean, unit-variance white noise process. On the other hand, $\{e(m)\}$ may be expressed as a sum of sinusoids with random amplitudes and phases,

$$e(m) = \int_{-\pi}^{\pi} e^{jwm} dZ(\omega) \tag{2.19}$$

where $Z(\omega)$ is a process with orthogonal increments, i.e.,

$$E[dZ(\omega_1)dZ^*(w_2)] = \frac{1}{2\pi}\delta(\omega_1 - \omega_2)dw_1 d\omega_2 \tag{2.20}$$

By substituting Equations (2.18) into (2.19), we can express the non-stationary process $\{x(n)\}$ as

$$x(n) = \int_{-\pi}^{\pi} H(n,\omega)e^{j\omega n} dZ(\omega) \tag{2.21}$$

where

$$H(n,\omega) = \sum_{m=-\infty}^{n} h(n,m)e^{-j\omega(n-m)} \tag{2.22}$$

is the time-frequency response of the LTV system, or the so called Zadeh's generalized transfer function [21] evaluated on the unit circle. The non-stationary signal provided in Equation (2.21) can be interpreted as an infinite sum of sinusoids with time-varying random amplitudes and phases.

Using Equations (2.18) to (2.22), the variance of $x(n)$ is given by

$$E[|x(n)|^2] = \frac{1}{2\pi}\int_{-\pi}^{\pi} |H(n,\omega)|^2 d\omega \tag{2.23}$$

illustrates the distribution of the power of a non-stationary process $x(n)$ at each time n, as a function of w. The Wold-Cramer (WC) evolutionary spectrum is defined as

$$S_{WC}(n,\omega) = |H(n,\omega)|^2. \tag{2.24}$$

which shows that the time-varying power spectral density of the output is equal to the magnitude squared of the time-varying frequency response of the filter.

2.4.1.1 Evolutionary Spectral Theory Using Gabor Expansion

The Wold-Cramer representation and Priestley's evolutionary spectrum [29, 31] provide a desirable representation and a time-dependent spectrum for non-stationary random signals. The Gabor expansion has been related to the evolutionary spectrum and it was possible to define a discrete evolutionary transform that represents the signal and gives the signal spectrum [15, 16, 17, 20]. For a non-stationary deterministic signal, or a deterministic signal with a time-dependent spectrum, $x(n)$, $0 \leq n \leq N-1$, an analogous Wold-Cramer representation is possible [17]:

$$x(n) = \sum_{k=0}^{K-1} X(n, w_k) e^{jw_k n} \qquad 0 \leq n \leq N-1 \tag{2.25}$$

where $w_k = \frac{2\pi k}{K}$, K is the number of frequency samples. The inverse discrete transformation that provides the evolutionary kernel $X(n,\omega_k)$ in terms of the signal is

$$X(n,\omega_k) = \sum_{l=0}^{N-1} x(l) W_k(n,l) e^{-j\omega_k l} \qquad 0 \leq k \leq K-1 \tag{2.26}$$

where $W_k(n,l)$ is, in general, a time and frequency dependent window. The DET and its inverse are then given by Equations (2.25) and (2.26).

To obtain the evolutionary kernel, specifically the window, we consider here the Gabor signal representation that uses a non-orthogonal basis. The classical Gabor expansion represents a signal as a weighted sum of Gaussian windows shifted in time and modulated by sinusoids.

The Gabor expansion can be seen as generating a rectangular tiling in the time-frequency plane. We consider the multi-window Gabor expansion [17] that generates a non-rectangular tiling with the signal represented as

$$x(n) = \frac{1}{I}\sum_{i=0}^{I-1}\sum_{k=0}^{K-1}\sum_{m=0}^{M-1} a_{i,m,k}h_i(n-mL)e^{jw_k n} \tag{2.27}$$

where $\{a_{i,m,k}\}$ are the Gabor coefficients, $\{h_i(.)\}$ are synthesis functions obtained by scaling a Gaussian window $g(n)$ as

$$h_i(n) = 2^{i/2}g(2^i n), \qquad i = 0, 1, ..., I-1, \tag{2.28}$$

and I is the number of scaled windows. The time step L is chosen as $L < K$, which corresponds to the oversampled Gabor expansion (See Appendix A). The Gabor coefficients are obtained using analysis functions $\{\gamma_i(.)\}$ that are orthogonal to the synthesis windows, so that

$$a_{i,m,k} = \sum_{n=0}^{N-1} x(n)\gamma_i^*(n-mL)e^{-j\omega_k n} \tag{2.29}$$

Comparing Equations 2.25 and 2.27 and substituting the expression for Gabor coefficients $\{a_{i,m,k}\}$, we get

$$\begin{aligned} X(n, w_k) &= \sum_{m=0}^{M-1} a_{m,k}h_i(n-mL) \\ &= \sum_{l=0}^{N-1} x(l)W(n,l)e^{-jw_k l}, \end{aligned} \tag{2.30}$$

where $W(n,l)$ is the time-varying window defined as

$$W(n,l) = \sum_{m=0}^{M-1} \gamma^*(l-mL)h(n-mL). \tag{2.31}$$

The energy density, or the evolutionary spectrum can be calculated as

$$S(n, w_k) = \frac{1}{K}|X(n, w_k)|^2. \tag{2.32}$$

as the magnitude square of the time-frequency evolutionary kernel divided by the frequency samples K.

Thus, the magnitude of the evolutionary kernel is the energy density in the time-frequency plane and is similar to the spectrogram, or the magnitude square of the STFT.

2.4.2 Frequency-Frequency Evolutionary Spectrum

In this section we show how to extend the time-frequency evolutionary spectrum to the frequency-frequency. In situations, like the one we consider later on the modeling of a time-varying channel, a frequency-frequency representation besides the time-frequency representation is required; here we consider how to obtain it. To motivate the development of the frequency-frequency evolutionary transform, let us consider a non-stationary signal $x(n) = \sum_k A(n, w_k)e^{jw_k n}$ as the input of a linear time invariant(LTI) system with impulse response $g(n)$. The output is given by

$$\begin{aligned} y(n) &= \sum_m g(n-m)x(m) \\ &= \sum_k \left[\sum_m X(m, w_k)g(n-m)e^{-jw_k(n-m)} \right] e^{jw_k n} \end{aligned} \tag{2.33}$$

where the term in the square brackets is the DET of $y(n)$ 2.26, can be denoted as $Y(n, w_k)$, and it can be expressed as a convolution in time:

$$Y(n, w_k) = X(n, w_k) * [g(n)e^{-jw_k n}] \tag{2.34}$$

Computing the discrete Fourier transform of **??** with respect to n, we obtain

$$Y(\Omega_s, w_k) = X(\Omega_s, w_k)G(\Omega_s + w_k) \tag{2.35}$$

which establishes a relationship between the input and the system response with frequency-frequency representation. Such a relation was used in the identification of non-stationary processes [27]. The above equation in the frequency-frequency representation simplifies the computation with the time convolution.

Now, the above relation can be extended to frequency-frequency transformation by computing the discrete Fourier transform of $X(n, w_k)$ with respect to n, so that it can be calculated directly from the signal $x(n)$, or from the evolutionary kernel $X(n, w_k)$, that is

$$\begin{aligned} X(\Omega_s, w_k) &= \sum_{l=0}^{N-1} x(l) W(\Omega_s, l) e^{-jw_k l} \\ &= \sum_{l=0}^{N-1} \sum_{n=0}^{N-1} x(l) W(n, l) e^{-j(\Omega_s n + w_k l)} \\ &= \sum_{n=0}^{N-1} X(n, w_k) e^{-j\Omega_s n} \end{aligned} \tag{2.36}$$

The inverse discrete evolutionary transform IDET 2.25 process can then be obtained from the frequency-frequency representation as

$$x(n) = \sum_{k} \sum_{s} X(\Omega_s, \omega_k) e^{j(w_k + \Omega_s)n} \tag{2.37}$$

Now it is possible to calculate the frequency-frequency evolutionary spectrum in a way similar to the time-frequency evolutionary spectrum by computing the magnitude square of the frequency-frequency kernel. Doing so produces the following:

$$S(\Omega_s, \omega_k) = \frac{1}{K} |X(\Omega_s, \omega_k)|^2 \tag{2.38}$$

One advantage to the frequency-frequency representation is the compactness of the information. At the new frequency domain Ω_s all information is concentrated around the DC value, allowing for less computations since the rest of the frequency-frequency plane can be ignored as will be shown in Chapter 5. A possible disadvantage is that the time information is now in the phase of the kernel, and cannot be seen in the frequency-frequency spectrum.

As an application we have used the frequency-frequency representation in the segmentation of non-stationary signals into locally stationary parts, and estimated their bandwidth by calculating the width function defined to measures the slowly time-varying processes. From that we obtained the characteristic width, defined as the interval at which the process was treated approximately stationary.

Example : In this example, we illustrate the time-frequency and frequency-frequency spectrum of a sinusoidal signal that is composed of two segments with a different frequency for each segment, defined as

$$x(n) = \begin{cases} exp(j0.5\pi n), & 0 \leq n \leq \frac{N}{2} - 1 \\ exp(j0.2\pi n), & \frac{N}{2} \leq n \leq N - 1 \end{cases}$$

with each segment having a length of M=64 samples. The length of the total signal is $N = 128$ samples and is equal to the length of the multi-scale Gabor window. The time-frequency and frequency-frequency spectra are shown in Figures 7 and 8 respectively.

Clearly the frequency-frequency spectrum is the Fourier transform of the time-frequency kernel with respect to time n as explained earlier. We notice that the output appears as large peaks located at low frequencies in the $frequency - \Omega$ domain, thus satisfying the slow-varying condition imposed on the evolutionary spectrum, and have original frequency values $\frac{\pi}{5}$ and $\frac{\pi}{2}$ in the $frequency - \omega$ domain.

2.5 SUMMARY

This chapter provides a review on the DSSS communication systems and the LTV channels considered in mobile communications. The multipath channel fading phenomenon was explained and its challenge in mobile communication was emphasized. The LTV-channel system functions were introduced with their relation. A bi-frequency representation of the signal has been introduced. This representation can be obtained from the time-frequency kernel, or from the signal directly using Gabor windows. The spectrum of this kernel depicts significant values around the dc value, $\Omega_s = 0$ and the corresponding frequency values ω_k. It compacts this information in a small region, which is a computational advantage in certain cases as can be shown in Chapter 6.

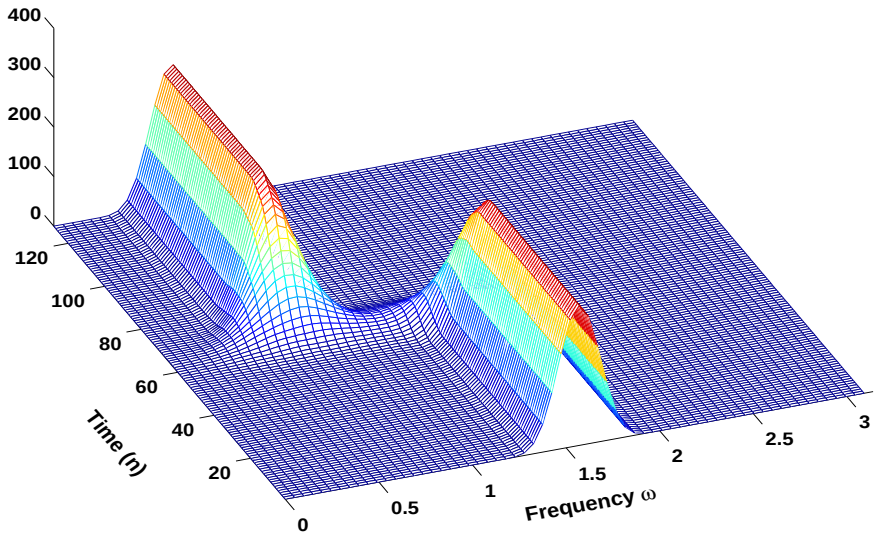

Figure 7: Time-frequency evolutionary spectrum.

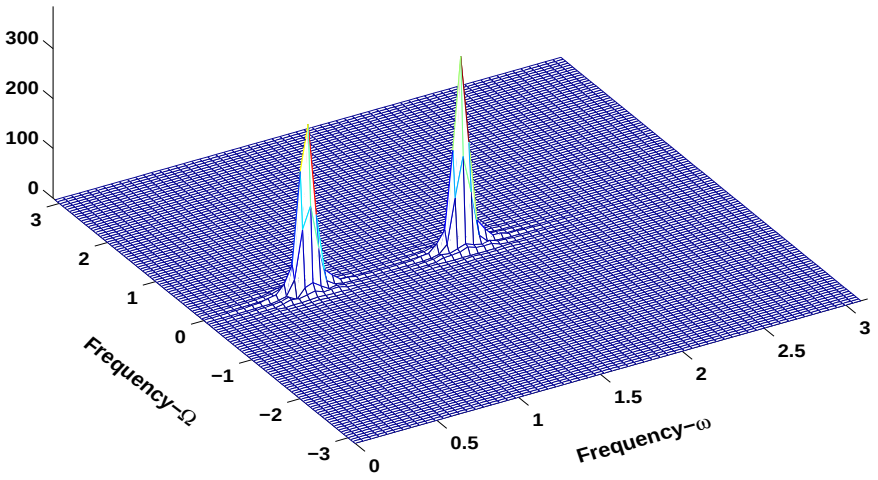

Figure 8: Frequency-frequency evolutionary spectrum.

3.0 SINGLE-USER CHANNEL MODELING AND ESTIMATION

Multi-path channel modeling and estimation pose a significant challenge in wireless communications. Because multi-path and Doppler effects in transmission channels spread the DSSS transmitted signal in both time and frequency, the channel models need to be random and time-varying which are difficult to deal with. Furthermore, blind estimation is needed using the only available data which are the received signal and the pseudo noise sequences at the receiver. In our estimation approach, we consider deterministic linear time-varying channel models with parameters that change randomly and our aim is to estimate such parameters. In this chapter we limit our discussion to a single user multipath channel.

In modeling and characterization of LTV channels, a discrete model is used. Therefore, if the system has $g(n, m)$ as its discrete impulse response, then its corresponding discrete time-varying frequency response, or Zadeh's function, is

$$G(n, \omega_k) = \sum_k g(n, m) e^{-j\omega_k m} \tag{3.1}$$

or the Fourier transform of $g(n, m)$ with respect to the delay variable k. The bifrequency function is then found by computing the Fourier transform of $G(n, \omega_k)$ with respect to n giving

$$B(\Omega_s, \omega_k) = \sum_n G(n, \omega_k) e^{-j\Omega_s n}. \tag{3.2}$$

Finally, the spreading function is the inverse Fourier transform of $B(\Omega_s, \omega_k)$ with respect to ω_k, or equivalently the Fourier transform of the impulse response function $g(n, m)$ with respect to the time variable n,

$$S(\Omega_s, k) = \sum_n g(n, m) e^{-j\Omega_s n}. \tag{3.3}$$

The evolutionary time-frequency kernel of the received signal is used to estimate the spreading function $S(\Omega_s, k)$ from which the channel parameters can be estimated. Based on this model, we will also describe in detail how the time-frequency evolutionary kernel of received multipath signal can be computed, and hence used to obtain the time-varying frequency response of the multipath channel. Once the time-varying frequency response is obtained, computing the spreading function is possible using the relation of the above channel system functions.

3.1 MULTIPATH CHANNEL MODELING

The baseband DSSS multipath transmission channel model is depicted in Fig. 9, where each path is considered an all-pass filter with an impulse response $\{h_\ell(n)\}$ characterizing the delay, and the functions $\{f_\ell(n)\}$ are the modulators that generate the frequency shift, or Doppler effect. The channel parameter $\{\alpha_\ell(n)\}$ is the attenuation factor, or the gain of the ℓ^{th} propagation path as a function of time. The impulse response of each path can be defined as

$$h_\ell(n) = \delta(n - N_\ell) \tag{3.4}$$

where N_ℓ is an integer delay representing the time difference between the first arrival signal and the signals that come through various paths due to reflection, scattering, and diffraction in the transmission channel. The Doppler shifts can be characterized by exponentials that modulate the delayed signals,

$$f_\ell(n) = e^{j\psi_\ell n}. \tag{3.5}$$

Using the time delays, Doppler shifts, and gain factors characterizations, the overall impulse response of the multipath channel can be written as

$$g(n, m) = \sum_{\ell=0}^{L(n)-1} \alpha_\ell(n)\delta(m - N_\ell(n))e^{j\psi_\ell(n)n}. \tag{3.6}$$

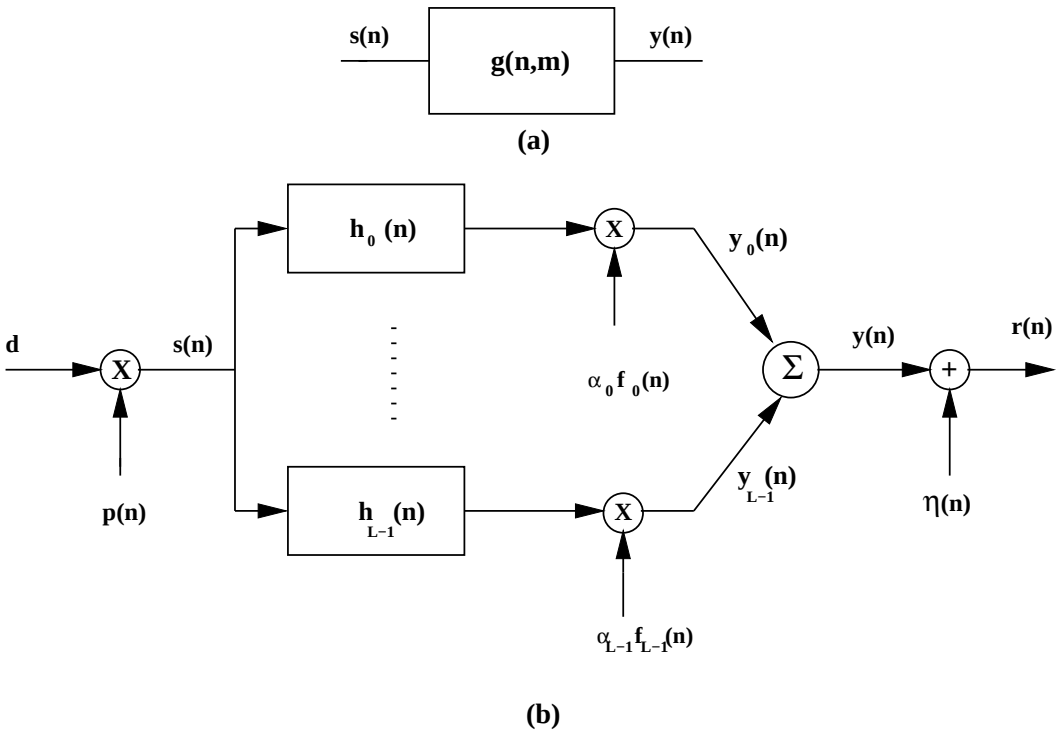

Figure 9: LTV channel model: a) System model, b) Baseband channel model

Assuming that the channel is almost constant during the transmission of a single data symbol, the channel model will then reduce to

$$g(n,m) = \sum_{l=0}^{L-1} \alpha_\ell e^{j\psi_\ell n} \delta(m - N_\ell) \tag{3.7}$$

as the number of paths L, path gain $\{\alpha_\ell(n)\}$, the delays $\{N_\ell(n)\}$ and the Doppler shifts $\{\psi_\ell(n)\}$ do not change during the small period of time equal to the time period of the transmitted bit, or the pseudo-noise signal.

The randomness of the channel appears as the model parameters, after one or more frames, obtain new values in an arbitrary fashion.

Under the above assumptions, the output signal $y(n)$ is given by

$$y(n) = \sum_{l=0}^{L-1} \alpha_\ell s(n - N_\ell) e^{j\psi_\ell n} \tag{3.8}$$

where $s(n) = dp(n)$ and $d = \pm 1$. The received signal for the corresponding bit d is given by

$$r(n) = y(n) + \eta(n) \tag{3.9}$$

where $\eta(n)$ is the interference signal due to channel noise and any possible interference in the medium.

To find the frequency response of the model we consider for simplicity $d = 1$, so that $s(n) = p(n)$ and is represented by its Fourier representation

$$p(n) = \frac{1}{2\pi} \int_{-\pi}^{\pi} P(\omega) e^{j\omega n} d\omega \tag{3.10}$$

If we replace Equations (3.10) into (3.8), we get

$$\begin{aligned} y(n) &= \frac{1}{2\pi} \sum_{\ell=0}^{L-1} \alpha_\ell e^{j\psi_\ell n} \int_{-\pi}^{\pi} P(\omega) e^{j\omega(n-N_\ell)} d\omega \\ &= \frac{1}{2\pi} \int_{-\pi}^{\pi} P(\omega) \sum_{\ell=0}^{L-1} \alpha_\ell e^{j\psi_\ell n} e^{-j\omega N_\ell} e^{j\omega n} d\omega \end{aligned} \tag{3.11}$$

or the equivalent response to $p(n)$ as an infinite sum of weighted exponentials

$$y(n) = \frac{1}{2\pi} \int_{-\pi}^{\pi} P(\omega) G(n, \omega) e^{j\omega n} d\omega \tag{3.12}$$

where $G(n, \omega)$ is the frequency response of the LTV system, which is given by the following equation after comparing (3.12) and (3.11)

$$G(n, \omega) = \sum_{\ell=0}^{L-1} \alpha_\ell e^{j\psi_\ell n} e^{-j\omega N_\ell} \tag{3.13}$$

which can be seen as the Fourier transform of the separable impulse response $g(n, m)$ given earlier.

Now, the bifrequency function $B(\Omega, \omega)$ is found by computing the discrete-time Fourier transform of $G(n, \omega_k)$ with respect to the n variable:

$$B(\Omega, \omega) = 2\pi \sum_{\ell=0}^{L-1} \alpha_\ell e^{-j\omega N_\ell} \delta(\Omega - \psi_\ell) \tag{3.14}$$

Finding the inverse discrete-time Fourier transform of $B(\Omega,\omega)$ with respect to ω we find that the spreading function is given by

$$S(\Omega,k)=2\pi\sum_{\ell=0}^{L-1}\alpha_\ell\delta(\Omega-\psi_\ell)\delta(k-N_\ell) \tag{3.15}$$

which displays peaks located at the delays and the corresponding Doppler frequencies, and with α_ℓ as their amplitudes. To express the above functions in the discrete domain and to relate them to the evolutionary kernels, assume that $s(n)$ has a support $0\leq n\leq M_p-1$, where M_p is the pseudo-noise length, y(n) can be obtained by replacing the discrete Fourier representation of $p(n)=\frac{1}{M_p}\sum_{k=0}^{M_p-1}P(k)e^{j\omega_k n}$:

$$\begin{aligned} y(n) &= \frac{1}{M_p}\sum_{k=0}^{M_p-1}P(k)\left[\sum_{\ell=0}^{L-1}d\alpha_\ell e^{j\psi_\ell n}e^{-j\omega_k N_\ell}\right]e^{j\omega_k n} \\ &= \sum_{k=0}^{M_p-1}Y(n,\omega_k)e^{j\omega_k n} \end{aligned} \tag{3.16}$$

where $\omega_k=\frac{2\pi k}{M_p}$, the Zadeh's time-varying frequency response $G(n,\omega_k)$ is the term in the square brackets and $Y(n,\omega_k)$ is the time-frequency evolutionary kernel. Thus we have that

$$\begin{aligned} G(n,\omega_k) &= \sum_{\ell=0}^{L-1}d\alpha_\ell e^{j\psi_\ell n}e^{-j\omega_k N_\ell} \\ &= \frac{M_pY(n,\omega_k)}{dP(k)}. \end{aligned} \tag{3.17}$$

The bi-frequency function $B(\Omega_s,\omega_k)$ is then found to be

$$\begin{aligned} B(\Omega_s,\omega_k) &= \frac{1}{M_p}\sum_{\ell=0}^{L-1}d\alpha_\ell\delta(\Omega_s-\psi_\ell)e^{-j\omega_k N_\ell} \\ &= \frac{M_pY(\Omega_s,\omega_k)}{dP(k)}, \end{aligned} \tag{3.18}$$

where $Y(\Omega_s,\omega_k)$ is the frequency-frequency evolutionary kernel of $y(n)$. Finally, the spreading function is given by

$$\begin{aligned} S(\Omega_s,k) &= \sum_{\ell=0}^{L-1}\alpha_\ell\delta(\Omega-\psi_\ell)\delta(k-N_\ell) \\ &= \mathcal{F}^{-1}_{\omega_k}\left[\frac{M_pY(\Omega_s,\omega_k)}{dP(k)}\right] \end{aligned} \tag{3.19}$$

which displays peaks of amplitude α_ℓ at the values of the delays and their corresponding Doppler shifts. If we extract this information from the received signal, we should then be able to figure out what d was. Furthermore, it is of interest to note that the above functions are related to the evolutionary time-frequency and frequency-frequency kernels. Such relations will be used in the estimation of the spreading function and in the development of fast algorithms to compute it.

3.1.1 General Model

In this section we will consider the general model which is similar to the baseband model shown in Fig. 9, except that it must include the carrier signal $e^{j\omega_c n}$ for modulation at the transmitter and its inverse $e^{-j\omega_c n}$ for demodulation at the receiver.

When the receiver, or channel objects are moving, the carrier frequency of multipath signals are shifted due to this movement, and new frequency values are obtained at the output shifted from the original frequency by an amount equal to the Doppler shifts. Therefore, the frequency of a received signal can be defined in terms of Doppler shift and the carrier frequency as

$$\omega_\ell = \omega_c + \psi_\ell \tag{3.20}$$

where ω_c is the carrier frequency and ψ_ℓ is the Doppler shift.

At the transmitter, the binary data is spread by the pseudo-noise sequence to have $dp(n)$, and then multiplied or modulated by the carrier signal producing the final transmitted signal

$$s(n) = dp(n)e^{j\omega_c n} \tag{3.21}$$

and therefore the noiseless received signal is given by

$$\begin{aligned} y(n) &= \sum_{\ell=0}^{L-1} d\alpha_l s(n - N_\ell) e^{j\psi_\ell n} \\ &= \sum_{\ell=0}^{L-1} d\alpha_\ell p(n - N_\ell) e^{j(\omega_c+\psi_\ell)n} e^{-j\omega_c N_\ell} \end{aligned} \tag{3.22}$$

Similar to the baseband model, to find the frequency response of the channel we replace $p(n)$ by its inverse discrete Fourier representation, and get

$$\begin{aligned} y(n) &= \sum_{k=0}^{M_p-1} \frac{P(k)}{M_p} \left[\sum_{\ell=0}^{L-1} d\alpha_\ell e^{j(\omega_c+\psi_\ell)n} e^{-j(\omega_c+\omega_k)N_\ell} \right] e^{j\omega_k n} \\ &= \sum_{k=0}^{M_p-1} Y(n, \omega_c+\omega_k) e^{j(\omega_c+\omega_k)n} \end{aligned} \tag{3.23}$$

where the term inside the square brackets is Zadeh's time-varying response $G(n, \omega_c + \omega_k)$ and $Y(n, \omega_c + \omega_k) = \sum_\ell Y_\ell(n, \omega_c + \omega_k)$ is the time-frequency evolutionary of $y(n)$, and

$$Y_\ell(n, \omega_c + \omega_k) = \frac{1}{M_p} P(k) d\alpha_\ell e^{j(\omega_c+\psi_\ell)n} e^{-j(\omega_c+\omega_k)N_\ell} \tag{3.24}$$

Letting $\omega_k^{'} = \omega_c + \omega_k$, the Zadeh's function $G(n, \omega_k^{'})$ can be expressed in terms of the evolutionary kernel as

$$\begin{aligned} G(n, \omega_k^{'}) &= \sum_{\ell=0}^{L-1} d\alpha_\ell e^{j(\omega_c+\psi_\ell)n} e^{-j(\omega_c+\omega_k)N_\ell} \\ &= \sum_{\ell=0}^{L-1} \frac{M_p}{dP(k)} Y_\ell(n, \omega_k^{'}) \\ &= \frac{M_p}{dP(k)} Y(n, \omega_k^{'}) \end{aligned} \tag{3.25}$$

Taking the discrete-time Fourier transform of the Zadeh's transfer function $G(n, k)$ with respect to n gives the bifrequency function

$$\begin{aligned} B(\Omega_s, \omega_k^{'}) &= \frac{1}{M_p} \sum_{\ell=0}^{L-1} d\alpha_\ell \delta(\Omega_s - \omega_\ell) e^{-j\omega_k N_\ell} e^{-j\omega_c N_\ell} \\ &= \frac{M_p Y(\Omega_s, \omega_k^{'})}{dP(k)}, \end{aligned} \tag{3.26}$$

where $Y(\Omega_s, \omega_{k'})$ is the frequency-frequency kernel of $y(n)$. Finally, finding the inverse Fourier transform of $B(\Omega_s, \omega_{k'})$ with respect to the frequency variable $\omega_{k'}$ we obtain the spreading function $S(\Omega_s, k^{'})$. There equations are similar to the ones for baseband model, so we only need to consider the baseband case.

3.2 SPREADING FUNCTION ESTIMATION VIA TIME-FREQUENCY EVOLUTIONARY KERNEL

In the last section we illustrated how modeling DSSS multipath channels provides the time-frequency representation of the channel. Now based on the above modeling of the channel, we consider estimating these functions blindly from the received signal in order to obtain estimates of the channel parameters. Both baseband and general models will be used for the parameter estimation.

Let us consider first the baseband model, where the output noiseless combined signal is $y(n)$, and is defined in (3.16). This signal can be considered as a non-stationary signal of length N, that can be represented in terms of either its time-frequency kernel $Y(n, \omega_k)$, or its corresponding bifrequency kernel $Y(\Omega_s, \omega_k)$. To compute the discrete evolutionary kernel, we need to consider what would be an appropriate function $V(m, n)$. Consider a noiseless multipath channel so that $y(n) = r(n)$, a non-stationary signal, of length M_p, that can be represented in terms of a time-frequency evolutionary or frequency-frequency kernels $Y(n, \omega_k)$ and $Y(\Omega_s, \omega_k)$. The discrete evolutionary transform (DET) and its inverse provide the following representations

$$\begin{aligned} Y(n, \omega_k) &= \frac{1}{M_p} \sum_m y(m) V_k(m, n) e^{-j\omega_k m} \\ y(n) &= \sum_k Y(n, \omega_k) e^{j\omega_k n}, \end{aligned} \tag{3.27}$$

where $V_k(m, n)$ is a frequency and time-varying window that can be obtained from the Gabor or the Malvar representation of $y(n)$ [20].

For the kernel $Y(n, \omega_k)$, computed from $y(n)$, to coincide with that in (3.16) an appropriate window $V(m, n)$ is needed. The conventional Gabor- or Malvar–based windows are not appropriate, and rather an adaptive function $V_q(m, n) = e^{j\omega_q(n-m)}$ needs to be used. In fact, when we replace $y(n)$ in (3.27) into the equation for the time-frequency evolutionary

kernel and introduce $V_q(m,n) = e^{j\omega_q(n-m)}$ we get

$$\begin{aligned} Y_q(n,\omega_k) &= \frac{1}{M_p}\sum_{s,\ell} d\alpha_\ell P(s) e^{-j\omega_s N_\ell} \\ &\quad \times \sum_{m=0}^{M_p-1} V_q(m,n) e^{j(\psi_\ell+\omega_s-\omega_k)m}, \end{aligned} \tag{3.28}$$

when $\omega_q = \psi_\ell$, the last term of the above equation gives

$$e^{j\psi_\ell n}\sum_{m=0}^{M_p-1} e^{j\frac{2\pi}{N}(s-k)m} = M_p e^{j\psi_\ell n}\delta(s-k),$$

Replacing this term back in equation (3.28) gives

$$Y_{\psi_\ell}(n,\omega_k) = \sum_{\ell=0}^{L-1} d\alpha_\ell P(k) e^{j(\psi_\ell n - \omega_k N_\ell)}, \tag{3.29}$$

which is $M_p Y(n,\omega_k)$ as in equation (3.16). If the frequency in $V_q(.)$ does not coincide with one of the Doppler frequencies, the result

$$Y_q(n,\omega_k) = \frac{1}{M_p}\sum_{s,\ell,m} \alpha_\ell P(s) e^{-j\omega_s N_\ell} e^{j\omega_q(n-m)} e^{j(\omega_\ell+\omega_s-\omega_k)m} \tag{3.30}$$

is a noise-like sequence and is completely different from the expected result. Once we can compute $Y(n,\omega_k)$, it is then possible to find the bifrequency and the spreading functions as indicated before.

Since the Doppler frequencies are not known, to implement the computation of $Y(n,\omega_k)$ and then the spreading function, we consider $V_q(m,n) = e^{j\omega_q(n-m)}$, where $0 \leq \omega_q \leq \pi$. When ω_q coincides with one of the Doppler frequencies, the spreading function displays a large peak at the corresponding delay and Doppler frequency. For those frequencies ω_q not equal to a Doppler frequency, the spreading function displays a random sequence of peaks spread over all possible delays. We then determine a threshold that allows us to obtain the most significant peaks of the spreading function corresponding to possible delays and Doppler frequencies.

For determining the desired peaks from the spreading function, we consider the ratio of the maximum value of the largest peak at each frequency in Doppler frequency domain and the mean value of all peaks in the time-delay domain

$$T_{\Omega_s} = \frac{max_k|(S(\Omega_s, k))|}{\frac{1}{M_p}\sum_{k=0}^{M_p-1}|S(\Omega_s, k)|} \tag{3.31}$$

as a decision parameter determining candidate peaks. Thus, when the window frequency coincides with any of the Doppler shift, a large peak will appear at that frequency ψ_ℓ as well as the corresponding time delay N_ℓ, and the ratio T_{Ω_s} explained above will determine if the peak at that location is a candidate peak. Repeating the same procedure for all possible frequencies provides all candidate peaks for the desired communication channel. From the experimental part we found that a good value for the decision parameter approximately is $T_{\Omega_s} \geq 2.5$ in order to separate and locate the desired peaks.

Finally, the attenuation values $\{\alpha_\ell\}$ can be estimated by considering the spreading function that matches the corresponding Doppler frequency. For instance, when there is a unique Doppler frequency ψ_q, the spreading function as computed using the evolutionary transform will be of the form

$$S_q(\Omega_s, k) \approx (M_p - N_q)\alpha_q\delta(\Omega - \omega_q)\delta(k - N_q) \tag{3.32}$$

so that finding its peak and dividing by the factor $M_p - N_q$ provides α_q. In the noisy cases, the above computations will be affected, but in general they can be done in a similar way.

In the following examples, we will illustrate our estimation approach as seen from both models with different channels parameters.

Example1 : In this example We consider a multipath channel (base-band) with a total number of paths $L = 4$. The received signal therefore will be composed of 4 signals having different time-delays N_ℓ, frequency Dopplers ψ_ℓ, and attenuation factors α_ℓ. We chose the original time delays of 0, 20, 40, and 80 samples with corresponding Doppler frequencies of $0.2\pi, 0.4\pi, 0.6\pi$, and 0.2π. The estimated spreading function obtained from the DET evolutionary kernel using the special window $V(m, n)$ provides the channel parameters as large peaks at frequencies that coincide with the Doppler frequencies corresponding to time

delays in the frequency-time plane. Figure 10-(a) shows the spreading function displaying a large peak at Doppler frequency 0.4π and a delay of 20 samples as expected, while Fig. 10-(b) shows the spreading function at a frequency that does not coincide with the Doppler frequency, displaying random peaks all over the time-delay domain. Using the proposed decision rule provides the desired peaks. When the frequency in use coincides with the Doppler frequency, the above ratio changes significantly from a case when they do not coincide. The thresholded spreading function obtained is shown in Fig. 10-(c). From these peaks, it was possible to compute the time delays N_ℓ, the associated Doppler frequencies ψ_ℓ, and an estimate of the attenuation factors $\hat{\alpha}_\ell$. Table 1 shows the values of estimated channel parameters along with the original values.

Example2 : In this example, We consider the general multipath channel model of 3 paths. The received signal is composed of 3 signals of different time-delays N_ℓ, frequency shifts $\omega_\ell = \omega_c + \psi_\ell$, and attenuation factors α_ℓ. The carrier frequency $\omega_c = \pi/2$ and has been shifted due to the Doppler effects to give a shifted version of the original carrier frequency. The spreading function corresponding to one path is shown in Fig. 11-(a), which displays a peak at the frequency $\omega_\ell = 0.5\pi$ with Doppler shift ($\psi_\ell = 0$). The final thresholded spreading function for this multipath channel is depicted in Fig. 11-(b) displaying three peaks corresponding to the three path signals. The estimated and original values are shown in Table 2.

Example3 : We consider in this example the general model as illustrated in example 2, but for the case of zero-Doppler in a multipath transmission channel. The initial spreading function is depicted in Fig. 12-(a), which displays three peaks at three different time-delays corresponding to the carrier frequency, since each multipath signals have zero Dopplers $\psi_\ell = 0$ or $\omega_\ell = \omega_c$. The thresholded spreading function is shown in Fig. 12-(b). The estimated values are shown in Table 3.

Table 1: Original and estimated values of the mulitpath channel parameters (example 1).

	Delay (samples)				**Amplitude (attenuation)**				**Frequency shifts (Doppler)**			
	τ_1	τ_2	τ_3	τ_4	α_1	α_2	α_3	α_4	ψ_1	ψ_2	ψ_3	ψ_4
Simulated	**2**	**20**	**40**	**80**	**1.0**	**0.8**	**0.6**	**0.4**	$0.2\,\pi$	$0.4\,\pi$	$0.6\,\pi$	$0.2\,\pi$
Estimated	**2**	**20**	**40**	**80**	**0.9850**	**0.7811**	**0.5881**	**0.4012**	$0.2\,\pi$	$0.4\,\pi$	$0.6\,\pi$	$0.2\,\pi$

Table 2: Original and estimated values of the mulitpath channel parameters (example 2).

	Delay (samples)			**Amplitude (attenuation)**			**Frequency shifts (Doppler)**		
	τ_1	τ_2	τ_3	α_1	α_2	α_3	ψ_1	ψ_2	ψ_3
Simulated	**1**	**27**	**43**	**1.0**	**0.8**	**0.7**	0.03π	**0**	$-0.02\,\pi$
Estimated	**1**	**27**	**43**	**0.9850**	**0.7911**	**0.6881**	0.03π	**0**	$-0.02\,\pi$

Table 3: Original and estimated values of the mulitpath channel parameters (example 3).

	Delay (samples)			**Amplitude (attenuation)**			**Frequency shifts (Doppler)**		
	τ_1	τ_2	τ_3	α_1	α_2	α_3	ψ_1	ψ_2	ψ_3
Simulated	**1**	**14**	**23**	**1.0**	**0.9**	**0.63**	**0**	**0**	**0**
Estimated	**1**	**14**	**23**	**0.9950**	**0.8911**	**0.6281**	**0**	**0**	**0**

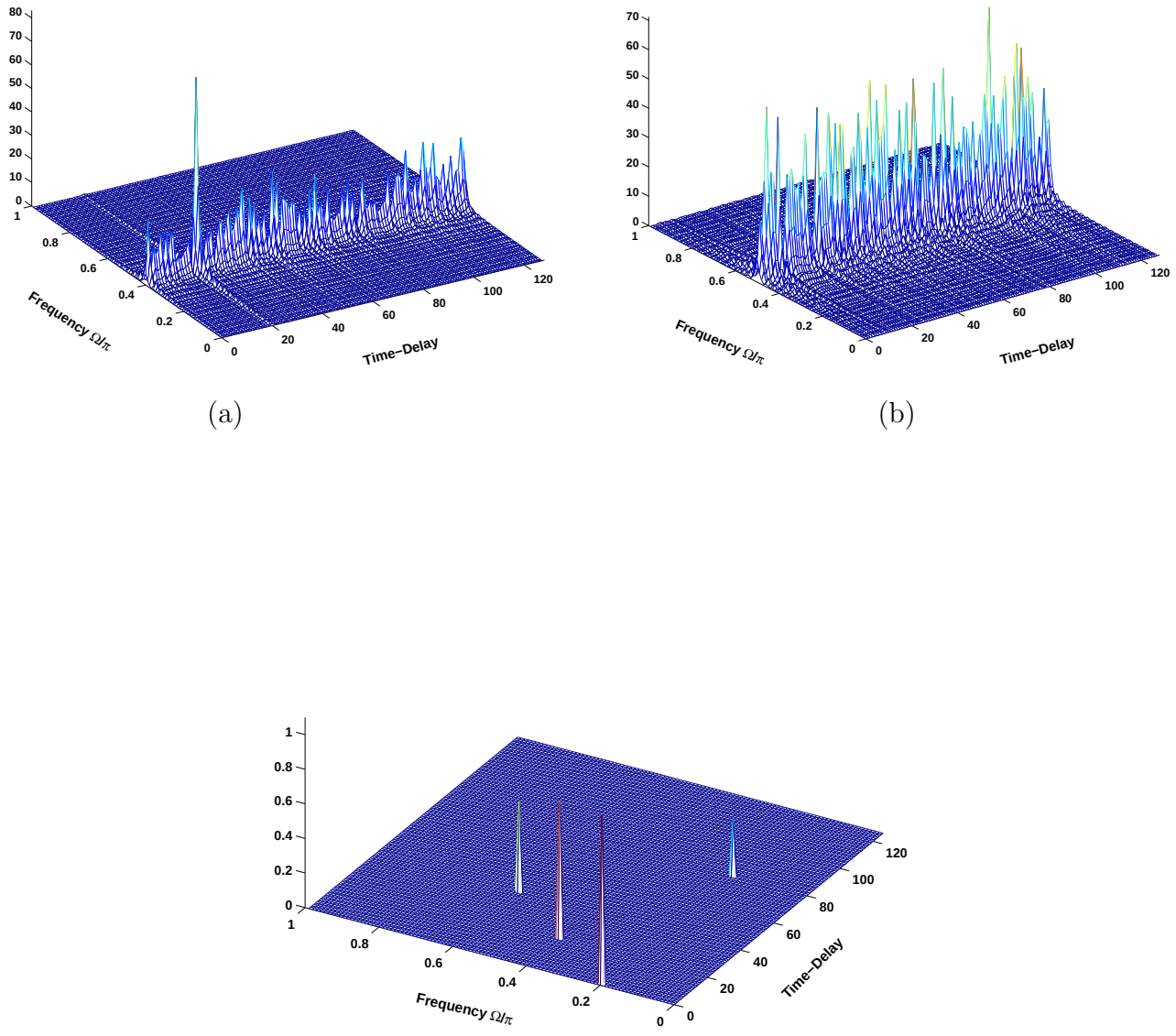

(a) (b)

(c)

Figure 10: Example 1: (a) SF at $\psi = 0.4\pi$, (b) SF at $\psi = 0.5\pi$, and (c) Final SF.

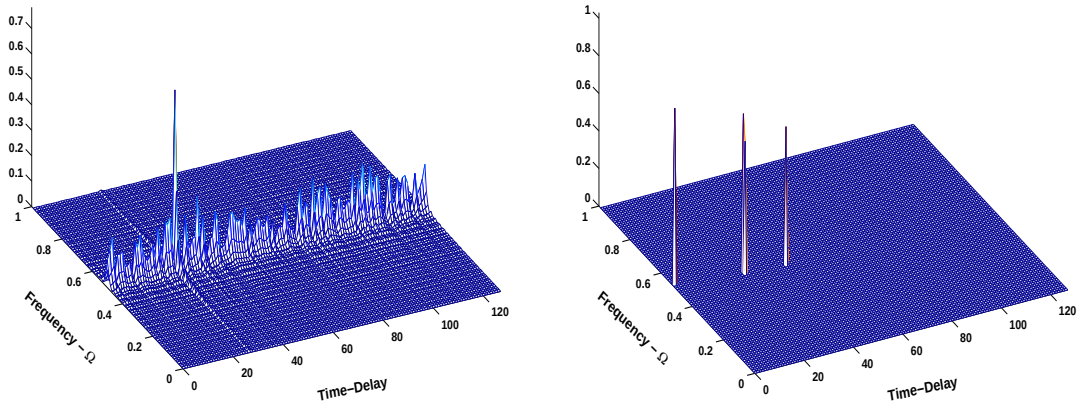

(a) (b)

Figure 11: Example 2: (a) SF for single path,(b) Final thresholded SF.

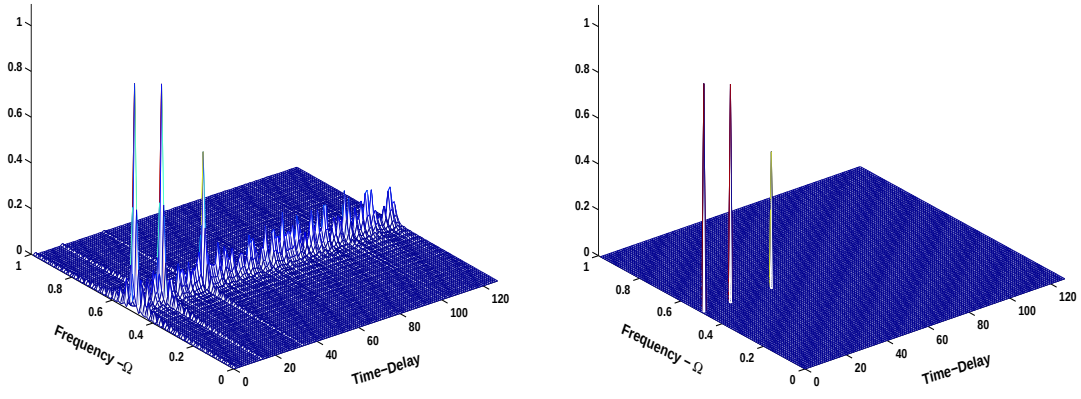

(a) (b)

Figure 12: Example 3: (a) Spreading function, (b) Final thresholded spreading function.

3.3 BIT DETECTION

In general, the DSSS receiver uses a locally generated replica of the pseudo-noise signal at the receiver to separate multiple signals. By cross correlation, the coded information can be obtained and interference suppressed. The multiple access advantage at the DSSS provides reducing the effect of interference due to jamming, multiuser interference, and self interference due to multipath propagations. In CDMA, to further reduce multipath effects, a RAKE receiver is usually employed, exploiting multipath diversity by combining at the receiver as many of the multipath signals as possible in a constructive way, which is done through a bank of correlators. The proposed receiver is a channel estimation based were the estimated channel parameters are used in a constructive way to detect the binary information bit.

3.3.1 Conventional Receiver

For this receiver, we would like to consider the signal component closest to the signal that has the smallest delay and the largest possible gain α to determine the value of d, or commonly known as the the line of sight (LOS) signal. At first, the receiver performs the channel estimation and computes the spreading function, which consists of the channel parameters as explained in the previous chapter.

Based on the baseband model, the combined received signal $r(n)$ that comes from various paths is

$$\begin{aligned} r(n) &= \sum_{\ell=0}^{L-1} y_\ell(n) + \mu(n) \\ &= \sum_{\ell=1}^{L-1} \alpha_\ell dp(n - N_\ell) e^{j\psi_\ell n} + \mu(n) \end{aligned} \tag{3.33}$$

where $\mu(n)$ is the channel noise. Now it is possible to despread the received signal by the shifted version of the pesudo-noise $p(n - N)$ with a shift equal to the shortest estimated

delay $N = \hat{N}_0$. The output despreaded signal is

$$\begin{aligned} r_0(n) &= r(n)p(n-\hat{N}_0) \\ &= p(n-\hat{N}_0)\left[\sum_{\ell=0}^{L-1} dp(n-N_\ell)\alpha_\ell e^{j\psi_\ell} + \mu(n)\right] \\ &= d\alpha_0 e^{j\psi_0 n} + \alpha_\ell dp(n-N_1)p(n-\hat{N}_0)e^{j\psi_1 n} \\ &\quad + ... + \alpha_{L-1}dp(n-N_{L-1})p(n-\hat{N}_0)e^{j\psi_{L-1}n} + p(n-\hat{N}_0)\mu(n). \end{aligned} \tag{3.34}$$

Demodulating and scaling the signal $r_o(n)$ with $e^{-j\psi_o n}/\alpha_0$, we get

$$\begin{aligned} \rho(n) &= d(n) + \left[\sum_{\ell=1}^{L-1} dp(n-N_\ell)e^{j(\psi_\ell - \hat{\psi}_o)n} + \mu(n)\right] p(n-\hat{N}_0)(1/\hat{\alpha}_0) \\ &= d(n) + \eta(n) \end{aligned} \tag{3.35}$$

where

$$\eta(n) = \left[\sum_{\ell=1}^{L-1} \alpha_\ell e^{j\psi_\ell n} dp(n-N_\ell) + \mu(n)\right] \frac{p(n-\hat{N}_0)e^{-j\hat{\psi}_0 n}}{\hat{\alpha}_0} \tag{3.36}$$

is noise-like term due to nonorthogonality between the shifted replicas of PN.

Given the pseudo noise nature of $p(n)$, and assuming it is uncorrelated with the noisy term $\mu(n)$, the expected value of $\rho(n)$ gives $E[\rho(n)] = d$, and using a short-term average we obtain an estimate of d.

We notice that this approach requires obtaining the channel parameters estimate of the first arrival signal in order to construct the desired receiver. Thus, our channel estimation approach used the information obtained from the estimated spreading function $S(\Omega, k)$, and repeats for all data bits. A complete structure of this receiver is shown in Fig. 13, which includes both estimation and detection. Figure 14 shows the estimated signal $\rho(n)$ obtained from information of the first arrival peak in the spreading function corresponding to the first arrival signal or simply the first path. We should mention here that the received signal is composed of 3 multiple signals with different delays, attenuations, and frequency shifts, and is transmitted in a noisy channel with an equivalent signal to noise ratio dB. The mean value of the estimated signal $\rho(n)$ gives 0.943, which means that the transmitted binary bit is $d = +1$.

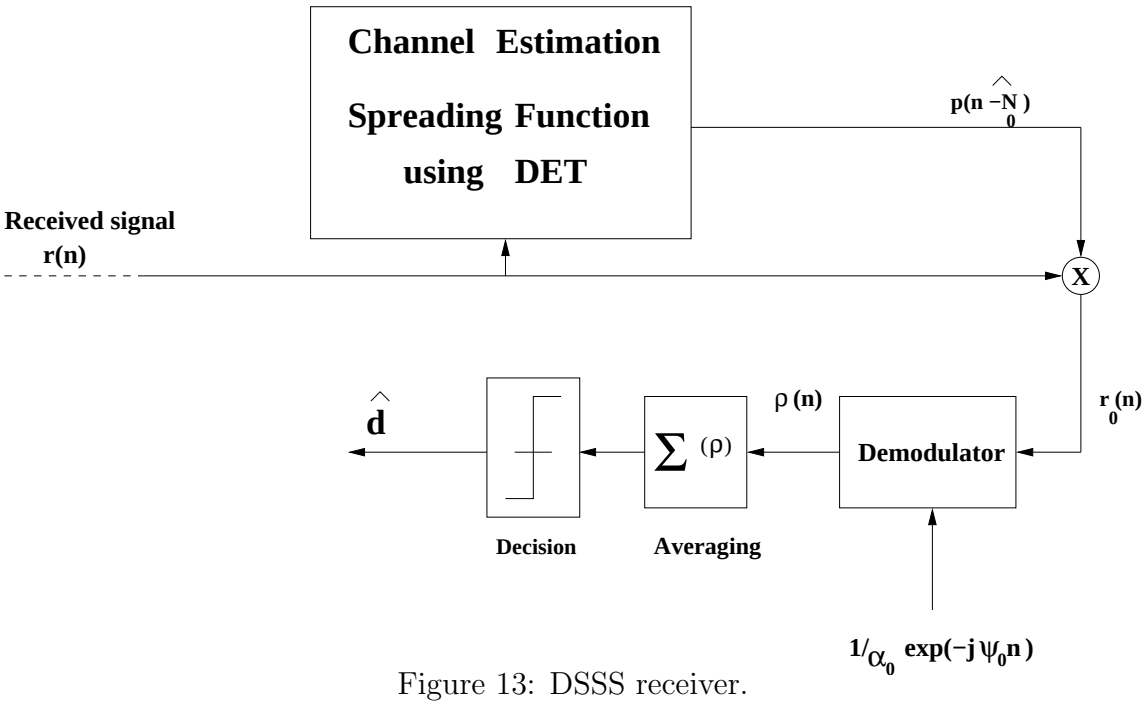

Figure 13: DSSS receiver.

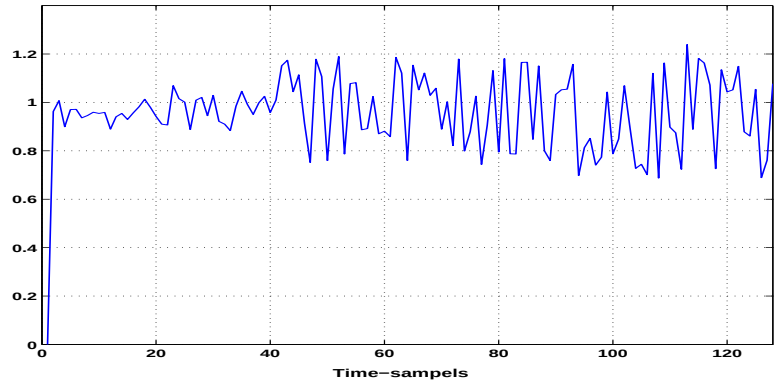

Figure 14: Demodulated, despreaded, and scaled signal $\rho(n)$ at the receiver

3.4 DOPPLER EFFECT

Doppler shifts are caused by changes in the carrier frequency due to the movement of the receiver, or moving objects in the communication channel. They negatively impact the detection of the correct transmitted information bits causing an increase in the bit error rate (BER). It is required to know these frequency shifts or Dopplers at the receiver, and then compensate for them in order to reduce the BER. The simulation at the end of Chapter 5 illustrates these effects by means of bit error rate.

Furthermore, to show this effect it is important to examine a simple case where the carrier frequency varies around a nominal frequency $\omega_c = \pi/2$ of the transmitted signal,

$$s(n) = dp(n)e^{j\omega_c n} \tag{3.37}$$

where p(n) is the pseudo-noise sequence, and d is the transmitted binary data and equals to $+1$. The channel in this case produces Doppler shifts ψ that have a different value at each transmission.

Under the assumption of perfect synchronization, the received signal is then demodulated and despreaded by a replica of pseudo-noise $p(n)$ at the receiver in order to recover or detect the binary data d. The demodulated and despreaded signal is

$$y(n) = dp(n)e^{j(\omega_c+\psi)n}p(n)e^{-j\omega_c n} \tag{3.38}$$

where for simplicity the channel noise has been neglected, and since $p(n)^2 = 1$, the final despread signal is

$$y(n) = de^{j\psi n} \tag{3.39}$$

Now, consider repeating the transmission for the same data bit $d = +1$ at different Doppler shifts, ψ_m, ($0.005\,\omega_c$ to $0.02\,\omega_c$), for $m = 1, 2, ..., 11$. At the output, the demodulated and despreaded signal $\hat{y}_m(n)$ is different for each transmission, and the average value of $\hat{y_m}(n)$ will decrease as the ψ_m increases. Notice here that the channel noise and multipath effects will affect the averaging and hence increase the probability of getting an error for the detected bit.

Figure 15 illustrates the output results of this example where the mean value of $\hat{y}(n)$ as the estimated data d_m decreases as the Doppler frequency shift increases and becomes totally dependent upon it. Thus, ignoring Doppler effects at the receiver increases the bit error rate BER as can be seen from the simple case result shown in Figure 15 and the simulation output shown in Figure 19.

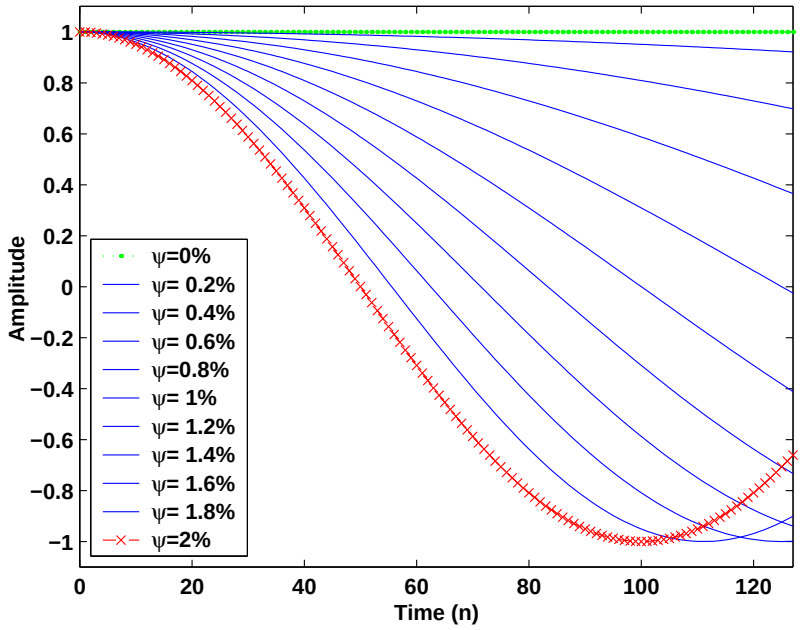

Figure 15: Real value of the despread and demodulated output signal at different Doppler shifts ψ_m defined as percentage changes of the carrier frequency ω_c

3.5 COMPUTATIONAL ASPECTS

In this section we will address two aspects regarding the reduction of computational load involved in the estimation approach. We will consider reducing the computations of the spreading function estimation, and to eliminate the need of estimating the channel for every single arrival bit avoiding the redundancy resulting from estimating channels with same or similar parameters due to their stationarity.

3.5.1 Fast Computation of Channel Spreading Function

For each arrival symbol, the spreading function is computed for all possible frequencies as obtained from the corresponding time-frequency kernel using the time-dependent windows $V(n,m) = e^{j\omega_q(m-n)}$. This window function can be computed *priori* to reduce the overall computational load. To show this, we have the evolutionary kernel as

$$\begin{aligned} Y(n,\omega_k) &= \frac{1}{M_p}\sum_{m=0}^{M_p-1} y(m)V(m,n)e^{-j\omega_k m} \\ &= \frac{1}{M_p}\sum_{\rho=0}^{M_p-1}\sum_{\ell=0}^{L-1} d\alpha_\ell P(\omega_\rho)e^{-j\omega_\rho N_\ell}\sum_{m=0}^{M_p-1} V(m,n)e^{j(\psi_\ell+\omega_\rho-\omega_k)m} \end{aligned} \tag{3.40}$$

and the Zadeh's transfer function was defined to be

$$G(n,\omega_k) = \frac{M_p Y(n,\omega_k)}{dP(\omega_k)} \tag{3.41}$$

Now when the window frequency ψ_q coincides with the Doppler frequency ψ_ℓ, the bifrequency kernel is

$$\begin{aligned} B(\Omega_s,\omega_k) &= \frac{1}{M_p}\sum_{m=0}^{M_p-1}\left[\sum_{\ell=0}^{L-1}\sum_{\rho=0}^{M_p-1} d\alpha_\ell e^{j\psi_\ell m}P(\omega_\rho)e^{j\omega_\rho(m-N_\ell)}\right]e^{-j\psi_q m}\delta(\Omega_s-\psi_\ell)e^{j(\omega_\rho-\omega_k)m}\frac{e^{-j\omega_k m}}{P(\omega_\rho)} \\ &= \frac{1}{M_p}\sum_{\ell=0}^{L-1} d\alpha_\ell e^{-j\omega_k N_\ell}\delta(\Omega_s-\psi_\ell)M_p\delta(\rho-k) \\ &= \sum_{\ell=0}^{L-1} d\alpha_\ell e^{-j\omega_k N_\ell}\delta(\Omega_s-\psi_\ell) \end{aligned} \tag{3.42}$$

showing peak at the frequency location when the signal frequency coincides with the frequency of the window function. Clearly, the above equation indicates that some terms are independent and can be computed *a priori*.

The bi-frequency function can be obtained by taking the discrete-time Fourier transform of the transfer function $G(n,\omega_k)$ with respect to n, or equivalently the window function $V(n,m)$ with respect to n, as,

$$\begin{aligned} B(\Omega_s,\omega_k) &= \sum_m y(m)\mathcal{F}_n\left\{V(m,n)\right\}\frac{e^{-j\omega_k m}}{P(\omega_k)} \\ &= \sum_m y(m)V(m,\Omega_s)\Phi(m,\omega_k) \end{aligned} \tag{3.43}$$

where $\Phi(m, \omega_k)$ is $M_p \times M_p$ matrix and is independent of the window function. The final spreading function is obtained by taking the inverse Fourier transform of the bifrequency function $B(\Omega_s, \omega_k)$, or equivalently the function $\Phi(m, \omega_k)$ with respect to k:

$$\hat{S}(\Omega_s, k) = \sum_m r(m) V(m, \Omega_s) \Theta(m, k) \tag{3.44}$$

where $\Theta(m, k)$ is the inverse Fourier transform of the the function $\Phi(m, \omega_k)$ and can be computed *a priori*.

In matrix, the spreading function can be obtained as

$$S = U \cdot \Theta \tag{3.45}$$

where U is $M_p \times M_p$ which can be obtained from the cross multiplications of the received signal and the adaptive function V as

$$\begin{bmatrix} u_{11} & u_{12} & \cdots & u_{1N} \\ u_{21} & u_{22} & \cdots & u_{2N} \\ \vdots & \vdots & \ddots & \vdots \\ u_{N1} & u_{N2} & \cdots & u_{NN} \end{bmatrix} = \begin{bmatrix} y^T \\ y^T \\ \vdots \\ y^T \end{bmatrix} \times \begin{bmatrix} v_{11} & v_{12} & \cdots & v_{1N} \\ v_{21} & v_{22} & \cdots & v_{2N} \\ \vdots & \vdots & \ddots & \vdots \\ v_{N1} & v_{N2} & \cdots & v_{NN} \end{bmatrix}.$$

The final spreading function is the result of the following inner product:

$$\begin{bmatrix} s_{11} & s_{12} & \cdots & s_{1N} \\ s_{21} & s_{22} & \cdots & s_{2N} \\ \vdots & \vdots & \ddots & \vdots \\ s_{N1} & s_{N2} & \cdots & s_{NN} \end{bmatrix} = \begin{bmatrix} u_{11} & u_{12} & \cdots & u_{1N} \\ u_{21} & u_{22} & \cdots & u_{2N} \\ \vdots & \vdots & \ddots & \vdots \\ u_{N1} & u_{N2} & \cdots & u_{NN} \end{bmatrix} \begin{bmatrix} \theta_{11} & \theta_{12} & \cdots & \theta_{1N} \\ \theta_{21} & \theta_{22} & \cdots & \theta_{2N} \\ \vdots & \vdots & \ddots & \vdots \\ \theta_{N1} & \theta_{N2} & \cdots & \theta_{NN} \end{bmatrix}.$$

We notice that the function $\Theta(m, k)$ can be computed *a priori*. For the window function, $V(m, \Omega_s)$, it can be generated for all possible frequency shifts corresponding to all possible Doppler shifts. Thus, computing both functions *a priori* at the receiver allows computing of the spreading function directly without obtaining other channel functions such as bi-frequency and transfer function. Therefore, with such fast computational approach, the computational load will be significantly reduced.

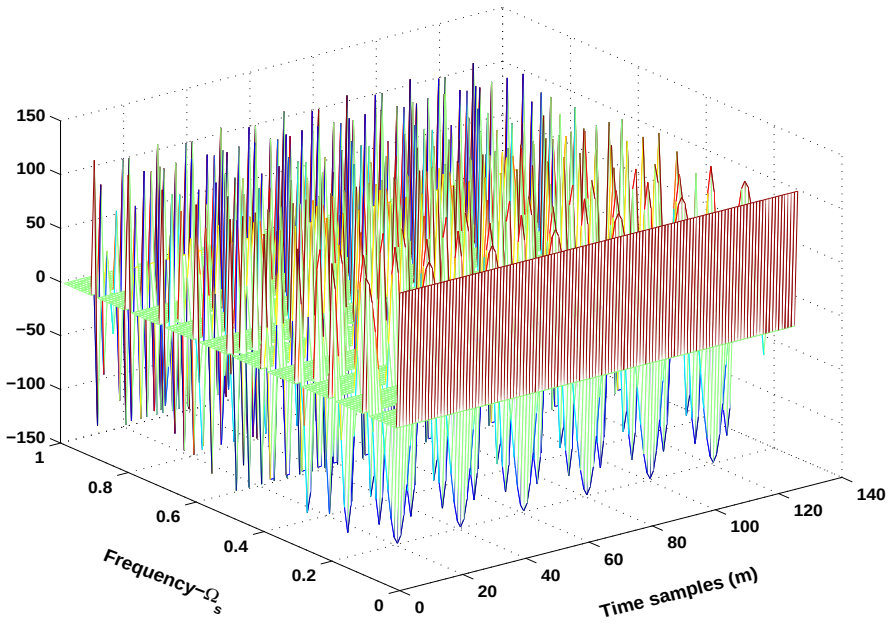

Figure 16: Real value of the adaptive window $V(\Omega_s, m)$

3.5.2 Computational Load Reduction from Channel Behavior

Another computational aspect is the estimation of redundant channels. In some communication applications such as TDMA, the receiver uses an equalization scheme with a pilot signal that is known at the receiver, and transmitted periodically so that the receiver can update channel coefficients. The disadvantage of this procedure is the that transmitting pilot signal comes at the cost of data rate. Another disadvantage is that the receiver performs channel equalization, even with stationary channels where channel parameters remain constant. In our approach, the estimated channel parameters for the previous bit data can be used for the current one until a significant change occurs in the channel behavior that makes it necessary for new updates. Therefore, the receiver should have self monitoring criteria that will allow the estimation process to work according to the channel behavior.

A better way to achieve this approach is by considering the absolute value of the average of the despreaded signal shown in Equation (3.35) as a required decision rule for determining

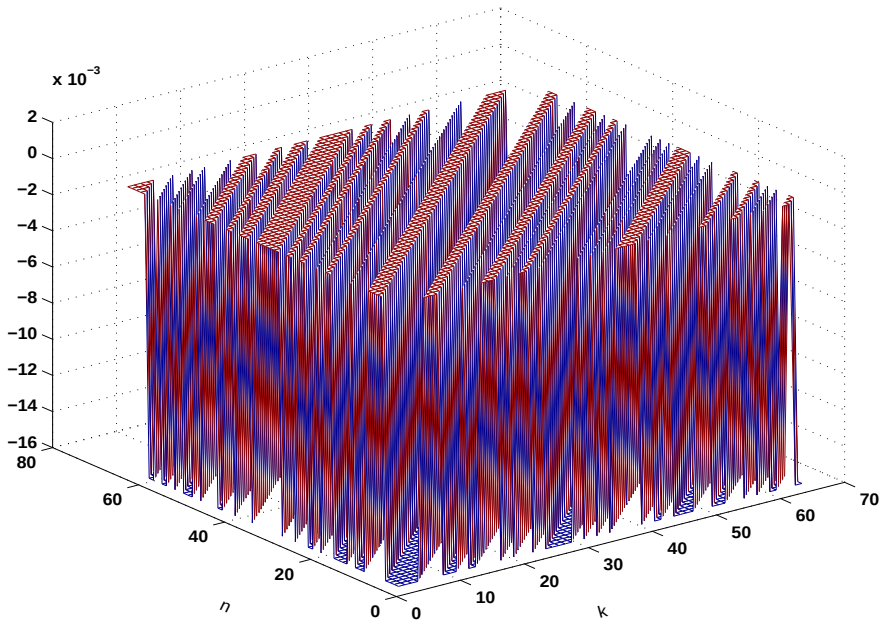

Figure 17: Real value of the 2-D function $\Phi(m, k)$

new channel estimation. Thus, avoiding the estimation of redundant channels during the transmission of stationary channels will significantly reduce the overall computational load. Figure 18 shows the mean value of the despreaded signal versus the transmission channels that change randomly; each remains constant for some period of time. It is shown that with any significant change in the channel parameters the value of $|d|$ becomes small, allowing the receiver to use a proper threshold value to initiate a new estimation process.

3.6 SIMULATIONS

To illustrate our estimation and bit-detection procedures we simulated the time-varying channel to vary at random in the number of paths (from 1 to 4), the delays (from 0 to $0.8M_p$), and the doppler frequencies (from $-0.005\omega_c$ to $0.005\omega_c$) where ω_c is the carrier

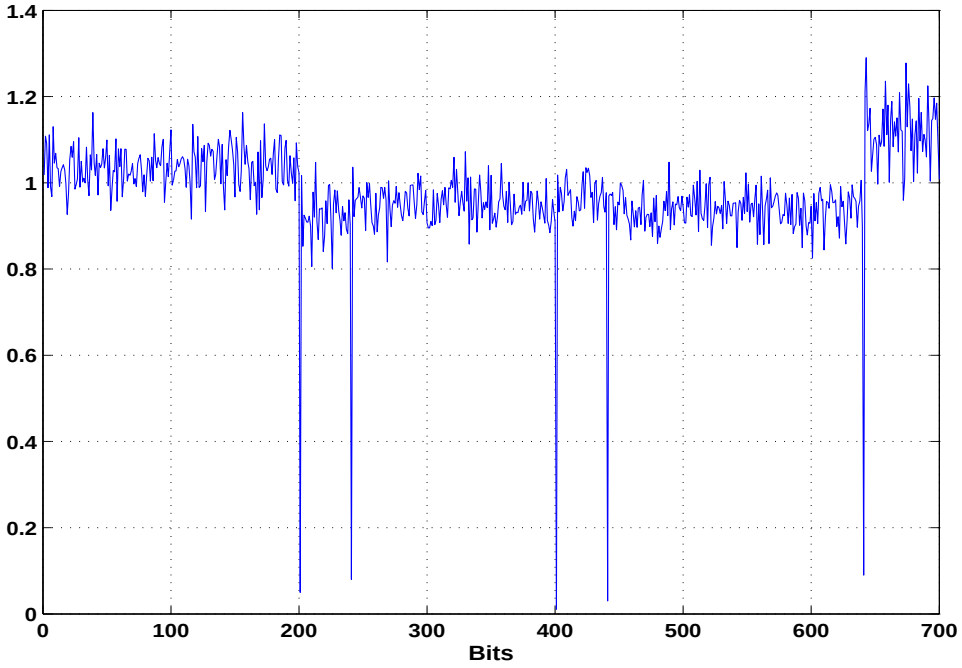

Figure 18: Channel variation as seen from the decision parameter at the receiver

frequency equals to $\pi/2$, and the gains α_ℓ were linearly related to the delays. The general model was considered; information from the shortest path signal obtained by the spreading function were efficiently employed to scale, demodulate, and despread the received signal with the estimated parameters $\hat{N}_0$, ψ_0, and α_o.

A Monte-Carlo simulation was performed to determine the goodness of our process. The model changes randomly from bit to bit as explained above in an attempting to simulate very fast fading. For each bit we performed 10000 trials with different media noise and with the same SNR. The chosen SNRs ranged from -2 dB to 16 dB. This simulation was performed for four different cases: when channel parameters are known to the receiver, when Doppler shifts are neglected, with no channel estimation, and finally with the consideration and compensation of Doppler shifts. The simulation results are provided in Fig. 19 as BER vs SNRs.

3.7 SUMMARY

The LTV channel model for the direct-sequence spread-spectrum communications (DSSS) is characterized by parameters such as time-delays, frequency shifts, and attenuation factors associated with signals coming from various paths. Modeling such channels using channel functions shows that they are characterized by means of spreading function.

At the estimation level, the discrete evolutionary transform DET has been used with an adaptive window to estimate the time-frequency kernel from the received signal. The connection between channel time-varying frequency response and Zadeh's transfer function was used to compute the spreading function, depicting the parameters of the channel as large peaks at frequency locations corresponding to the time-delays of the multipath signals with amplitudes equal to their gains.

An efficient DSSS receiver has been introduced that is dependent on the channel estimation approach, where only the information of the spreading function, particularly the set of parameters corresponding the shortest path signal, is needed for bit detection. This receiver avoids the cross-correlation and bank of filters process as the case of RAKE receiver.

Doppler shifts were proved to have a negative impact on the detection part. It was shown experimentally that the bit error rate decreases as the Doppler increases, and to correct it, the receiver must compensate for those frequency shifts.

At the computational level, a newer, faster algorithm has been proposed for estimating the spreading function with much less computational cost.

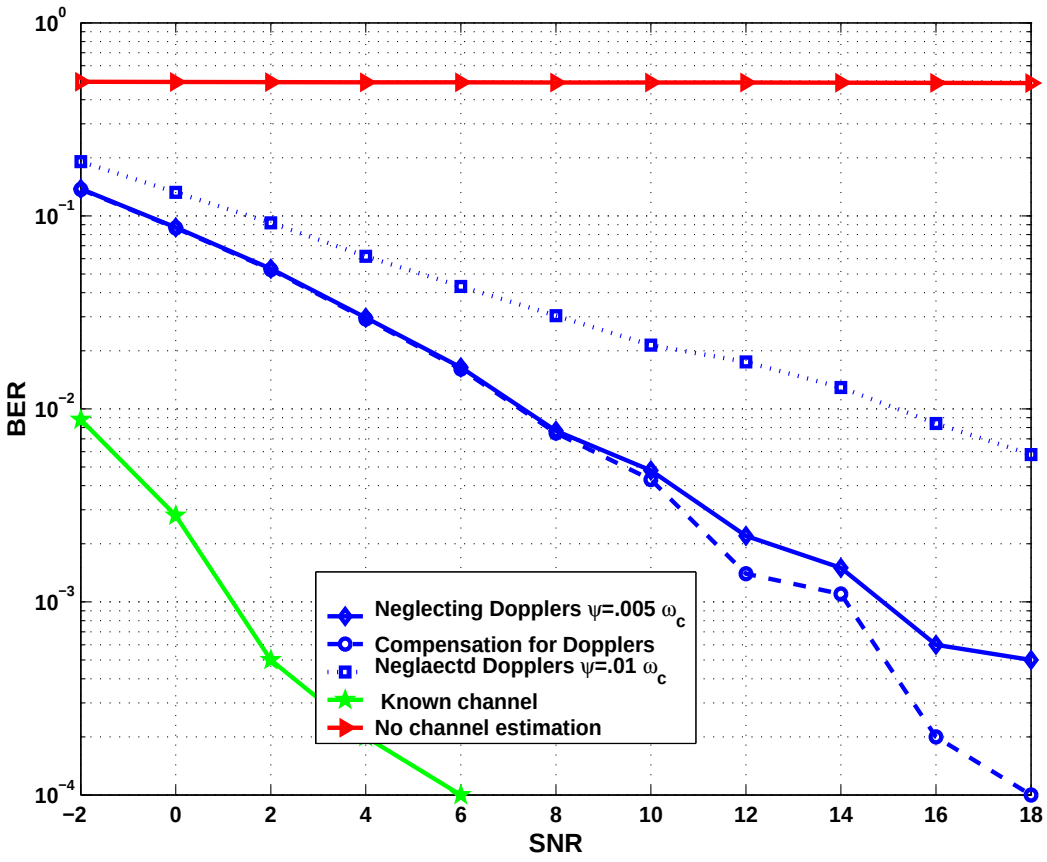

Figure 19: Bit error rate (BER) vs SNR

4.0 MULTIUSER CHANNEL MODELING AND ESTIMATION

The proposed channel estimation approach presented in Chapter 3 considers only the single user scenario. In this chapter, we extend our approach for higher level estimation considering multiuser communication channels. In practice, as is the case with wireless communications, multiple users can be actively communicating simultaneously with the base station at both the up and down links. At the down-link, the base station transmits signals of multiple users, however it is up to the receiver to determine which signal belongs to the appropriate receiver. In the uplink, the base station receives multiple signals that come from active users at different time delays depending on the distance and location of each user. In this case, the base station must utilize a receiver that detects different signals corresponding to different users. The interference is coming from channel noise, multipath, and multiuser interferences only. We will consider how to deal with these interferences now and leave intentional jammer for the following chapter.

4.1 UPLINK MULTI-USER DSSS COMMUNICATION CHANNEL MODELING AND ESTIMATION

In uplink transmission, the base station receives signals –each affected by a different channel– from different users and locations. The main function of the base station receiver is to somehow separate these signals and detect the transmitted bits corresponding to a particular user. The problem is then how to estimate the parameters of the channel corresponding to one of the users from the received signal knowing his unique transmitted pseudo-noise sequence, and then how to use these channel parameters in the detection of the sent data.

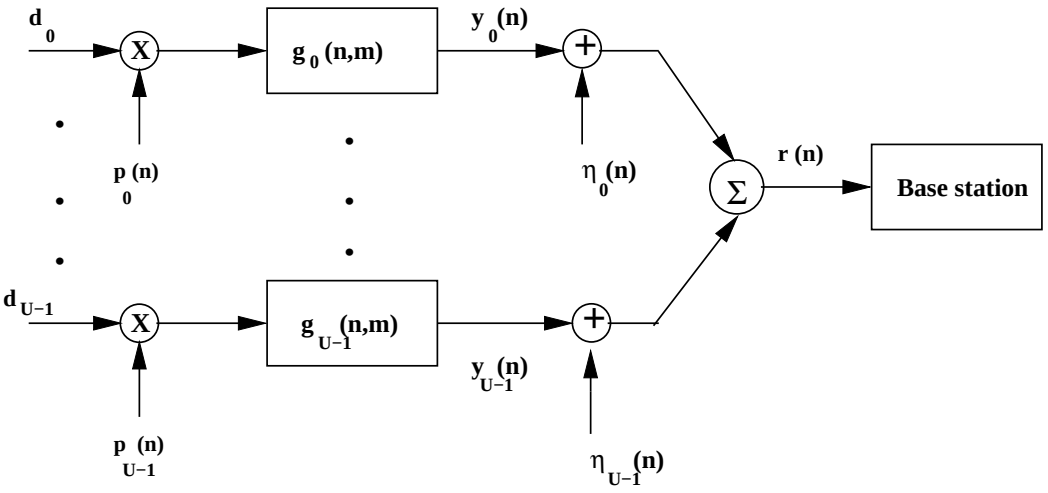

Figure 20: Multiuser communication channel (uplink).

4.1.1 Uplink Channel Modeling

Figure 20 illustrates the DSSS uplink transmission for U users, each having a different channel with impulse response $g_u(n,m)$, modeled as in the single user case. If $p_u(n)$ is the unique pseudo-noise assigned to user u, the spread signals $\{s_u(n) = d_u p_u(n)\}$, $u = 0, \cdots, U-1$, are transmitted over the different channels and

$$r(n) = y(n) + \eta(n) + j(n),$$

is the received signal, where $\eta(n)$ is the cumulative channel noise, and we consider the presence of a cumulative intentional jammer $j(n)$. For simplicity in the analysis, we assume each $p_u(n)$ to have the same length M_p.

Analogous to the single-user case, when we replace $p_u(n)$ by its Fourier representation, the noiseless received signal becomes

$$\begin{aligned} y(n) &= \sum_{k=0}^{M_p-1} \left\{ \sum_{u=0}^{U-1} d_u \frac{P_u(k)}{M_p} \left[\sum_{\ell=0}^{L_u-1} \alpha_{u,\ell} e^{-j\omega_k N_{u,\ell}} e^{j\psi_{u,\ell} n} \right] \right\} e^{j\omega_k n} \\ &= \sum_{k=0}^{M_p-1} Y(n,\omega_k) e^{j\omega_k n} \end{aligned} \tag{4.1}$$

where the term in brackets is the time-varying frequency response function, $G_u(n,\omega_k)$, of the channel corresponding to the u^{th} user, and $Y(n,\omega_k)$ is the time-frequency evolutionary kernel corresponding to $y(n)$. As in the single user, for each user the channel functions are similarly related, and it is found again that the spreading function $S_u(\Omega_s,k)$ provides the parameters of the channel for user u and is connected with the kernel $Y_u(n,\omega_k)$. The problem with the uplink case is that the overall time-varying frequency response function is a matrix, given that the system is multiple input/single input, and cannot be used to obtain the corresponding spreading functions. Instead, we will show that the $S_u(\Omega_s,k)$ can be computed from $Y(n,\omega_k)$. In fact, from (4.1) we have for a user i

$$Y(n,\omega_k)=\frac{d_iP_i(k)}{M_p}G_i(n,\omega_k)+\frac{1}{M_p}\sum_{u\neq i}d_uP_u(k)G_u(n,\omega_k)$$

from which we solve for $G_i(n,\omega_k)$ and find the corresponding spreading function as

$$S_i(\Omega_s,k)=\mathcal{F}^{-1}_{\omega_k}\left[\frac{M_pY(\Omega_s,\omega_k)}{d_iP_i(k)}-\frac{1}{d_iP_i(k)}\sum_{u\neq i}d_uP_u(k)B_u(\Omega_s,\omega_k)\right]. \tag{4.2}$$

The last term in the above equation displays the influence of the other users in the determination of the channel parameters for a specific user, and again the connection with the evolutionary discrete kernels. We will see that when estimating the parameters of the channel for some user, the effect of the other users is minimal.

4.1.2 Uplink Channel Parameter Estimation

The DET of $y(n)$, letting $V_q(n,m)=e^{j\omega_q(n-m)}$, is whenever $\omega_q=\psi_{i,\ell}$

$$\begin{aligned}Y_{\psi_{i,\ell}}(n,\omega_k) &= d_i\sum_{s=0}^{M_p-1}\frac{P_i(s)}{M_p}\left[\sum_{\ell=0}^{L_i-1}\alpha_{i,\ell}e^{-j\omega_sN_{i,\ell}}e^{j\psi_{i,\ell}n}\right]\\ &\quad\times\sum_{m=0}^{M_p-1}e^{j(\omega_s-\omega_k)m}+\Gamma(n,\omega_k)\\ &= d_iP_i(k)G_i(n,\omega_k)+\Gamma(n,\omega_k),\end{aligned} \tag{4.3}$$

where the last equation is due to the fact that the summation with respect to m gives $M_p\delta(s-k)$, and that the effect of the other users is defined as

$$\begin{aligned}\Gamma(n,\omega_k) &= \sum_{u\neq i} d_u \sum_{s=0}^{M_p-1} \frac{P_u(s)}{M_p}\left[\sum_{\ell=0}^{L_u-1} \alpha_{u,\ell} e^{-j\omega_s N_{u,\ell}}\right] \\ &\quad \times \sum_{m=0}^{M_p-1} e^{j\psi_{u,\ell}m} e^{j\psi_{i,\ell}(n-m)} e^{j(\omega_s-\omega_k)m},\end{aligned}$$

From equation (4.3), we then have that

$$G_i(n,\omega_k) = \frac{Y_{\psi_{i,\ell}}(n,\omega_k) - \Gamma(n,\omega_k)}{d_i P_i(k)}. \tag{4.4}$$

from which the spreading function $S_i(\Omega_s,k)$ is found to be

$$S_i(\Omega_s,k) = \mathcal{F}^{-1}_{\omega_k}\left[\frac{Y_{\psi_{i,\ell}}(\Omega_s,\omega_k)}{d_i P_i(k)}\right] - \frac{\Gamma(\Omega_s,k)}{d_i P_i(k)} \tag{4.5}$$

where

$$\Gamma(\Omega_s,k) = \frac{1}{M_p}\sum_{u\neq i}\sum_{s=0}^{M_p-1}\sum_{\ell=0}^{L_u-1} d_u P_u(s)\alpha_{u,\ell} e^{-j\omega_s(N_{u,\ell}-k)} e^{j(\psi_{u,\ell}-\psi_{i,\ell})k}\delta(\Omega_s-\psi_{i,\ell}),$$

which is a noise-like component that occurs only at the Doppler frequencies.

Thus, the spreading function $S_i(\Omega_s,k)$ found this way provides the corresponding channel parameters for user i, with a certain amount of noise from the other users, when considering frequencies that coincide with the Doppler shift frequencies. For any other frequency, the spreading function appears noise-like. As before, it is also possible to obtain a fast computation in this case by adapting the matrices to the i-user. Figure 22 illustrates the computation of a user spreading function in the multi-user uplink transmission.

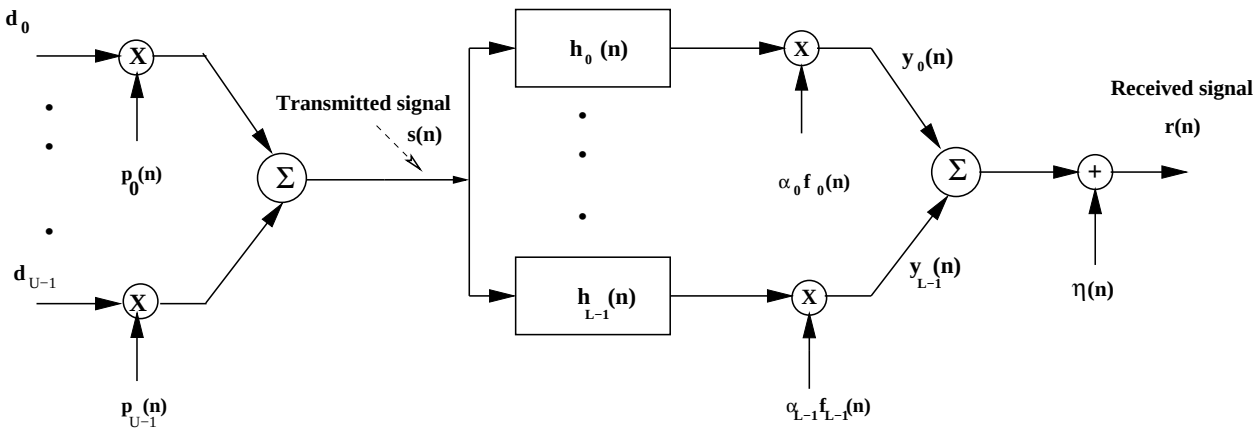

Figure 21: Multiuser downlink channel model.

4.2 DOWNLINK TRANSMISSION

In the downlink transmission, the base station transmits the received information to all required users simultaneously, and each user's receiver detects its own information using its unique pseudo-noise sequence. Figure 21 depicts the downlink communication channel model. In this case, there is only one channel to model and estimate, but again it needs to be estimated in a blind fashion from the received signal.

4.2.1 Downlink Channel Modeling

For the case of U users, the downlink noiseless baseband received signal, $y(n)$, becomes after expanding the pseudo-noise sequences $\{p_u(n)\}$, $u = 0, \cdots, U$, using their Fourier representations

$$\begin{aligned} y(n) &= \sum_{k} \left\{ \sum_{u=0}^{U-1} d_u \frac{P_u(k)}{M_p} \left[\sum_{\ell=0}^{L-1} \alpha_\ell e^{-j\omega_k N_\ell} e^{j\psi_\ell n} \right] \right\} e^{j\omega_k n} \\ &= \sum_{k=0}^{M_p-1} Y(n, \omega_k) e^{j\omega_k n} \end{aligned} \tag{4.6}$$

where the term inside the square brackets is $G(n,\omega_k)$, and $Y(n,\omega_k)$ is the time-frequency evolutionary kernel of $y(n)$.

Just as before, the spreading function can be shown to be connected to the parameters of the channel, and related to the evolutionary kernel of the received signal. In fact, from equation (4.6) we can find $G(n,\omega_k)$ and as before from it find the following expression for the spreading function

$$\begin{aligned} S(\Omega_s,k) &= \sum_{\ell=0}^{L-1}\alpha_\ell\delta(\Omega_s-\psi_\ell)\delta(k-N_\ell) \\ &= \mathcal{F}^{-1}_{\omega_k}\left[\frac{M_p}{\sum_u d_u P_u(k)}Y(\Omega_s,\omega_k)\right]. \end{aligned} \tag{4.7}$$

4.2.2 Downlink Estimation

In the downlink, the parameter estimation is much simpler than in the uplink since there is only one channel. As before, using the adaptive function $V_q(m,n)=e^{j\omega_q(m-n)}$ permits us to obtain the spreading function from the received signal. First, replacing $V_q(m,n)$

$$\begin{aligned} Y_q(n,\omega_k) &= \sum_{u=0}^{U-1}\sum_{s=0}^{M_p-1}\frac{d_u P_u(s)}{M_p}\sum_{\ell=0}^{L-1}\alpha_\ell e^{-j\omega_s N_\ell}e^{j\omega_q n} \\ &\quad\times\sum_{m=0}^{M_p-1}e^{j(\psi_\ell-\omega_q)m}e^{j(\omega_s-\omega_k)m}, \end{aligned}$$

and whenever $\omega_q=\psi_\ell$, we obtain as before

$$Y_{\psi_\ell}(n,\omega_k)=\sum_{u=0}^{U-1}d_u P_u(k)\sum_{\ell=0}^{L-1}\alpha_\ell e^{-j\omega_k N_\ell}e^{j\psi_\ell n}$$

which will then give

$$Y_{\psi_\ell}(\Omega_s,\omega_k)=\sum_{u=0}^{U-1}d_u P_u(k)B(\Omega_s,\omega_k).$$

For a user i, for which we know its unique PN sequence and consequently its Fourier coefficients $\{P_i(k)\}$, an estimate of its bifrequency is obtained by

$$\begin{aligned} B_{\psi_\ell i}(\Omega_s,\omega_k) &= \frac{Y_{\psi_\ell}(\Omega_s,\omega_k)}{d_i P_i(k)} \\ &= \left[1+\frac{\sum_{u\neq i}d_u P_u(k)}{d_i P_i(k)}\right]B(\Omega_s,\omega_k), \end{aligned}$$

from which we obtain

$$S_{\psi_\ell i}(\Omega_s, \omega_k) = S(\Omega_s, \omega_k) + \Lambda(\Omega_s, \omega_k), \tag{4.8}$$

where $S(\Omega_s, \omega_k)$ is the desired channel spreading function, and $\Lambda(\Omega_s, \omega_k)$ is a noise-like term that corresponds to the other users. As before, the above computation is when ω_p coincides with the Doppler frequency shifts, otherwise, the above process just gives a noise-like sequence. Again, a fast computation of the above spreading function is possible using the matrix procedure.

4.3 BIT DETECTION USING ESTIMATED CHANNEL PARAMETERS

Once the parameters of the channel for a certain user are found it is then possible to detect the corresponding data using the correlation of the pseudo-noise sequences in the uplink as well as the downlink situations. We consider two cases: (i) when the received signal is only affected by channel noise, which is the typical situation in commercial wireless communications, the other is (ii) when a jammer besides the channel noise is present, as in military wireless communications. Next, we will give the analysis with the simulations for the first case, while the second case (Wiener receiver) is introduced in the following Chapter.

4.3.1 Conventional Receiver

As seen, the spreading function provides a way to characterize the changes in the channel, either bit by bit or for a group of bits, and also to determine the value of the bit sent as we show next. To detect the sent bit, corresponding to a user u, our approach is to obtain the transmitted signal closest to the line of sight; i.e. the received signal having the smallest delay, the least attenuation and some Doppler shift and use these parameters to determine the sent bit. The reason for this choice is that such a signal is clearly the strongest signal being received, and thus its parameters are probably better estimated than for other weaker signals.

In the uplink transmission, to recover the bit d_u, corresponding to the user u, assuming the parameters $\hat{N}_{u,0}$, $\hat{\psi}_{u,0}$ and $\hat{\alpha}_{u,0}$ correspond to the path closest to the line of sight, the received signal $r(n)$ is de-spread by a shifted replica $p_u(n-\hat{N}_{u,0})$ of the user's pseudo-noise $p_u(n)$, scaled by $1/\hat{\alpha}_{u,0}$ and demodulated by $e^{-j\hat{\psi}_{u,0}n}$ giving

$$\begin{aligned}\rho_u(n) &= d_u p(n-\hat{N}_{u,0})^2 + \left[\sum_{i\neq u}\sum_{\ell=1}^{L_i-1}\alpha_{i,\ell}d_i p_i(n-N_{i,\ell})e^{j\psi_{i,\ell}n} + \eta(n)\right] \\ &\quad \times\frac{p_u(n-\hat{N}_{u,0})e^{-j\hat{\psi}_{u,o}n}}{\hat{\alpha}_{u,0}} \end{aligned} \tag{4.9}$$

Given the pseudo noise nature of $p_u(n)$, and assuming it is uncorrelated with the channel noise $\eta(n)$, the expected value of $\rho_u(n)$ gives $E[\rho(n)] = d_u$, and using a short-term average being we obtain an estimate of d_u.

Likewise in the downlink transmission, the de-spread, scaled and demodulated received signal of user u, letting $\hat{N}_0$, $\hat{\psi}_0$ and $\hat{\alpha}_0$ correspond to the path closest to the line of sight, is given by

$$\rho_u(n) = d_u p_u(n-\hat{N}_0)^2 + \left[\sum_{\ell=1}^{L-1}\alpha_\ell e^{j\psi_\ell n}\sum_{i\neq u} d_i p_i(n-N_\ell) + \eta(n)\right]\frac{p_u(n-\hat{N}_0)e^{-j\hat{\psi}_0 n}}{\hat{\alpha}_0}, \tag{4.10}$$

which again, under similar assumptions, gives that the expected value of $\rho_u(n)$ is $E[\rho(n)] = d_u$, and the short-term average is an estimate of d_u. These possible receivers would be special cases of the RAKE receiver, simplified and improved by the information from the channel estimation.

4.4 SIMULATION

To illustrate the performance of the proposed procedures we simulate a multiple user uplink and downlink base-band system to transmit BPSK coded data. The aim of these simulations is to show the robustness of the estimation under very restrictive conditions. Thus, the channel models are allow to vary at random from bit to bit within certain restrictions. The number of paths is allowed to vary from 1 to 4, the delays can vary from 0 to $0.8M_p$, and

the Doppler shifts to vary from the 0 to π. The attenuation factors are set to vary linearly with the delays. Clearly, these simulations exceed real situations, where the model is valid for much more than the duration of a bit, and the delays are not as large, and in particular the Doppler frequency shifts are not as significant as it would require a rather large velocity difference between the user and the receiver. The results are thus related to a very worst situation, and despite this we will show that the results are encouraging. Using the fast computation of the spreading function, indicated before, makes the simulations not very computationally complex . We wish to determine the goodness of the process in detecting the correct sent bit for both cases when the received signal is affected by Gaussian channel noise. We thus perform for different situations 10,000 Monte-Carlo trials for each signal to noise ratio (SNR) value of the channel noise (ranging from -2 dB to 14 dB). The bit error rate (BER) is computed for the range of SNRs for several users (ranging from 1 to 7) in uplink and downlink situations. The results are compared to the situation where no channel estimation is performed and the received signal is just processes using the corresponding pseudo noise sequence for a user (corresponding to an upper bound) and in the ideal situation when the corresponding channel is known (corresponding to a lower bound).

The simulations results, shown in Figs. 24 and 25, correspond to the cases of uplink and downlink transmission affected by Gaussian channel noise. As expected, the performance of the procedures degrades as the number of users increases, although the performance is not significantly different for 4 or 7 users as shown. Clearly, the estimation of the parameters is improved as the noise SNR increases. In these simulations, no significant differences are noticed between the uplink and the downlink cases. Considering the stringent conditions imposed on the simulations, these results seem to indicate that the performance of our procedures when these conditions would be a lot better.

4.5 SUMMARY

In this chapter, we showed an important extension of the proposed estimation approach to supporting higher level multiuser applications that are encountered in wireless communi-

cations and other applications. In multiuser uplink and down link wireless communication channels, multiple users communicate simultaneously through a base station, and estimating individuals' channels parameters was possible by means of spreading function. The estimated spreading function in this case depicts only the information for the desired user, while others' information appear as a noise. Our approach is capable of estimating individual user channel parameters in both scenarios.

In bit detection at each user level, the first set of channel parameters obtained from the desired user's spreading function is used to determine the correct data bit. For each user, the interference of other users appears as a noise-like component with zero mean that can be eliminated at the despreading level. When the interference is of a broadband type with non-zero-mean, then detection will be affected, and requires an exciser to suppress the interference and improve the BER, as can be explained in the following chapter.

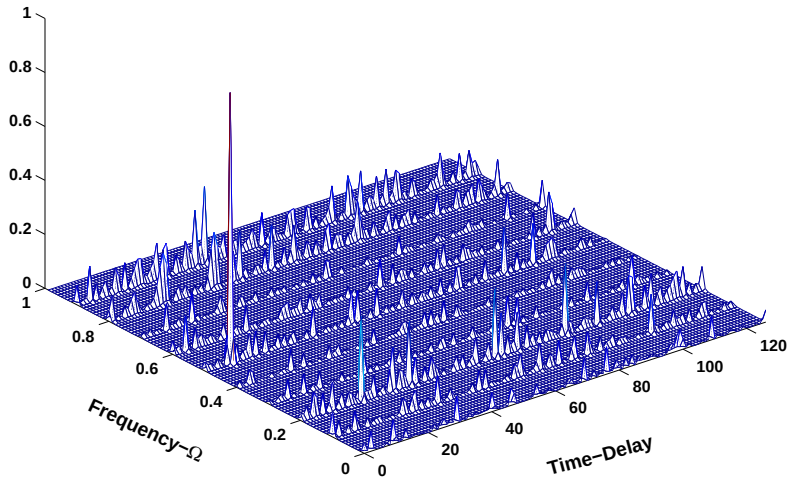

Figure 22: SF of user 2 in multiuser communication channel (uplink) of 6 users.

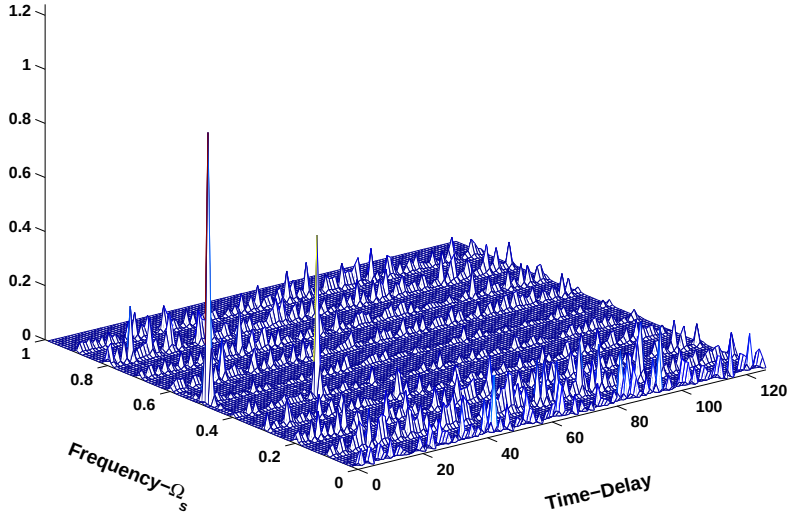

Figure 23: SF corresponds to user 1 in multiuser channel (downlink) of 4 users.

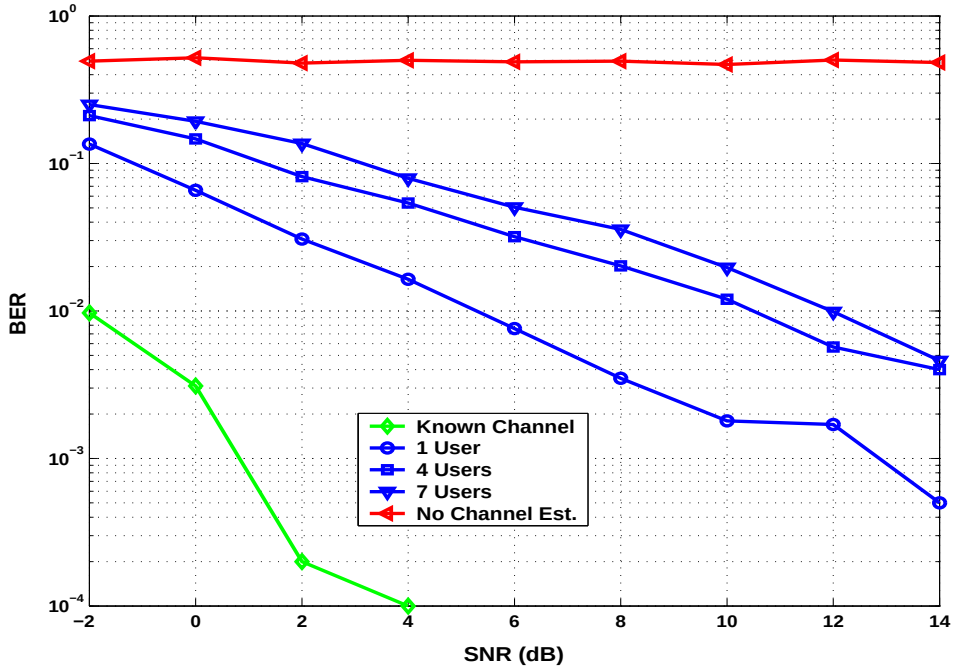

Figure 24: Multiuser uplink output as BER vs SNR

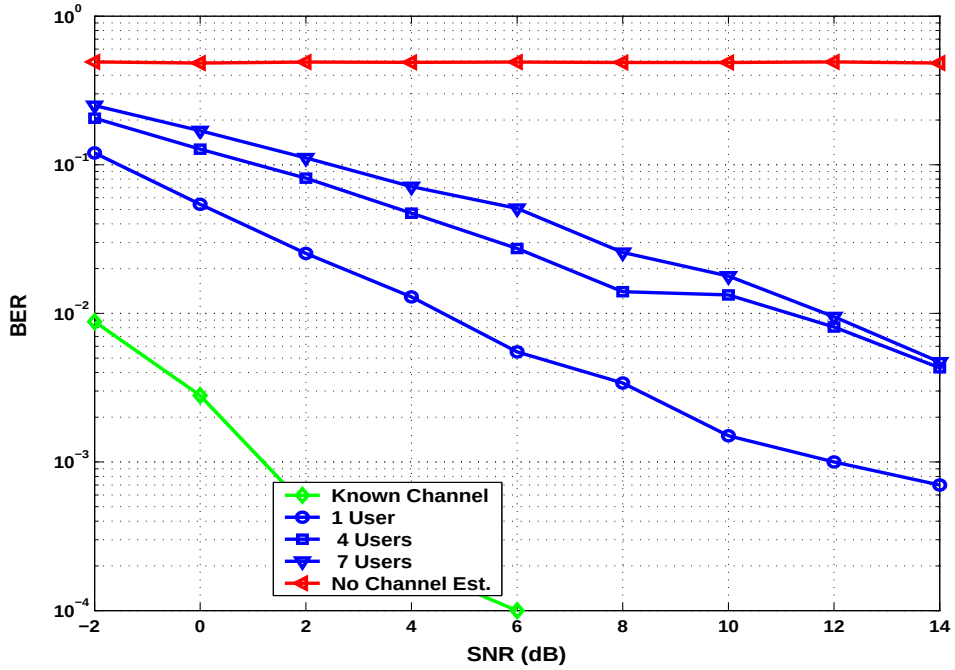

Figure 25: Multiuser downlink output as BER vs SNR

5.0 INTERFERENCE EXCISION AND A WIENER-MASK RECEIVER

One of the advantages to using DSSS in communication systems is the ability to resist the interference of narrow-band signals. For non-stationary broad-band interference, the DSSS is not robust [41]. Recently, time-frequency analysis has been used for excising a non-stationary broad-band jammer [40, 54]. Amin was the first to propose the use of tme-frequency to construct a time-varying notch filter [44]. A projection filter implemented by using the time-frequency signature of jammers is given in [42]. Barabarossa uses the Wigner-Hough transform to estimate the jammer instantaneous frequency, setting up an adaptive time-varying excision filter [47]. Instantaneous bandwidth was used to the notch-width of the filter to excise AM-FM jammers [48, 49]. Suleesathira and Chaparro examined the use of instantaneous frequency estimated from the discrete evolutionary transform for jammer excision [45]. Jang and Loughlin examined the use of interference bandwidth for excising AM-FM jammers in direct sequence spread spectrum communication systems [48, 49]. Additionally, the discrete evolutionary and the Hough-transforms and singular value decomposition have been implemented for interference mitigation in spread spectrum [45, 4].

In this chapter, two methods of interference excising will be introduced. Both of these methods implement the masking techniques from the frequency-frequency spectrum using the frequency-frequency discrete evolutionary and Wiener theory [54]. In the next two sections, the discussion and the implementation of both approaches are based on free-space DSSS communication channels with the assumption of perfect synchronization at the receiver. In the final section we will discuss the mitigation of broadband interference in the presence of multipath phenomenon in single and multiuser communication channels.

5.1 FREQUENCY-FREQUENCY MASKING

This method is based on the discrete frequency-frequency evolutionary representation of non-stationary signals as explained earlier in Chapter 2. We are using the fact that the spreading sequence PN is known at both the transmitter and the receiver.

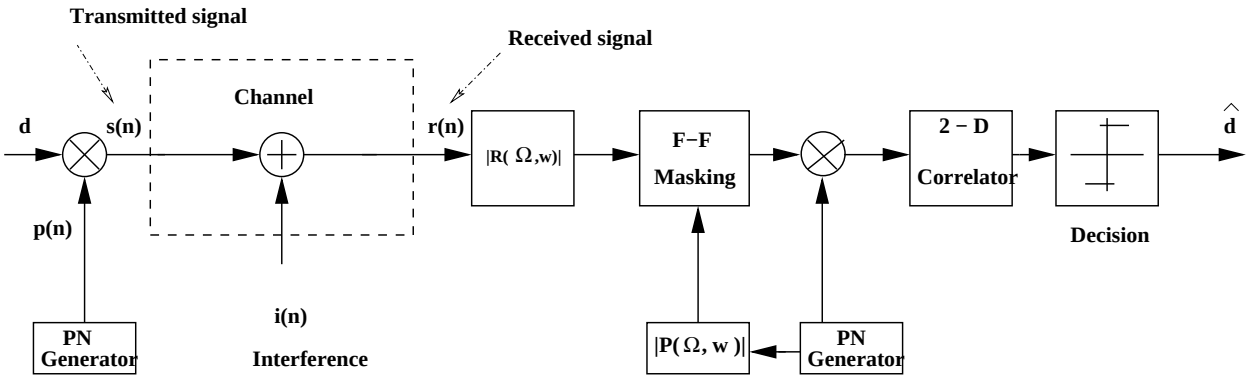

Figure 26: Frequency-frequency masking exciser

Consider first the case when the channel effects are not considered. The model of the DSSS system, including the frequency-frequency masking exciser for that is shown in Fig. 26. When transmitting the m^{th} data the received baseband signal is given by

$$r_m(n) = d_m p(n) + i_m(n) \qquad 0 \leq n \leq (M_p - 1) \tag{5.1}$$

where the data bit is $d_m = \pm 1$, $p(n)$ is a pseudo-noise signal of length M_p chips, and the interference signal is

$$i_m(n) = j_m(n) + \eta_m(n) \qquad 0 \leq n \leq (M_p - 1) \tag{5.2}$$

composed of possible interference signal $j_m(n)$, and the channel white noise $\eta_m(n)$ for that bit. Having the knowledge that the spreading code is known at both the transmitter and

the receiver, the frequency-frequency DET of $p(n)$ can be computed for the spreading code as *a priori* information as

$$P(\Omega_s, \omega_k) = \sum_l p(l) W_k(l, \Omega_s) e^{-j\omega_k l} \tag{5.3}$$

where $W_k(l, \Omega_s)$ is the Gabor window defined in Equation 2.31.

Similarly, the frequency-frequency DET of the received signal $r_m(n) = d_m p(n) + i_m(n)$ can be computed to give

$$R_m(\Omega_s, \omega_k) = d_m P(\Omega_s, \omega_k) + I_m(\Omega_s, \omega_k) \tag{5.4}$$

where $P(\Omega_s, \omega_k)$ and $I_m(\Omega_s, \omega_k)$ are the frequency-frequency DET_s of the pseudo-noise and the interference signal respectively and assuming p(n) and $i_m(n)$ are statistically independent or uncorrelated. In the stationary case, interference is eliminated by designing a filter with a bandwidth coinciding with that of the desired signal. But in this non-stationary broadband case, we define a mask

$$M_k(\Omega_s, \omega_k) = \frac{|P(\Omega_s, \omega_k)|}{|R_m(\Omega_s, \omega_k)|} \tag{5.5}$$

to do the interference excision. Notice here that the value of $|P(\Omega_s, \omega_k)|$ is independent of the sign of the received bit.

This approach works by taking the frequency-frequency DET of the PN code as *a priori* information, and the frequency-frequency DET of the received signal. The mask will be unity for some points in the frequency-frequency plane where the support of the interference kernel does not overlap with the support of the kernel of the pseudo-noise signal. Once the unity points are defined, a 2-D correlator will be used to correlate these points with their equivalents from the known frequency-frequency kernel of the PN signal. Taking the average of these points will allow us to obtain a decision for the estimated bit $\hat{d}$.

Thus, in the case of interference that has a frequency-frequency kernel with a support that does not cover the whole frequency-frequency plane, whenever the mask is close to unity (given that the white noise has as support the whole frequency-frequency plane) the kernel of the received signal $R_m(\Omega_s, \omega_k)$ provides an estimate of the kernel $d_m P(\Omega_s, \omega_k)$. Such a procedure works well whenever no channel noise is present, and the interference kernel is

not spread over the whole frequency-frequency plane. The actual type of interference is not important. When the interference has as support the whole frequency-frequency plane, or when the channel noise is very strong, this method would not work well as explained in the experimental section.

5.2 INTERFERENCE EXCISION VIA WIENER MASKING

In this approach we consider the implementation of the special case of the non-stationary Wiener filter [54] for jammer excision in DSSS communications. Wiener masking requires obtaining the time-frequency spectrum of both the received signal and reference signal using DET.

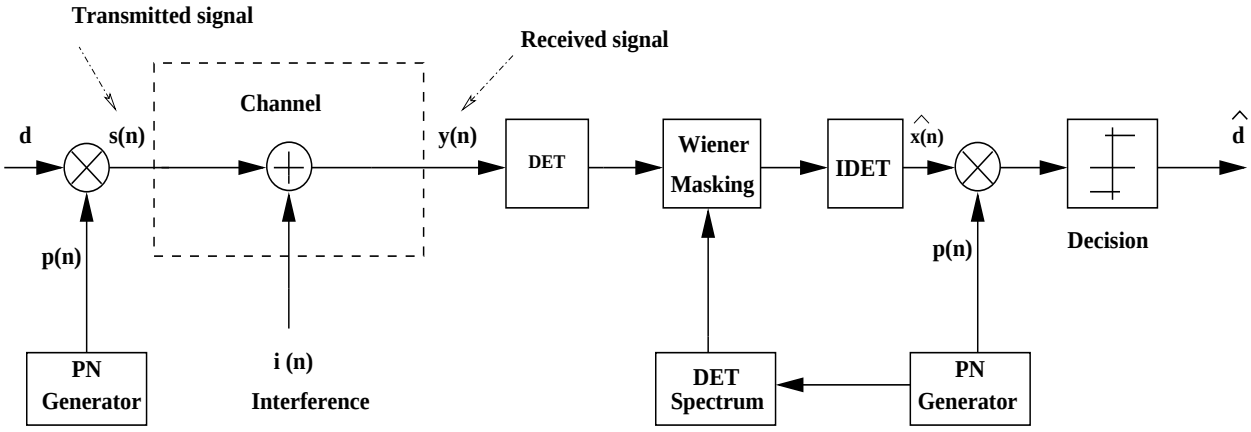

Figure 27: Wiener exciser

One piece of information that is critical for the direct sequence spread spectrum technique to work properly is that the pseudo noise sequence used as the spreading function in the transmitter is known at the receiver. Thus, for each bit, information regarding the spreading sequence does not change and we can compute *a priori* its evolutionary spectrum, $|P(n,\omega)|^2$. This spectrum and the spectrum of the received baseband signal $y(n) = r_m(n)$ can be used to obtain a mean-square estimate of the DS signal, $x(n) = d_m p(n)$. This is a special case

of the non-stationary Wiener filtering [54], where we want a linear time-varying estimator for a signal $x(n)$ embedded in a non-stationary interference $i_m(n)$. The Wiener filtering problem can be setup by letting the desired signal be $x(n) = d_m p(n)$, and the data $y(n) = x(n) + i_m(n)$, assuming $x(n) + i_m(n)$ are non-stationary and not correlated, or independent. When transmitting the m^{th} data bit using DSSS, the received baseband signal is given by Equation 5.1, and an estimate can be found by minimizing the mean-square error

$$\varepsilon(n) = E|x(n) - \hat{x}(n)|^2, \tag{5.6}$$

where $\hat{x}(n)$ is the output of a linear time-varying filter or mask. The masking estimator has the Wold-Cramer representation

$$\hat{x}(n) = \int_{-\pi}^{\pi} Y(n,\omega) B(n,\omega) e^{j\omega n} dZ_y(\omega) \tag{5.7}$$

where $Y(n,\omega)$ is the evolutionary kernel of $y(n)$, $B(n,\omega)$ is a masking function, and $Z_y(\omega)$ is the process of orthogonal increments correspondsing to the non-stationary signal $y(n)$. The minimization of $\varepsilon(n)$ requires, according to the orthogonality principle, that

$$E[x(n) - \hat{x}(n)]\hat{x}^*(n) = 0 \tag{5.8}$$

which can be shown to be equivalent to

$$\int_{-\pi}^{\pi} \left[\frac{S_x(n,\omega)}{Y^*(n,\omega)} - G(n,\omega) \right] G^*(n,\omega) d\omega = 0, \tag{5.9}$$

where we have defined $G(n,\omega) = Y(n,\omega)B(n,\omega)$. To minimize the above equation we let

$$G(n,\omega) = Y(n,\omega)B(n,\omega) = \frac{S_x(n,\omega)}{Y^*(n,\omega)}, \tag{5.10}$$

so that the mask is given by

$$B(n,\omega) = \frac{S_x(n,\omega)}{S_y(n,\omega)} \tag{5.11}$$

or the ratio of the evolutionary spectra of $x(n)$, and that of the data $y(n)$. This result is analogous to the non-casual stationary Wiener filter. The optimal estimator and the minimum mean square error are found to be

$$\begin{aligned} \hat{x}(n) &= \int_{-\pi}^{\pi} \frac{S_x(n,\omega)}{Y^*(n,\omega)} dZ_y(\omega), \\ \varepsilon_{min}(n) &= \int_{-\pi}^{\pi} \frac{S_x(n,\omega) S_\psi(n,\omega)}{S_y(n,\omega)} d\omega. \end{aligned}$$

The Wiener mask, using DET implementation, is given by the ratio of the spectrum of $d_m p(n)$ and the spectrum of $r_m(n)$. The evolutionary spectrum of $d_m p(n)$ is the same independent of d_m, and the spectrum of the received signal is available for every bit transmitted. Finally, the estimated message signal is the inverse discrete evolutionary transform of the kernel $R_m(n,\omega)B(n,\omega)$. The above is only possible because of the connection between the evolutionary kernel and the signal.

5.3 EXPERIMENTAL RESULTS

In this experimental section, we consider two examples of different interference signals for free path communication channel. The first example is with interference that is composed of monocomponent signals with narrow support; the second one is the interference of broad support as of two chirp signals. Both methods require acquiring *a priori* the evolutionary spectrum of the pseudo-noise $S_p(n,\omega_k)$, and the frequency-frequency kernel $P(\Omega_s,\omega_k)$ for the frequency-frequency masking. These two *a priori* pieces of information are illustrated in Fig. 27. The time-frequency and frequency-frequency spectrum of the received signal with both narrow support and broad support interference are shown in Fig. 5.3.1.

5.3.1 Simulation

In the simulation, the goodness of algorithms at estimating the sent bit was measured by the bit error rate (BER), where 5000 trials at each SNR (corresponding to the DS signal and the channel noise) were performed. A multipath free channel was considered with perfect

synchronization at the receiver. In each method, the interference-to-signal ratio (ISR) was 25 dB. The SNR values in each case varied from 0 to 20 dB. The results are shown in Figs. 30 and 31.

As expected, the performance of the frequency-frequency algorithm is better than those from the Wiener algorithm when the support of the interference is narrowly concentrated. In the case of broad support interference, the frequency-frequency algorithm does not work well, as there are no regions where the mask is close to unity and so the estimation of d_m is not accurate, while the Wiener masking algorithm method performs better.

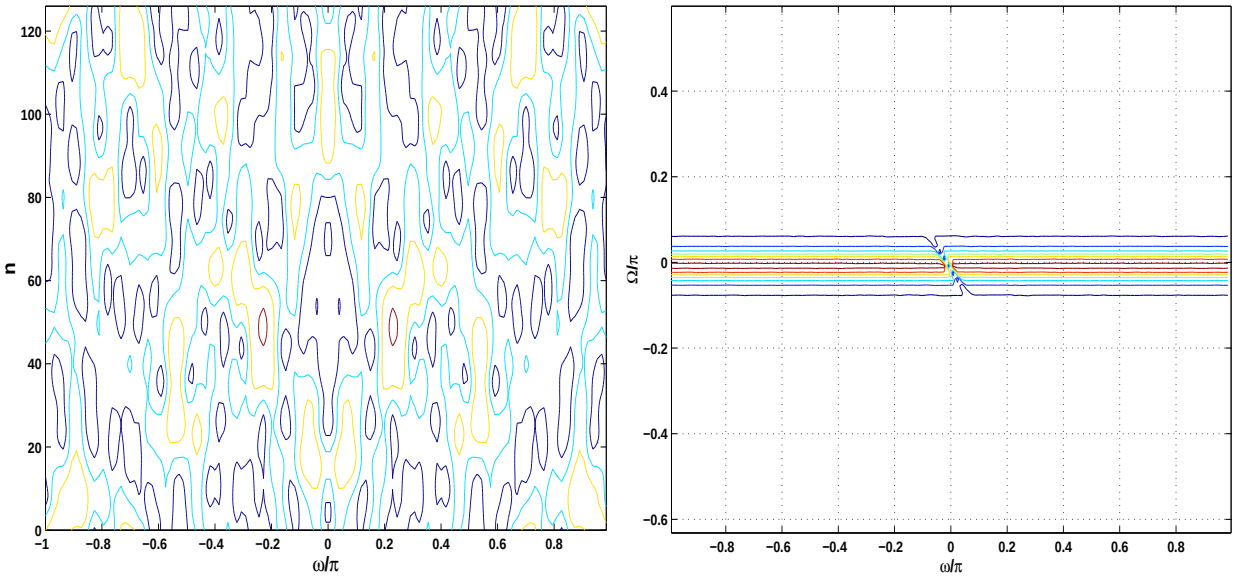

(a) (b)

Figure 28: (a) Time-frequency spectrum of PN, (b) Frequency-frequency spectrum of PN.

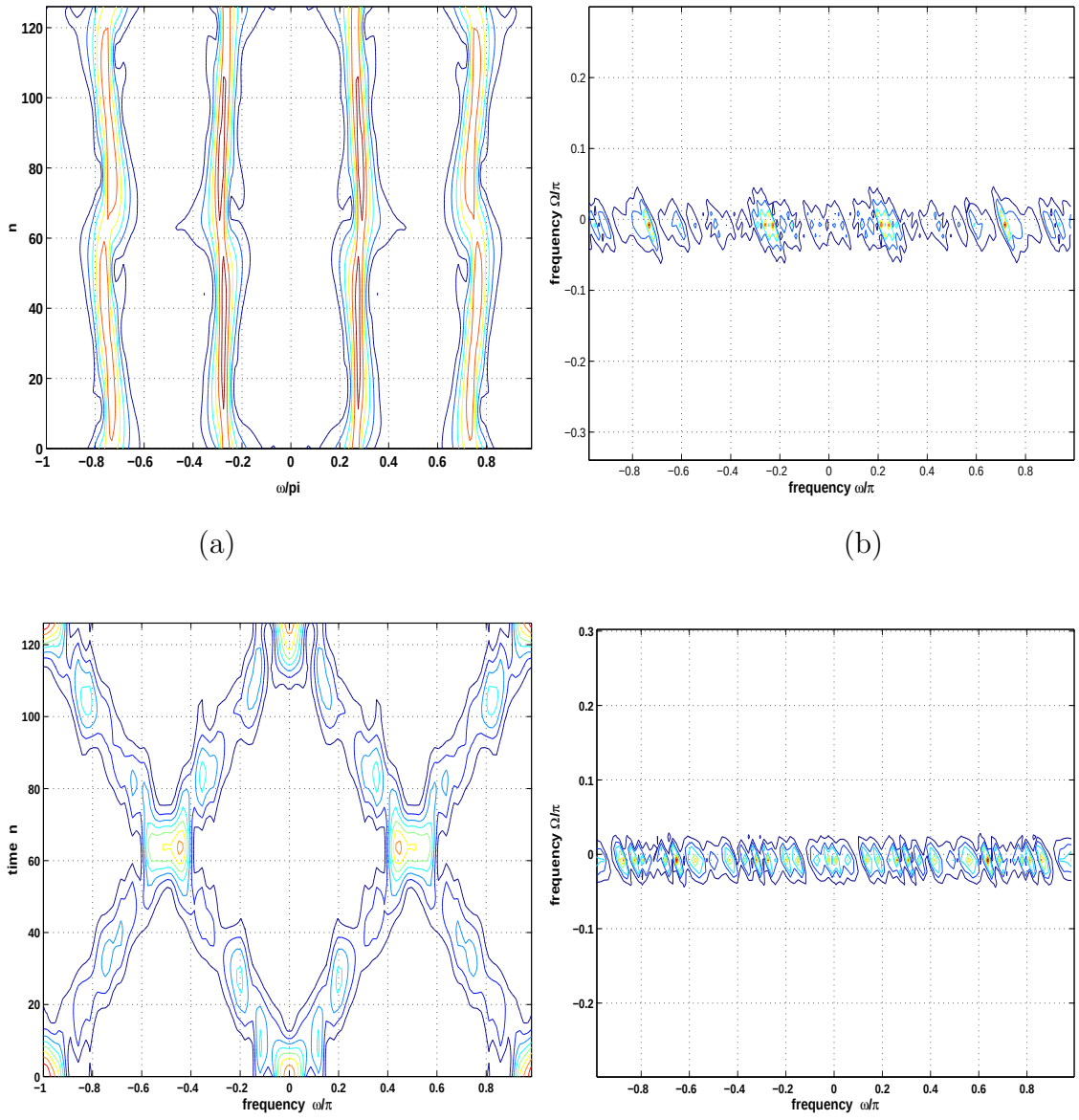

Figure 29: (a) Time-frequency spectrum of the received signal with jammer of (narrow support), (b) Frequency-frequency spectrum (narrow support), (c) Time-frequency spectrum (broad support), (d) Frequency-frequency spectrum (broad support).

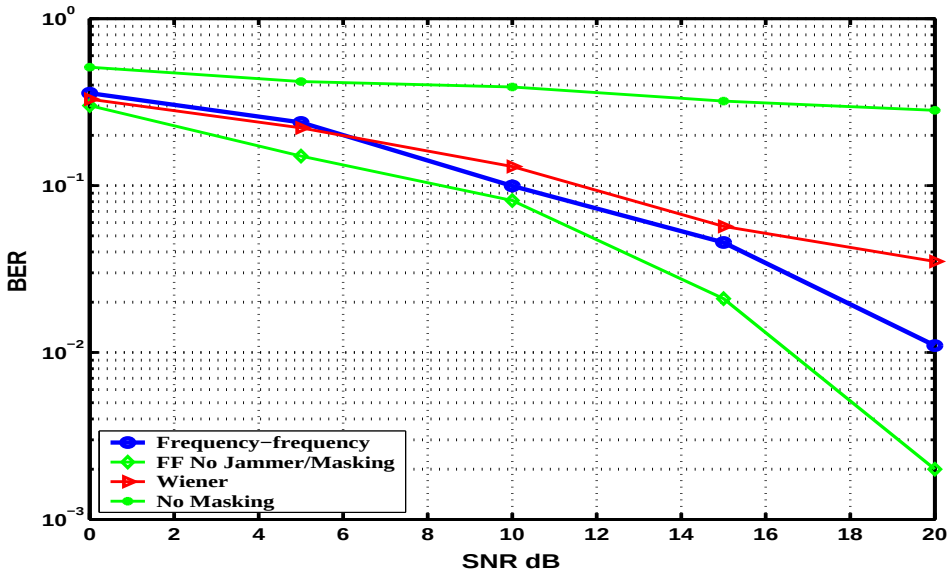

Figure 30: Excision of interference of narrow support.

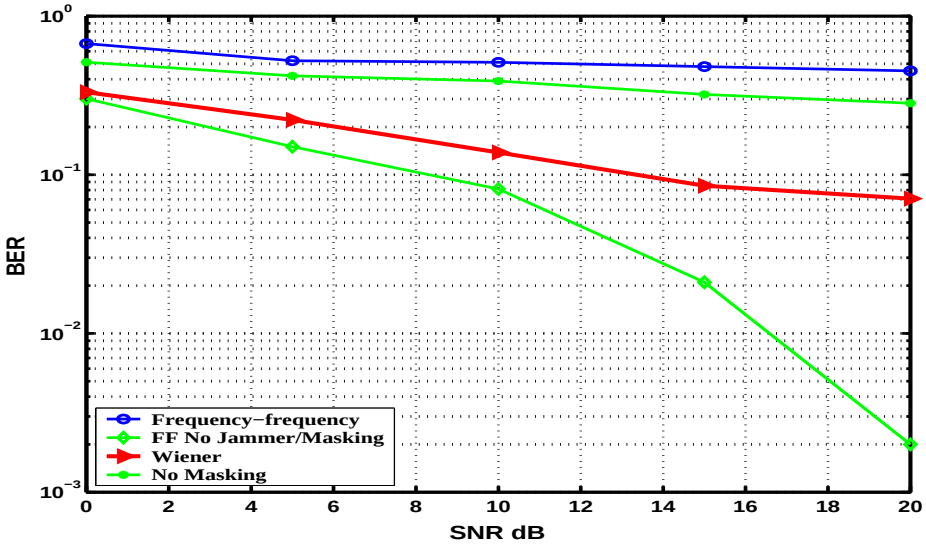

Figure 31: Excision of interference with broad support.

5.4 BROADBAND JAMMER EXCISION IN MULTIUSER AND MULTIPATH DSSS

In section 6.2, it was shown that the Wiener masking receiver is robust for excising interferences of broad support such as chirps and non-stationary jammers. In this section, we use Wiener masking in the multiuser DSSS receiver to deal with jammers. The function of the Wiener masking filter in this case is to mitigate chirp jamming signals, interference caused by multipath effects, and channel noise as well.

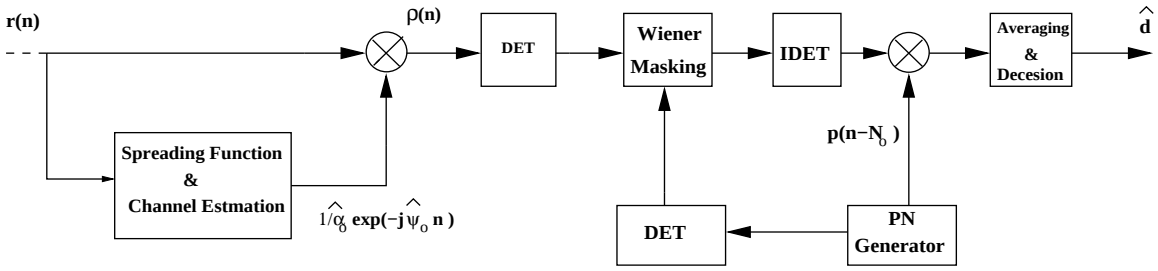

Figure 32: DSSS Receiver with Wiener masking

5.4.1 Wiener Masking in Downlink

Based on channel estimation, the received signal $r(n)$ is demodulated and scaled by $e^{j\hat{\psi}_0 n}/\hat{\alpha}_0$ corresponding to the shortest path signal obtained from the estimated spreading function. For user i, among a total of U users, the scaled and demodulated output signal is

$$\begin{aligned}
\rho_i(n) &= r(n) \times \frac{e^{-j\hat{\psi}_o n}}{\hat{\alpha}_o} \\
&= \left[\sum_{\ell=0}^{L-1} \alpha_\ell e^{j\psi_\ell n} \sum_{u=0}^{U-1} d_u p_u(n - N_\ell) + \eta(n) + j(n)\right] \frac{e^{-j\hat{\psi}_0 n}}{\hat{\alpha}_o} \\
&= d_i p_i(n - \hat{N}_0) + \gamma(n), \qquad (5.12)
\end{aligned}$$

where

$$\gamma(n) = \left[\sum_{\ell=1}^{L-1} \alpha_\ell e^{j\psi_\ell n} \sum_{u\neq i} d_u p_u(n - N_\ell) + \eta(n) + j(n)\right] \frac{e^{-j\hat{\psi}_0 n}}{\hat{\alpha}_o}, \qquad (5.13)$$

is the total interference, which includes channel noise $\eta(n)$, multipath interference, and the chirp jamming signal $j(n)$. Excising $\gamma(n)$ is then possible by means of Wiener masking, which gives a good estimate of $d_i p_i(n - N_0)$. Figure 32 illustrates the Wiener receiver at the desired user.

The demodulated and scaled signal $\rho_i(n)$ is the input to the Wiener mask and has an evolutionary kernel

$$R_i(n, w_k) = \sum_{n=0}^{N-1} \rho_i(n) W(n, m) e^{-j\omega_k m}$$

where $W(n, m)$ is time-varying window obtained from Gabor expansion defined in (2.31). The reference signal is the shifted version of the pseudo-noise $p_i(n - \hat{N}_o)$ generated at user i. Thus, for each bit, information about the spreading sequence does not change, and we can compute *a priori* its time-frequency evolutionary spectrum, $|P_i(n, \omega)|^2$.

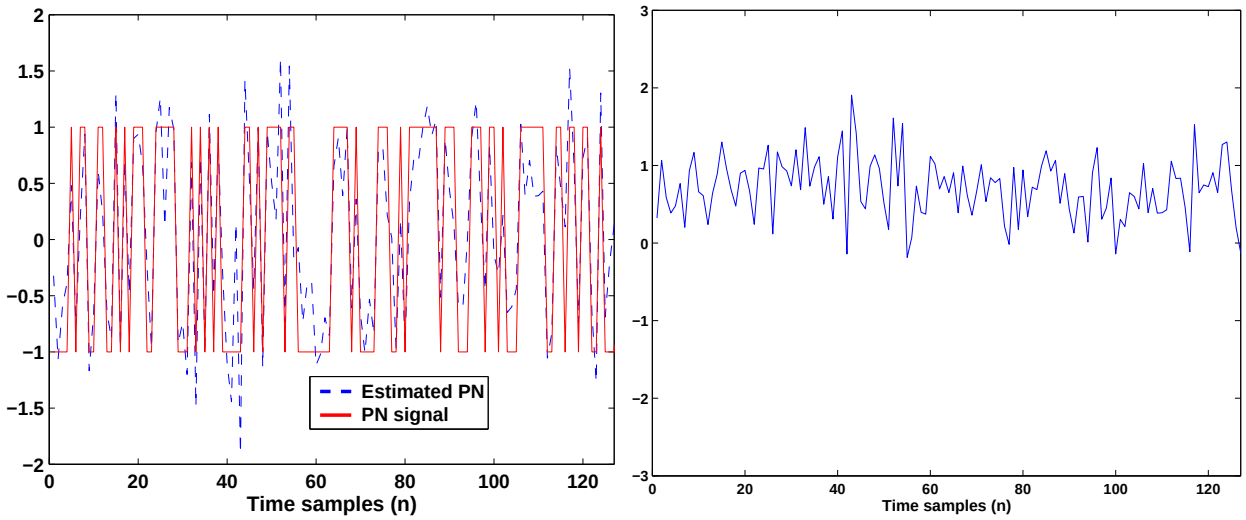

(a) (b)

Figure 33: Example 2 results: (a) Estimated (dotted line) and original PN sequence (solid line), (b) Despreaded signal from Wiener masking.

This spectrum and the spectrum of the received modulated signal $\rho_i(n)$ can be used to obtain a mean-square estimate of the signal, $x_i(n) = d_i p_i(n - \hat{N}_0)$. The estimated signal is

the output of the time-varying filter or mask which has the Wold-Cramer representation

$$\hat{x}_i(n) = \int_{-\pi}^{\pi} R_i(n,\omega) M(n,\omega) e^{j\omega n} dZ_u(\omega) \tag{5.14}$$

where $R(n,\omega)$ is the evolutionary kernel of $\rho_i(n)$, and $M(n,\omega)$ is the masking function given by

$$M_i(n,\omega) = \frac{|P_i(n,\omega)|^2}{|R_i(n,\omega)|^2} \tag{5.15}$$

or the ratio of the evolutionary spectra of $x(n) = p_i(n - \hat{N}_0)$ and that of the data $\rho_i(n)$.

The estimated signal $\hat{x}_i(n)$ is obtained by taking the inverse discrete evolutionary transform IDET of the masked evolutionary kernel. Multiplying it with the the reference signal $p_i(n - \hat{N}_0)$, and taking the average will give the transmitted binary bit $\hat{d} = \pm 1$. Figure 33-a shows for user 0 the original pseudo-noise $p_0(n - \hat{N}_0)$ (solid line), along with the estimated pseudo-noise signal $\hat{p}_i(n - \hat{N}_0)$ (dashed line) obtained from Wiener masking output in a multiuser channel (2 users) with chirp jammer (JSR=3 dB) and channel noise (SNR=10dB). Figure 33-b shows the despreaded signal $p_i(n - \hat{N}_0) \times d_u \hat{p}_i(n - \hat{N}_0)$. The average of this signal clearly gives the value of the transmitted bit d_i.

5.4.2 Wiener Masking in Uplink

Similarly, based on the channel estimation, for user i, the received signal $r(n)$ is demodulated and scaled by $e^{j\hat{\omega}_{i,0}(n-\hat{N}_{i,0})}/\hat{\alpha}_{i,0}$, corresponding to the shortest path signal obtained from the estimated spreading function. At the base station received signals coming from active users, each with different channel characterizations are added together to have one combined signal. Each user has its reference receiver at the base station, and for user i, the scaled and demodulated output signal is

$$\begin{aligned}
\rho_i(n) &= r(n) \times \frac{e^{-j\hat{\omega}_{i,o}n}}{\hat{\alpha}_{i,o}} \\
&= \left[\sum_{u=0}^{U-1} d_u \sum_{\ell=0}^{L-1} \alpha_{u,\ell} e^{j\psi_{u,\ell}n} p_u(n - N_{u,\ell}) + \eta(n) + j(n) \right] \frac{e^{-j\hat{\omega}_{i,0}n}}{\hat{\alpha}_{i,o}} \\
&= d_i p_i(n - \hat{N}_{i,0}) + \beta(n)
\end{aligned} \tag{5.16}$$

where

$$\beta(n) = \left[\sum_{u \neq i} d_u \sum_{\ell=0}^{L-1} \alpha_{u,\ell} e^{j\psi_{u,\ell} n} p_u(n - N_{u,\ell}) + \eta(n) + j(n)\right] \frac{e^{-j\hat{\omega}_{i,0} n}}{\hat{\alpha}_{i,o}} \tag{5.17}$$

as the total interference includes channel noise $\eta(n)$, multipath interference, multiuser interference, and the chirp jamming interference signal $j(n)$.

Like the downlink process explained in the last section, the signal $\rho_i(n)$ is defined as the input signal to the Wiener mask, and the reference signal for *useri* is its pseudo-noise signature shifted with amount of shift equal to the estimated delay $N_{i,o}$. The Wiener mask is obtained as in Equation (5.5) using the discrete evolutionary transform. The output of the Wiener mask is the estimated pseudo-noise for that user. The final receiver diagram is same as the downlink receiver shown in Figure 32.

5.5 SIMULATION

To illustrate the performance of the Wiener masking receiver, for the uplink and the downlink, a linear FM jammer is added to the received signal. We considered jammer to signal ratios (JSR) ranging from -2 dB to 8 dB. For each user, we modeled the channel as time-varying channel varying randomly in the number paths (from 1 to 4), delays (from 1 to $0.8M_p$), and Doppler frequency shifts ψ_ℓ (from 0 to π). The gains α_ℓ were linearly related to the delays. Figures 34 and 35 show the BER vs JSR results at different SNRs for the uplink and downlink transmissions, respectively. As expected, the Wiener mask helps not only in the excision of the jammer but also in de-noising the received signal from the channel noise as well as interferences from the same user and other users. The performance of the channel parameter estimation is greatly affected by jammers with significant JSR. More sophisticated approaches would be needed.

5.6 SUMMARY

In this chapter we have proposed two methods to excise interference in DSSS: one that uses a frequency-frequency DET masking approach, and the other an application of the non-stationary evolutionary Wiener filtering with mean-squared based mask. In the first part, the analysis was for a single user and neglecting multipath effects. In both approaches it is assumed that the pseudo noise signal is available, and we wish to determine the value of the sent bit d_m. No special characterization for the interference is made; we only need to know if it is narrowly or broadly supported. Given the compression of data in the frequency-frequency kernels, it is shown that by locating the regions in the frequency-frequency plane where the interference is not present, or has less power, an estimate of the sent bit can be obtained. When the interference is of broad support, the Wiener masking method performs better than the frequency-frequency method. The application of one algorithm instead of the other depends on *a-priori* information about the type of support of interference, rather than on its characterization. Also, Wiener masking depends on the connection between the signal and the kernel, a unique property of the evolutionary methods.

The results obtained in the first part indicate that the Wiener masking scheme is robust with a jammer of broad support, alloying one to employ it in multiuser channels to excise such interference. Another reason for choosing Wiener masking over the frequency-frequency scheme is the type of broadband interference that comes form multiple-user interference in such situations. A Wiener masking receiver was implemented which follows the channel estimation and capable of excising broad band jammers.

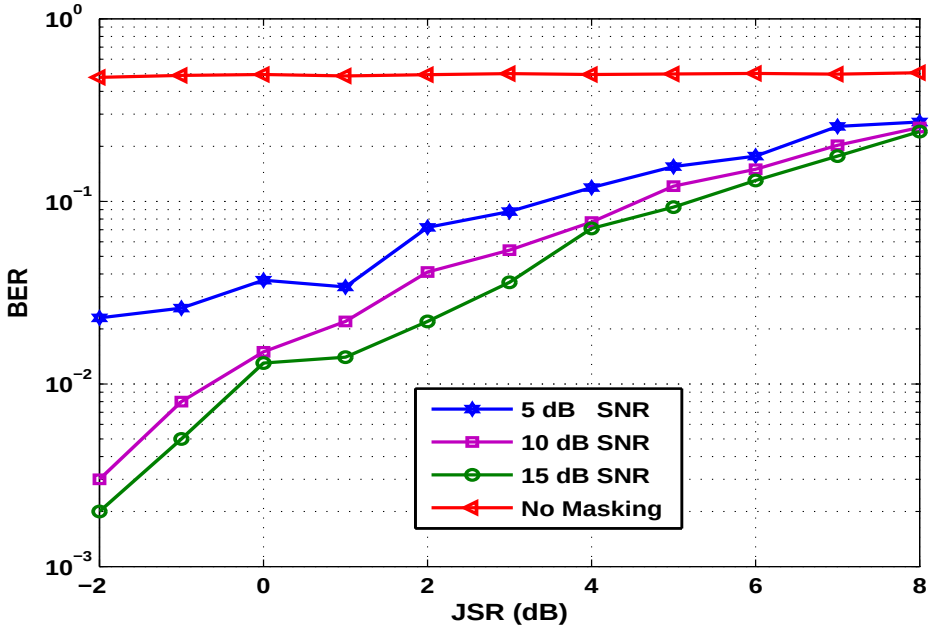

Figure 34: Bit error rate BER vs JSRs for different SNRs for uplink

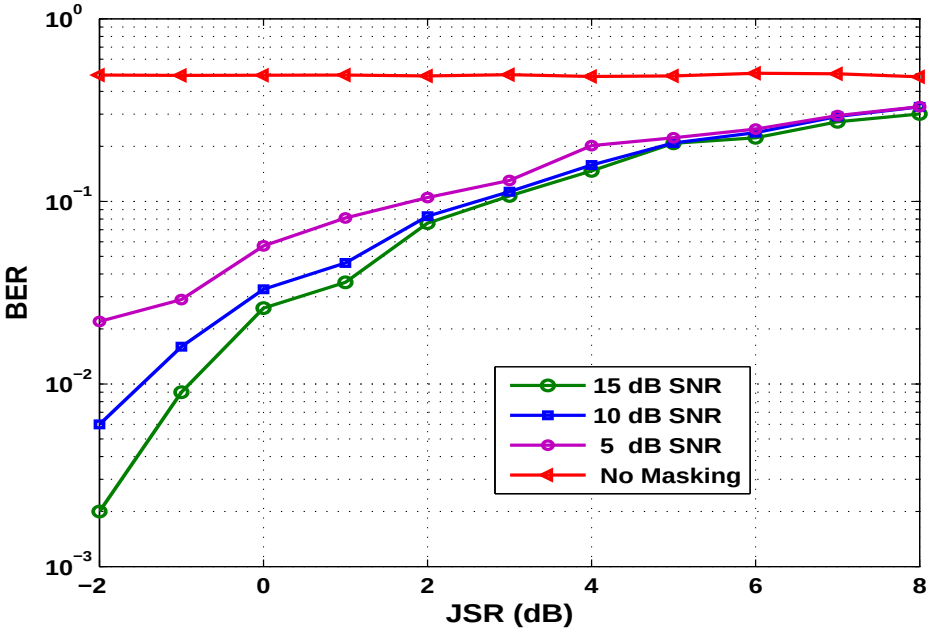

Figure 35: Bit error rate BER vs JSRs for different SNRs for downlink

6.0 CONCLUSIONS

This dissertation addressed the problem of blindly estimating multipath communication channel parameters such as time-delays, Doppler frequency shifts, and attenuation factors in direct sequence spread spectrum communication systems. The channel is characterized by means of the spreading function obtained from the time-frequency evolutionary kernel of the overlapped received signal.

The assumption of a constant channel during the transmission of a single data symbol or frame allows the use of formulas of linear time invariant systems to calculate the channel impulse response. The proposed LTV channel model has been related to direct-sequence spread-spectrum communication systems (DSSS); such a model is characterized by parameters such as time-delays, frequency shifts, and attenuation factors associated with signals coming from various paths. This model contains all-pass filters that characterize the delays, constant attenuation factors, and exponential modulators that characterizes the frequency or Doppler shifts. The discrete evolutionary transform DET has been used for computing the time-frequency kernel from the received signal. The connection between channel time-varying frequency response and Zadeh's transfer function was used to compute the spreading function, which depicts the parameters of the channel as large peaks corresponding to the Doppler shifts frequency locations corresponding to the time-delays of the multipath signals with amplitudes equal to their gains.

The use of time-frequency representation in the mitigation of interference signals has been of great concern. The two schemes we have proposed are time-frequency based by means of masking the time-frequency spectrum, utilizing the fact that the spreading signal is always known at both the transmitter and at the receiver; therefore the direct sequence has the same spectrum independent of the sign of the sent bit. When interference is of broad

support, the Wiener masking method performs better than the frequency-frequency method.

The Wiener masking scheme has been used to excise any intentional broadband jammer and multiuser interference. The implementation of Wiener masking was possible for multiuser transmission situations, both uplink and downlink.

6.1 CONTRIBUTIONS

The contributions made in this dissertation are related to the issues of identifying and estimating multipath channel parameters from the overlap DSSS signal at the receiver. We developed a DSSS communication channel modeling and estimation technique for single and multiuser transmission channels using the evolutionary theory that provides the time-frequency evolutionary kernel, which is related to Zadeh's transfer function known as the LTV channel transfer function, or time-varying frequency response of the LTV channel. Using the spreading function obtained from the time-varying frequency response of the channel could provide a blind estimation of channel parameters directly from the combined received signal. We presented this approach as a new idea of using time-frequency analysis in blind multipath DSSS channel estimation. We addressed and used the time-varying channel functions and their relations to obtain the spreading function that provides estimates of channel parameters from its peaks. We also developed an evolutionary frequency-frequency spectrum, that has been presented in the thesis as an extension of the evolutionary time-frequency spectrum, capable of compacting information in a small region around low frequencies.

We proposed two interference mitigation techniques that were developed based on the time-frequency and frequency-frequency evolutionary kernels by means of spectrum masking. In both approaches, the priori knowledge of the PN at the receiver has been used to obtain the time-frequency and frequency-frequency evolutionary kernels. We compared both approaches for interferences to narrow and wide support. The frequency-frequency based masking shows superior performance in the case of narrow support, while time-frequency wiener masking performs better under broad support interference.

In the detection part, we implemented 2 DSSS receivers based on channel estimates

obtained from the spreading function. The first scheme is a generalized approach, while the second is for bit detection and excision of broadband jammers. Both methods use the channel estimates of the first, or shortest path signal to detect the correct binary data. The estimated parameters are efficiently utilized to demodulate, scale, and shift the received signal providing a signal that has a mean value equal to $\pm d$.

Furthermore, a proper implementation of the Winer masking approach has been employed to excise broadband interference in multiuser DSSS applications, namely in uplink and downlink communication channels.

6.2 FUTURE WORK

The problem of efficient channel estimation when both Doppler and time-delay are present in the channel remains an area for further research. At the present, this research focuses on the modeling and estimation of direct sequence spread spectrum communication channels only. It is important to extend this work to other communications schemes such as orthogonal frequency division multiple aces (OFDM), multi-carrier code division multiple aces (MC-CDMA), and multi-carrier direct sequence (MC-DS).

In chapter 2, the developed frequency-frequency evolutionary spectrum does not reveal time information, and only shows peaks at the zero frequency of the new frequency domain Ω corresponding to frequency components of the signal at frequency domain ω. However, the phase contains time information and it is important to exploit it and examine its significance, and investigating more appropriate applications. One possible application is in the case of jammer excision for multiple users, similar to the case of Wiener excision developed in 6.4.2. It is also important to look at the instantaneous frequency and instantaneous bandwidth described in such a representation.

APPENDIX A

GABOR EXPANSION

In conventional Fourier transform, the signal is represented via complex sinusoidal functions. Because sinusoidal basis functions spread over the entire time domain and are not concentrated in time, the Fourier transform does not explicitly indicate how a signal's frequency contents evolve in time. A natural way to characterize a signal in time and frequency simultaneously is to represent it the signal with elementary functions that are concentrated in both time and frequency domains, such as the frequency modulated Gaussian function. Gaussian-type functions are optimally concentrated in the joint time and frequency domains, reflecting the signal's behavior in local time and frequency.

Gabor expansion represents a signal in terms of time and frequency shifted basis functions, and has been used in various applications to analyze the time-varying frequency content of a signal [10, 13, 15, 17]. Elementary basis or logons of the Gabor representation are obtained by translating and modulating a single window function. This single window function has a Gaussian shape and called the mother Gabor function, and is given by

$$h(n) = \frac{1}{(\pi\sigma^2)^{\frac{1}{4}}} exp\left\{-\frac{[n-0.5(N-1)]^2}{2\sigma^2}\right\} \tag{A.1}$$

where σ is the standard deviation constrained by $3\sigma \leq (N-1)/2$. This function is shown in Fig. 36.

The discrete-time Gabor representation:

A discrete-time Gabor representation was defined from the continuous-time representa-

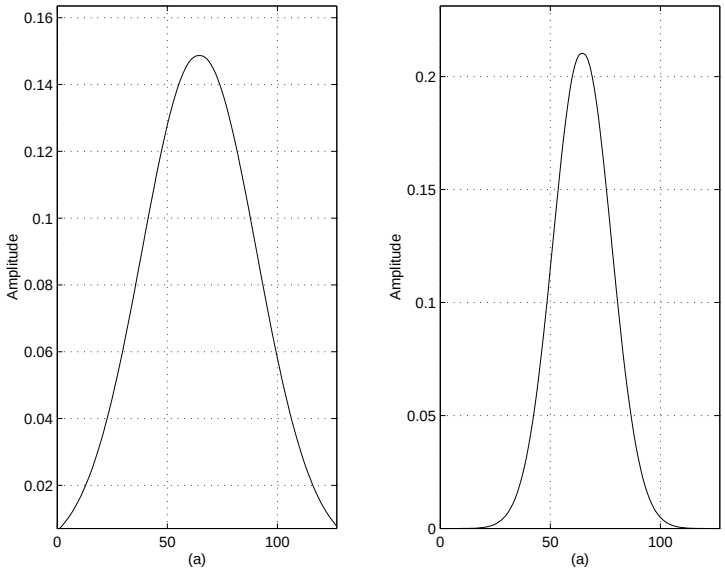

Figure 36: Gaussian window $h(n)$ with two different scales.

tion by applying sampling theory and the discrete Poisson-sum formula [5]. The discrete Gabor expansion of a discrete-time, finite extent signal $x(n)$ is given by

$$x(n) = \sum_{m=0}^{M-1} \sum_{k=0}^{K-1} a_{m,k} \widetilde{h}_{m,k}(n) \qquad 0 \leq n \leq N-1 \tag{A.2}$$

where the elementary signal is

$$\widetilde{h}_{m,k}(n) = \widetilde{h}(n - mL) e^{jw_k n} \tag{A.3}$$

and $\widetilde{h}(n)$ is a periodic extension of the synthesis window $h(n), i.e.,$

$$\widetilde{h}(n) = \sum_{r} h(n + rN) \tag{A.4}$$

and $w_k = \frac{2\pi L^{'}}{N} k$, and positive integers M, K, L and $L^{'}$ are constrained according to

$$ML = KL^{'} = N. \tag{A.5}$$

where M and K are the number of samples in time and frequency respectively.

There are several methods to calculate Gabor coefficients [21]: using biorthogonal functions, the Zak transform, or by deconvolution of the sample Short-Time Fourier transform. We use the first method here which was introduced by Bastiaans [11] and uses an auxiliary function $\gamma(n)$ called the biorthogonal window, or dual function of $h(n)$. The Gabor coefficients are evaluated by

$$a_{m,k}(n) =< x(n), \widetilde{\gamma}_{m,k} >= \sum_{n=0}^{N-1} x(n)\widetilde{\gamma}^*_{m,k}(n) \tag{A.6}$$

where $\widetilde{\gamma}_{m,k}(n)$ is obtained from the biorthogonal analysis window $\widetilde{\gamma}(n)$ as

$$\widetilde{\gamma}_{m,k}(n) = \widetilde{\gamma}(n - mL)e^{jw_k n}. \tag{A.7}$$

High Resolution Gabor Expansion:

Higher resolution in Gabor expansion is obtained by using scaled versions of the synthesis window [17]. This approach called the multi-scale Gabor expansion and the scaled window generated from a the mother Gabor window $h(n)$ by scaling, i.e.,

$$h_i(n) = 2^{\frac{i}{2}} h(2^i n), \qquad 0 \leq n \leq N-1, \qquad i = 0, 1, ..., I-1 \tag{A.8}$$

Thus the multi-scale expansion for a finite energy signal $x(n)(0 \leq n \leq N-1)$ is

$$x(n) = \frac{1}{I} \sum_{i=0}^{I-1} \sum_{m=0}^{M-1} \sum_{k=0}^{K-1} a_{i,m,k} \tilde{h}_{i,m,k}(n) \qquad 0 \leq n \leq N-1 \tag{A.9}$$

where I is the number of resolutions used in the analysis of the signal. The multi-scale Gabor expansion representation of the signal $x(n)$ is given as the average of I representations, each obtained at a different resolution level or scale. The logon $\tilde{h}_{i,m,k}(n)$ is centered at $n = mL$ and is localized over a time domain determined by the scale 2^i. The Gabor coefficients are evaluated as before by

$$a_{i,m,k} =< x(n), \tilde{\gamma}_{i,m,k}(n) >= \sum_{n=0}^{N-1} x(n)\tilde{\gamma}^*_{i,m,k}(n) \tag{A.10}$$

where

$$\tilde{\gamma}_{i,m,k}(n) = \tilde{\gamma}_i(n - mL)e^{jw_k n} \tag{A.11}$$

is the scaled analysis (biorthogonal) window obtained from the biorthogonality condition, similar to the regular discrete Gabor expansion introduced in the last section.

APPENDIX B

PSEUDORANDOM SEQUENCE

The pseudo-noise (PN) or pseudorandom sequence is a binary sequence generated using sequential logic circuits. Although it is deterministic, a pseudonoise sequence has many characteristics that are similar to those of random binary sequences. As a result of having randomness, it is used in several applications of communication systems such as data scrambling, spread spectrum, and encryption [3, 9]. It is generated using sequential logic circuits known as a feedback shift register. A feedback shift register, which is shown in Fig 29, consists of consecutive stages of two state memory devices and feedback logic [57]. Binary sequences are shifted through the shift registers in response to clock pulses, and the output of the various stages are logically combined and fed back as input to the first stage.

When the feedback logic consists of exclusive-OR gates, which is usually the case, the shift register is called a linear PN sequence generator. If a linear shift register reaches zero state at some point of time, it should always remain in the zero state, and the output would subsequently be all 0's. The period of a sequence generated by an m-stage shift register is $L = 2^m - 1$ bits. The pseudo-noise sequence p(n) after each clock cycle n is the content from the first stage register. Therefore, the content of the $(i-1)^{th}$ stage is placed by the content of the i^{th} stage, denoted as $a_i(n)$. The last stage can be obtained by

$$a_m(n) = \sum_{i=1}^{m} a_i(n-1)b_i(mod2)$$

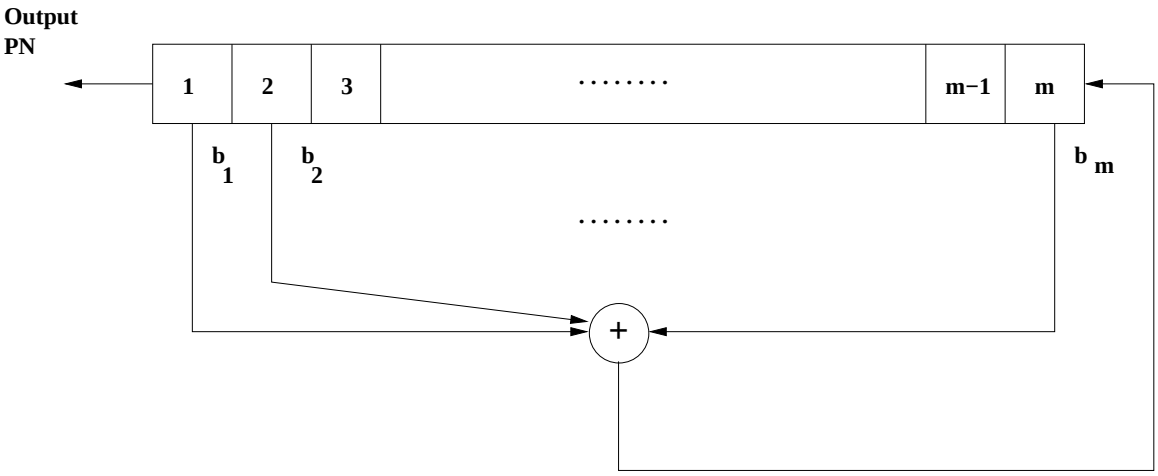

Figure 37: Binary linear shift register sequence generator.

where the initial $a_i(0)$ is

$$a_i(n) = \begin{cases} 1, & \text{i=1} \\ 0, & \text{i=2,...,m} \end{cases}$$

and b_i for $i\epsilon 1, ..., m$ is a stage connector to the modulo-2 adder. In DSSS, the PN sequence of 0's and 1's is changed to a corresponding set of -1's and 1's called a bipolar sequence.

PN Autocorrelation Function

The autocorrelation function $R_p(\tau)$ of PN sequence $p(t)$, with period T_0, can be given in normalized form as

$$R_p(\tau) = \frac{1}{K}(\frac{1}{T_0}) \int_{-\frac{T_0}{2}}^{\frac{T_0}{2}} p(t)p(t+\tau)dt \tag{B.1}$$

where

$$K = \frac{1}{T_0} \int_{-\frac{T_0}{2}}^{\frac{T_0}{2}} p^2(t)dt \tag{B.2}$$

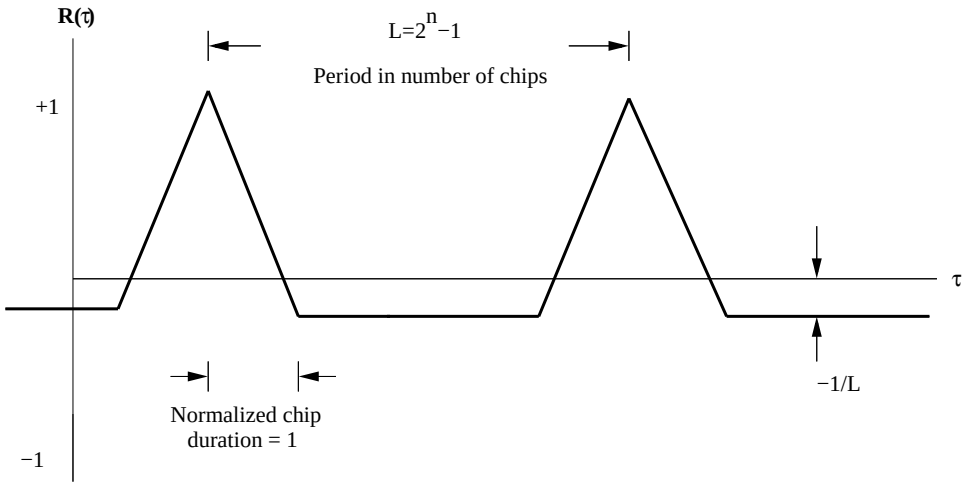

Figure 38: Autocorrelation function of PN code signal.

When $p(t)$ is a periodic pulse waveform representing a PN code, we refer to each fundamental pulse as a PN code symbol or a chip. The normalized autocorrelation function for a maximal length sequence, $R_p(\tau)$, is shown in Figure (38).

It is clear that for $\tau = 0$, that is, when $p(t)$ and its replica are perfectly matched, $R_p(\tau) = 1$. However, for any cyclic shift between $p(t)$ and $p(t - \tau)$ with $(0 \leq \tau < L - 1)$, the autocorrelation function is equal to $-1/L$ (for large L, the sequences are virtually decorrelated for a shift of a single chip). Since PN is periodic, the autocorrelation function $R_p(\tau)$ is also periodic, with the same period L as shown in Figure (38).

APPENDIX C

RAKE RECEIVER

A RAKE receiver, shown in Figure (39) below, is essentially a diversity receiver designed specifically for CDMA, where diversity is provided by the fact that multipath components are practically uncorrelated from one another when their relative propagation delays exceed a chip period [62].

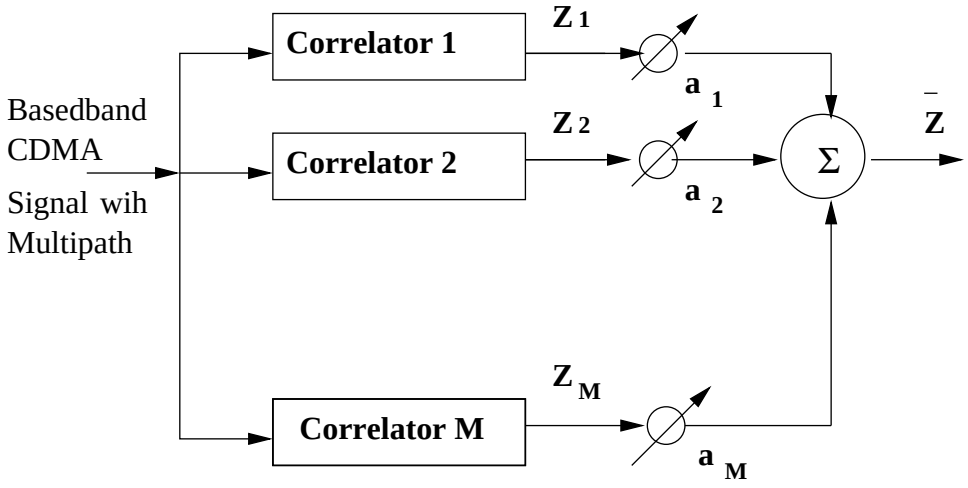

Figure 39: RAKE receiver.

A RAKE receiver utilizes multiple correlators to separately detect the M strongest multipath components. The output of each correlator is weighted to provide a better estimate of the transmitted signal than provided by a single component. Demodulation and bit decisions are then based on the weighted outputs of M correlators. The M decision statistics

are weighted to form an overall decision statistic as shown in Fig 33 above. The outputs of the M correlators are denoted as Z_1, Z_2, ... and Z_M, and are weighted by a_1, a_2, ... and a_M, respectively. These weighting coefficients are based on the power of the SNR from each correlator output. If the power, or SNR from a particular correlator is small, it will be assigned a minimal weighting factor. The overall combined signal $\bar{Z}$ is given by

$$\bar{Z} = \sum_{m=1}^{M} a_m Z_m$$

The weighting coefficients a_m are normalized to the output signal power of the correlator in such a way that the coefficients sum to unity

$$a_m = \frac{Z_m^2}{\sum_{m=1}^{M} Z_m^2}$$

In the combining process, the various signal inputs are individually weighted and added together as

$$\begin{aligned} r(t) &= a_1 r_1(t) + a_2 r_2(t) + ... + a_M r_M(t) \\ &= \sum_{m=1}^{M} a_m r_m(t) \end{aligned} \tag{C.1}$$

where $r_m(t)$ is the envelope of the i^{th} signal, and a_m is the weight factor applied to the i^{th} signal. Since the goal of the combiner is to improve noise performance of the system, the analysis of combiners is generally performed in terms of SNR. Several combining methods are used such as selection-combiner, maximal-ration combining, and equal-gain combining [62, 57].

BIBLIOGRAPHY

[1] Proakis, J., *Digital Communications.* McGraw-Hill, New York, 1995.

[2] Sklar, B., *Digital Communication.* Academic Press, London, 1988.

[3] Proakis, J. and Salehi, M., *Communication Systems Engineering.* Prentice Hall, 1978.

[4] Rappaport, T. S., *Wireless Communication.* Prentice Hall 1996.

[5] Sklar, B., "Rayleigh fading channels in mobile digital communication systems part I: Characterization," *IEEE Communications Magazine*, Vol. 35, Issue 7, pp.90-100, July 1997.

[6] Sklar, B., "Rayleigh fading channels in mobile digital communication systems part II: Mitigation," *IEEE Communications Magazine*, Vol. 35, Issue 7, pp.102-109, July 1997.

[7] Bello, P. A., "Characterization of randomly time-variant linear channels," *IEEE Trans. Commun. Syst.,* Vol. CS-11, pp.360-393, Dec. 1963.

[8] Kay, S. M. and Doyle, S. B., "Rapid Estimation of the Range-Doppler Scattering Function," *IEEE Trans. Signal Processing.,* Vol. 51, No. 1, pp.255-268, Jan. 2003.

[9] Garg, V. K. *Wireless Network Evolution : 2G to 3G.* Prentice Hall, NJ, 2000.

[10] Cohen, L., *Time-Frequency Analysis.*Prentice Hall, Englewood Cliffs, NJ, 1995.

[11] Priestley, M.B., *Non-linear and Non-stationary Time Series Analysis.* Academic Press, London, 1988.

[12] Rabiner, L.R., and Schafer, R.W. *Digital Processing of Speech Signals.* Prentice Hall, Englewood Clifs, NJ., 1978.

[13] Wexler, J., and Raz, S., "Discrete Gabor Expansions," *Signal Processing,* Vol. 21, No. 3, pp.207-220, Nov. 1990.

[14] Priestley, M.B., *Spectral Analysis and Time Series.* Academic Press, London, 1981.

[15] Akan, A., and Chaparro, L.F., "Evolutionary Spectral Analysis and the Generalized Gabor Expansion," *IEEE Proc. ICASSP-95,* Vol. 3, pp. 1537-1540, Detroit, MI, May 1995.

[16] Akan, A., and Chaparro, L.F., "Evolutionary Spectral Analysis Using a Warped Gabor Expansion," *IEEE ICASSP,* Vol. 3, pp. 1403-7, Atlanta GA, May 1996.

[17] Akan, A., and Chaparro, L.F., "Multi-window Gabor Expansion for Evolutionary Spectral Analysis," *Signal Processing,* Vol. 63, No.3, pp. 249-62, Dec. 1997.

[18] Qian, S., and Chen, D., *Joint Time-Frequency Analysis: Methods and Applications.* Prentice Hall, NJ, 1996.

[19] Bastiaans, M.J., "Gabor's Expansion of a Signal into Gaussian Elementary Signals," *Proc. IEEE* Vol. 68, No. 4, pp. 538-39, Apr. 1980.

[20] Suleesathira, R., Chaparro, L.F., and Aydin, A., "Discrete Evolutionary Transform for Time-Frequency Signal Analysis," *Journal of the Franklin Institute,* Special Issue on Time-Frequency Signal Analysis and Its Applications, Vol. 337, No. 4, pp. 347-64, Jul. 2000.

[21] Suleesathira R., T., and Chaparro, L.F., "Evolutionary Spectral Analysis Using Malvar Wavelet Transform, " *Proceedings of the IEEE-SP International Symposium on Time-Frequency and Time-Scale Analysis,* PP. 673-6 Pittsburgh, Oct. 1998.

[22] Suleesathira, R., Chaparro, L.F., and Aydin, A., "Discrete Evolutionary Transform for Time-Frequency Analysis," *Proceedings of 32^{th} Asilomar Conference on Signals, Systems and Computers,* pp. 812-6, California, Nov. 1998.

[23] Qian, S., "Discrete Gabor Transform," *IEEE Transactions on Signal Processing.* Vol. 41, No. 7, pp. 2429-39, July 1993.

[24] Qian, S., "A Complement to a Derivation of Discrete Gabor Expansions," *IEEE Signal Processing Letters,* Vol. 2, No. 2, pp. 31-33, Feb. 1995.

[25] Kayhan A.S., El-Jaroudi A., and Chaparro L.F., "Evolutionary Periodogram for Non-Stationary Signals," *IEEE Trans. on Signal Proc.,* Vol. 42, No. 6, pp. 1527-36, June 1994.

[26] Choi, H., and Williams, W.J., "Improved Time-Frequency Representation of Multicomponent Signals Using Exponential Kernels," *IEEE Trans. on ASSP,* Vol. 37, No. 6, pp. 862-71, June 1989.

[27] Al-Shoshan, A., and Chaparro, L.F., "Identification of Non-minimum Phase Systems Using Evolutionary Spectral Theory," *Signal Processing,* Vol. 55, No. 1, pp. 79-92, Nov. 1996.

[28] Melard, G., and Schutter, A.H., "Contributions to Evolutionary Spectral Theory," *Journal Time Series Analysis,* Vol. 10, pp.41-63, Jan. 1989.

[29] Cramer, H., "On Some Classes of Non-stationary Stochastic Processes," *Proc. of the Fourth Berkely Symp. on Math. Stat. and Prob.,* pp. 57-78, 1961.

[30] Aydin, A. *Time–Frequency Signal Analysis in Gabor Spaces.* PhD Dissertation, University of Pittsburgh, Pittsburgh, PA, 1996.

[31] Priestley M.B. "Evolutionary Spectral and Non-stationary Processes," *J. R. Statistics Soc. B.,* pp. 204-237, 1965.

[32] Kayhan, A.S., and El-Jaroudi, A., and Chaparro, L.F. "Data-Adaptive Evolutionary Spectral Estimation," *IEEE Trans. on Signal Proc.,* pp. 204-213, 1995.

[33] Detka, C., and El-Jaroudi, A., and Chaparro, L "Relating the Bilinear Distributions and the Evolutionary Spectrum," *IEEE Proc. ICASSP'93,* Vol. IV, pp. 496-499, 1993.

[34] Shah, S.I., and Chaparro, L.F., and Kayhan, A.S. "Evolutionary Maximum Entropy Spectral Analysis," *IEEE Proc. ICASSP'94,* Vol. IV, pp. 285-288, 1994.

[35] Al-Shoshan A. I. *System Identification and Modeling of Nonstationary Signals.* PhD Dissertation, University of Pittsburgh, Pittsburgh, PA, 1995.

[36] Khan H. A. *Time–Frequency Masking and Signal Estimation Using Evolutionary Spectral Theory.* PhD Dissertation, University of Pittsburgh, Pittsburgh, PA, 1996.

[37] Papoulis, A., *Probability, Random Variables, and Stochastic Processes.* McGraw-Hill, Inc., 1991.

[38] Oppenheim, A. V., and Schafer, R. W. *Discrete-Time Signal Processing.* Prentice-Hall, Englewood Cliffs, N.J., 1989.

[39] Cohen L., "Time-Frequency Distributions — A Review," *Proc. IEEE* Vol. 77, No. 7, pp. 941-981, July, 1989.

[40] Suleesathira R., "Jammer Excision In Spread Spectrum Using Discrete Evolutionary-Hough Transform," *Ph.D. Dessertation*, University of Pittsburgh, 2001.

[41] Amin, M.G. and Akansu, N.A., "Time-Frequency for Interference Excision in Spread Spectrum Communications," *IEEE Signal Precessing Magazine*, Vol. 16, No. 2, pp.33-4, Mar. 1999.

[42] Amin, M.G., and Mandapati, R.G., "Nonstationary Interference Excision in Spread Spectrum Communications Using Projection Filtering Methods," *Preceedings of* 34^{th} *Asilomar Conference on Singals, Systems, and Computers*, pp.827-31, California, Nov. 1998.

[43] Amin, M.G., "Interference Mitigation in Spread Spectrum Communication Systems Using Time-Frequency Distributions," *IEEE Trans. on Signal Processing*, Vol. 45, No. 1, pp.90-101, Jan. 1997.

[44] Amin, M.G., Wang, C., and Lindsay, A.R., "Optimum Interference Excision in Spread Spectrum Communications Using Open-loop Adaptive Filters." *IEEE Trans. on Signal Processing,* Vol. 47, No.7, pp.1966-76, Jul. 1999.

[45] Chaparro, L.F. and Suleesathira, R., "Non-stationary jammer excision in spread spectrum communications via discrete evolutionary and Hough transforms," *Singnal Processing* , Vol.83, pp.1117-1133, 2003.

[46] Suleesathira, R., and Chaparro, L.F., "Jammer Excision in Spread Spectrum Using Discrete Evolutionary-Hough Transform and Singular Value Decomposition," *Proceedings of* 10^th *IEEE Workshop on Statistical signal and Array Processing,* pp.519-24, Poconos, PA, Aug.2000.

[47] Barabarossa, S., and Scaglione, A., "Adaptive Time-varying Cancellation of Wide-band Interference in Spread Spectrum Communications Based on Time-frequency Distributions," *IEEE Trans. on Signal Processing,* Vol.47, No.4, pp.957-65, Apr. 1999.

[48] Jang, S., and Loughlin, P.J., "Effect and Suppression of Wideband AM-FM Interference in Direct Sequence Spread Spectrum Communication Systems," *Int. Conf. Telecommunications,* Acapulco. Mexico, May 2000.

[49] Jang, S., and Loughlin, P.J., "Use of Instanteneous Bandwidth for Excising AM-FM Jammers in Direct Sequence Spread Spectrum Communication Systems," *SPIE Int. Symp. on Optical Science and Technology*, San Diego CA, Jul. 2000.

[50] Chaparro, L.F., Suleesathira, R., Aydin, A., and Basar, "Instantaneous Frequency Estimation Using Discrete Evolutionary Transform for Jammer Excision," *Proceedings of the IEEE ICASSP*, Salt Lake City, Utah, May 2001.

[51] Bultan, A., and Akansu, N.A. "A Novel Time-frequency Exciser in Spread Spectrum Communications for Chirp-like Interference," *Proceedings of the IEEE ICASSP*, pp. 3265-8, Seattle, WA, May 1998.

[52] Yimin, Z., and Amin, M.G., "Array Processing for Nonstationary Interfernce Suppression in DS/SS Communications Using Subspace Projection Techniques," *Trans. on Signal Processing*, Vol. 49, No. 12, Dec. 2001.

[53] Ertugrul, S., and Akan, A. "Broadband Jammer Excision in Spread Spectrum Communication Systems Using Time-Frequency Masking," *Proceedings of of the IEEE Signal Processing Workshop*, pp.48-51, 1999.

[54] Khan, H., and Chaparro, L.F., "Formulation and implementation of the non-stationary evolutionary Wiener filtering," *Signal Proc.*, pp.253-67, 1999.

[55] D. Greenwood and L. Hanzo, *Characterization of Mobile Radio Channels,* Mobile Radio Communications, by R. Steele, Ed., Ch. 2, London Pentech press, 1994.

[56] K. Pahlavan and A. H. Levesque, *Wireless Information Networks,* Chs. 3 and 4, New York: Wiley, 1995.

[57] T. S. Rappaport, *Wireless Communications,* Chs. 3 and 4, Upper Saddle River, NJ:Prentice Hall, 1996.

[58] R. L. Bogusch, et. al., "Frequency Selective Propagation Effects on Spread-Spectrum Receiver Tracking," *Proc. IEEE*, vol. 69, no. 7, Jully 1981, pp. 787-96

[59] F. Amoroso, "Use of DS/SS Signaling to Mitigate Rayleigh Fading in a Dense Scatterer Environment," *IEEE Pers. Commun.*, vol. 3, no2, pp. 52-61, Apr. 1996,.

[60] R. H. Clarke, "A Statistical Theory of Mobile Radio Reception," *Bell Sys. Tech. J.*, vol. 47, no. 6, pp. 957-1000, July-Aug. 1968.

[61] F. Amoroso,"Instantaneous Frequency Effects in a Doppler Scattering Environment," *Proc, IEEE ICC* '87, Seattle, WA, pp. 1458-66, June 7-10, 1987

[62] V. K. Garg, *Wireless Network Evolution 2G to 3G,* Upper Saddle River, NJ:Prentice Hall, 2002

[63] Geraniotis, E., "Noncoherent Hybrid DS-SFH Spread-Spectrum Multiple Access Communications," *IEEE Trans. Commun.*, vol. COM34, no. 9, pp. 862-72, Sept, 1986.

[64] Lee, W. C. Y., "Elements of Cellular Mobile Radio Systems," *IEEE Trans. on Vehicular Technology,* vol. V-35, no. 2, pp. 48-56., May 1986.

[65] Andersen, J. B., Rappaport, T. S., Yoshilda, S., "Propagation Measurements and Models for Wireless Communications Channels.", *IEEE Communications Magazine,* vol. 33, no. 1, pp. 42-49, Jan. 1995.

[66] Amoroso, F. "Use of DS/SS Signaling to Mitigate Rayleigh Fading in a Dense Scatterer Environment ," *IEEE personal Communications*, vol. 3, no. 2, pp. 52-61, April 1996.

[67] Amoroso, F., "Instantaneous Frequencyly Effects in a Doppler Scattering Enfironment," *IEEE International Conference on Communications*, June 7-10, 1987, pp. 1458-66.

[68] Price, R. and Green P. E. Jr., "A Communication Technique for Multipath Channels," *Proceedings of the IRE*, vol. 46, pp. 555-70, March 1958.

[69] Fazel K., Kaiser S., *Multi-Carrier Spread-Spectrum and Related Topics. ,* 2001.

[70] A. M. Sayeed, A. Sendonaris, and B. Aazhang, "Multiuser detection in fast-fading multipath environments," *IEEE Journal on Selected Areas in Commun.,* vol. 16, no. 9, pp. 1691-1701m Dec. 1998.

[71] A. M. Sayeed, and B. Aazhang, "Joint multipath-Doppler diversity in fast fading channels," *IEEE International Conference on Acoustics, Speech and Signal Processing*, vol. 6, pp. 3237-40, 1998.

[72] S. Bhashyam, A. M. Sayeed, and B. Aazhang, "Time-selective signaling and reception for communication over multipath fading channels," *IEEE Trans. on Commun.*, vol.48, No. 1,pp. 83-94, Jan. 2000.

[73] A. Feng, Q. Yin, J. Zhang, and Z. Zhao., "Joint Space-multipath-Doppler Rake receiver in DS-CDMA systems over Time-selective fading channels," *IEEE International symposium on circuit and systems,* vol. 1, pp. 601-604, May 2002.

[74] W. C. Y. Lee., "Antenna Spacing Requirements for a Mobile Radio Base Station Diversity," *Bell System Technical Journal,* vol. 50, July-Aug. 1971.

[75] J. C. Liberti, and T. Rappaport., *Smart Antennas for Wireless Communications,* Prentice Hall: Upper Saddle River, NJ, 1999.

[76] F. Amoroso and W. Jones, "Modeling direct sequence pseudonoise(DSPN) signaling with directional antennas in the dense scaterrer mobile environment, " in Proc. *IEEE Veh. Tech. Conf.,* Philadelphia, PA, pp. 419-26, May 1988.

[77] Akbar M. Sayeed and Behnaam Aazhang, "Multiuser Detection in Fast-Fading Multipath Environments," *IEEE Journal of Selected Areas in Communications,* vol. 16, No. 9, pp. 1691-1701, Dec. 1998.

[78] Akbar. M. Sayeed, and B. Aazhang, "Joint multipath-Doppler diversity in mobile wireless communications," *IEEE Trans. on Comm.*, vol. 47, pp. 123-131, January 1999.

[79] Giannakis G. B. and Tepedelenloioglu C, "Basis Expansion Models and Diversity Techniques for Blind Identification and Equalization of Tiem-Varying Cahnnels," *Proceedings of the IEEE,* vol. 86, no. 10, pp. 1969-86, October 1998.

[80] Giannakis G. B., Tepedelentioglu C., and Liu H., Adaptive Blind Equlaization of Time-varying Channels," *IEEE ICASSP 97*, vol. 5, pp. 4033-36.

[81] Tsatsanis M. K. and Giannakis G. B. "Equalization of Rapidly Fading Channels: Self-Recovering Methods", *IEEE Trans. on Comm.*, vol. 44, no. 5, pp. 619-30, May 1996.

[82] Liu H. and Giannakis G. B.' "Deterministic Approaches for Blind Equalization of Time-Varying Channels with Antenna Arrays", *IEEE Trans. on Signal Processing,* vol. 46, no. 11, pp.3003-13, Nov. 1998.

[83] Tsastsanis M. K. and Giannakis G. B., "Subspace Methods for Blin Estimation of Time-Varying FIR Channels," *IEEE Trans. on Signal Processing,* vol. 45, no. 12, pp. 3084-93, December 1997.

[84] Tsatsanis M. K. and Giannakis G. B., "Modeling and Equalization of Rapidly Fading Channels," *Int. Journal of Adaptive Control and Signal Processing,* vol. 10, pp. 159-76, 1996.

[85] Tsatsanis K. K. and Giannakis G. B., "Blind Estimation of Direct Sequence Spread Spectrum Signals in Multipath," *IEEE Trans. on Signal Processing,* vol. 45, No. 5, pp. 1241-52, May 1997.

[86] Tsatsanis K. K. and Giannakis G. B., "Acquisition of PN sequences in chip synchronous DS/SS systems using a random sequence model and the SPRT," *IEEE Trans. Commun.,* vol. 42, pp. 2325-33, June 1994.

[87] Chaparro, L. F. and Alshehri, A., "Jammer Excision in Spread Spectrum Communications via Weiner Masking and Frequncy-frequency Evolutionary Transform," *IEEE ICASSP 2003,* Volume: 4 , April 6-10, 2003.

[88] Alexandra D.H., Jack H., and Zoran Z., "Multiuser Detection for CDMA Systems," *IEEE Personal Communications,* April, 1995.

[89] M. Honig, U. Madhow, and S. Verdu, "Blind Adaptive Multiuser Detection", *IEEE Trans. on Information Theory,* vol. 41, no. 4, pp. 944-960, July 1995.

[90] Mark D. Hahm, and Zoran I. Mitrovwski, "Deconvolution in the Presence of Doppler with Application to Specular Multipath Parameter Estimation", *IEEE Trans. on Signal Processing.,* vol. 45, No. 9, pp. 2203-2219.